DETERMINATION OF WIND POWER POTENTIAL AND OPTIMAL WIND POWER PLANT LOCATIONS IN TURKEY

A THESIS SUBMITTED TO
THE GRADUATE SCHOOL OF NATURAL AND APPLIED SCIENCES
OF
MIDDLE EAST TECHNICAL UNIVERSITY

BY

HALE ÇETİNAY

IN PARTIAL FULFILLMENT OF THE REQUIREMENTS
FOR
THE DEGREE OF MASTER OF SCIENCE
IN
ELECTRICAL AND ELECTRONICS ENGINEERING

MAY 2014

Approval of the thesis:

DETERMINATION OF WIND POWER POTENTIAL AND OPTIMAL WIND POWER PLANT LOCATIONS IN TURKEY

submitted by **HALE ÇETİNAY** in partial fulfillment of the requirements for the degree of **Master of Science in Electrical and Electronics Engineering Department, Middle East Technical University** by,

Prof. Dr. Canan Özgen _____
Dean, Graduate School of **Natural and Applied Sciences**

Prof. Dr. Gönül Turhan Sayan _____
Head of Department, **Electrical and Electronics Engineering**

Prof. Dr. Ali Nezih Güven _____
Supervisor, **Electrical and Electronics Eng. Dept., METU**

Dr. Osman Bülent Tör _____
Co-Supervisor, **EPRA**

Examining Committee Members:

Prof. Dr. Arif Ertaş _____
Electrical and Electronics Engineering Dept., METU

Prof. Dr. Ali Nezih Güven _____
Electrical and Electronics Engineering Dept., METU

Dr. Osman Bülent Tör _____
Manager, EPRA

Prof. Dr. Muammer Ermiş _____
Electrical and Electronics Engineering Dept., METU

Mahmut Erkut Cebeci, M.Sc. _____
Chief Researcher, TUBITAK

Date: 21.05.2014

I hereby declare that all information in this document has been obtained and presented in accordance with academic rules and ethical conduct. I also declare that, as required by these rules and conduct, I have fully cited and referenced all material and results that are not original to this work.

Name, Last name : Hale Çetinay

Signature :

ABSTRACT

DETERMINATION OF WIND POWER POTENTIAL AND OPTIMAL WIND POWER PLANT LOCATIONS IN TURKEY

Çetinay, Hale
MS, Department of Electrical and Electronics Engineering
Supervisor : Prof. Dr. Ali Nezih Güven
Co-Supervisor: Dr. Osman Bülent Tör

May 2014, 144 pages

Due to increased environmental concerns, utilization of the renewable energy, especially the wind power, gains importance. Like developed countries which have set their renewable energy targets for the long term integration, Turkish government has also set the goal as 20 GW of total wind power installed capacity in 2023. In this thesis, the wind power potential in Turkey is analyzed and different cases are studied to determine optimal locations for wind power plant establishment.

In order to determine the wind power potential, annual and seasonal average wind speeds and Weibull distribution parameters of the speed are calculated for every 6 km x 6 km area in Turkey. Moreover, using calculated parameters of the speed, wind power densities and capacity factors of the potential power plant are determined. To visualize results via maps, Plate Carrée map transformation is utilized.

The calculated wind speed parameters, the altitude and urban data of Turkey are used to find the set of feasible locations for wind power plant establishment and possible transformer substation connections for wind power plants. Then, among the set of feasible locations, linear programming optimization method is performed in the expected 2017 summer peak scenario of Turkey to determine optimal locations of wind power plants which lead maximum annual wind power production. While solving the optimization problem, DC load flow equations are utilized by taking the transmission constraints into account and the impact of wind power penetration on Turkish grid is analyzed.

Keywords: Wind Power, Weibull Distribution, Wind Power Density, Capacity Factor, Linear Programming

ÖZ

TÜRKİYE'DE RÜZGAR ENERJİSİ POTANSİYELİNİN VE RÜZGAR ENERJİ SANTRALİ KURULUMU İÇİN OPTİMUM YERLERİN BELİRLENMESİ

Çetinay, Hale
Yüksek Lisans, Elektrik ve Elektronik Mühendisliği Bölümü
Tez Yöneticisi : Prof. Dr. Ali Nezih Güven
Ortak Tez Yöneticisi : Dr. Osman Bülent Tör

Mayıs 2014, 144 sayfa

Yenilenebilir enerji, özellikle rüzgar enerjisi, son yıllarda çevresel kaygılarla beraber giderek artan şekilde önem kazanmaktadır. Diğer gelişmiş ülkeler gibi Türkiye de uzun dönem yenilenebilir enerji hedefini belirlemiştir: 2023 yılında Türkiye'deki rüzgar santralleri kurulu gücünün toplamda 20 GW'a ulaşılması hedeflenmiştir. Bu tezde Türkiye'de rüzgar enerjisi potansiyeli ve rüzgar enerjisi santrali kurulumu için en uygun yerler belirlenmiştir.

Türkiye'de rüzgar enerjisi potansiyelini analiz etmek için her bir 6 km x 6 km'lik alana ait yıllık ve mevsimlik ortalama rüzgar hızları ve hızın Weibull dağılım parametreleri hesaplanmıştır. Ayrıca hesaplanan parametreler kullanılarak, rüzgarın güç yoğunluğu ve bu alana kurulabilecek rüzgar enerji santralinin kapasite faktörü

hesaplanmıştır. Sonuçları haritalar aracılığıyla görselleştirmek için Plate Carrée harita projeksiyonu kullanılmıştır.

Hesaplanan rüzgar parametreleri, Türkiye rakım ve kentsel verileri kullanılarak Türkiye'de rüzgar enerji santrali kurulumuna uygun yerler ve bağlantı trafo merkezleri bulunmuştur. Daha sonra, belirlenen yerler arasından, yıllık rüzgar enerjisi üretimini en yüksek değere taşıyacak alanlar, beklenen 2017 Türkiye yaz puant senaryosunda Lineer Programlama optimizasyon modeli kullanılarak belirlenmiştir. Optimizasyon problemi çözülürken, DC yük akışı denklemleri, iletim kısıtları ile beraber göz önüne alınmış ve üretimin Türk Elektrik Sistemi üzerindeki etkisi analiz edilmiştir.

Anahtar Kelimeler: Rüzgar Enerjisi, Weibull Dağılımı, Rüzgar Güç Yoğunluğu, Kapasite Faktörü, Lineer Programlama

To My Family

ACKNOWLEDGMENTS

First of all, I would like to thank my supervisor, Prof. Dr. Ali Nezih Güven, and my co-supervisor, Dr. Osman Bülent Tör, for their guidance, advice, criticism and encouragement throughout the study.

I would also like to express my deepest gratitude to my family for their unconditional support, love and encouragement throughout my life.

I also wish to thank all members of the Power Systems Group of TÜBİTAK MAM for their support, intimate friendship and for creating an excellent working environment. I especially thank Mahmut Erkut Cebeci for his advises and Erman Terciyanlı who has provided the necessary data for calculations and excellent information throughout the study.

TABLE OF CONTENTS

LIST OF TABLES

TABLES

LIST OF FIGURES

FIGURES

LIST OF ABBREVIATIONS

AD	Air Density
A.G.L.	Above Ground Level
CDF	Cumulative Distribution Function
CF	Capacity Factor
ECMWF	European Centre for Medium-Range Weather Forecasts [4]
EMRA	Energy Market Regulatory Authority
EPDK	Republic of Turkey Energy Market Regulatory Authority
GIS	Gas Insulated Substation
HV	High Voltage
PC	Power Curve
PDF	Probability Density Function
PP	Power Plant
REPA	Turkish Wind Atlas Prepared by Ministry of Energy and Natural Resources [23]
RITM	Monitoring and Forecasting System Development for Wind Generated Electrical Power in Turkey [15]
ROR	Run of River
TEIAS	Turkish Electricity Transmission Company [26]
TS	Transformer Substation
TSO	Transmission System Operator
TUBITAK	The Scientific and Technological Research Council of Turkey
WPD	Wind Power Density
WPP	Wind Power Plant

CHAPTER 1

INTRODUCTION

Aim of this thesis is to analyze the wind power potential in Turkey and to investigate optimal wind plant locations taking into account both the investors' point of view and transmission system operators' point of view.

As the green energy idea becomes more and more popular due to environmental concerns, renewable energy gains importance. So far, the main source of the renewable energy is wind: The utilization of wind energy has increased throughout the world in recent years. This rapid development of wind power technology has certain impacts on the power generation; since, the increase in wind power generation will result in the decrease in the domination of fossil fuel power plants.

Like developed countries which set their renewable energy targets for long term integration, Turkish government has set the goal as attaining a total 20 GW of installed wind power plants in 2023 [1]. In order to make this ambitious goal fulfilled, Turkey takes both economic and technical measures: Government encourages investors financially by feed-in tariffs which even increase by the use of local resources in the construction [2] and the transmission system operator plans necessary improvements to ensure Turkish power system becoming convenient for large scale renewable integration.

Large scale wind power integration cannot be established without a well planning process. In this perspective, one of three plans can be selected: Firstly, in scope of

the transmission operator, new generating plants are welcomed to the places where demands for electricity are high. However, these locations may not be favorable for the wind power generation. Secondly, places with strong wind are locations where investors would like to establish wind power plants. However, these areas may be remote from load centers or wind power plant establishment can lead to high transmission system investments to secure the system. Lastly, various combinations with different weather patterns in order to smooth wind output can be established [3]. However, since the demand for electricity in Turkey is still increasing with changing peak hours and due to lack of real measured data, this option is not feasible. The combination of first and second plans is more suitable for Turkey: For wind power plants investments, locations which will lead the maximum wind power production while taking the transmission system security into account should be promoted.

TUBITAK Marmara Research Center has prepared a national database including forecasts of the wind speed, the wind direction, the ambient temperature and the air pressure values for every hour of last 8 years. These values are deduced from satellite data which are purchased from the European Centre for Medium-Range Weather Forecasts (ECMWF) [4] in the scope of European Wind Atlas Project. Then, by applying WAsP technique [5], the mentioned database in TUBITAK is constructed. In the database, there are more than 38000 data points, each of which represents a 6 km x 6 km area in Turkey. In addition, values in the database are dependent on altitude. As wind turbines nowadays are mostly installed at between 80 and 100 meters above the ground level [6], in this study, the data belonging to 80 meters are taken into account.

Main parameters which affect a wind power plant investment are the average wind speed, the wind power density and the capacity factor of the probable unit at that location. There is a relation between these parameters; however, before deciding on a place to invest; each of them should be investigated carefully. For instance, the same average speed from different wind patterns can lead to different wind power densities and capacity factors which will directly affect the wind power generation.

The wind pattern depends on the climate so as the average wind speed, the power density and the capacity factor. Therefore, in addition to performing annual analyses, it is useful to investigate seasonal results. The results of the seasonal analyses are also important and useful in generation dispatch planning since peak and off-peak demands of Turkey are also dependent on the season.

The work accomplished in this thesis consists of two main parts: In the first part, in Chapter 3, by using the data deduced from ECMWF, the analyses are accomplished to determine the wind power potential in Turkey. This part starts with acquiring the 8 years of hourly wind speed, wind direction, ambient temperature and pressure variations from the database for each data point. Then, by using Matlab [7] software and necessary formulae; calculations of the average wind speed, Weibull Distribution parameters of the speed, the air density of the area, and the wind power density for different seasons are performed. In addition, by proposing an adequate wind turbine for each data point, the capacity factors of the potential wind power plants are calculated. All results are visualized via prepared maps by introducing a map transformation.

In the second part of the study, in Chapter 4, integration of wind power to Turkish grid and optimal locations for wind power plant establishment are investigated. This part starts with finding feasible areas and connection transformer substations for wind power plant establishment, using the calculated wind speed parameters in Chapter 3, the altitude and urban data of Turkey. Then, based on the forecasted 2017 summer peak data of the Turkish network, linear programming technique with DC load flow are used to determine the optimal places for wind power establishment which will lead maximum annual wind power production by taking the transmission constraints into account. The optimization is simulated for two cases: In Case 1, the maximum installed capacity of wind power plants in a region is bounded by the regional wind power connection capacities declared by TEIAS [8] and the optimal locations are selected accordingly. In Case 2, the declared regional capacities are not taken into account and locations for WPP establishment which will lead maximum wind power generation in Turkey are found without any regional constraints.

CHAPTER 2

OVERVIEW OF WIND POWER

2.1. Definition of Wind Power

Wind power can be defined as the conversion of wind energy into a useful form of energy. Wind turbines are used to convert the kinetic energy in the wind into rotational kinetic energy in the turbine and then to electrical energy that can be supplied, via the national grid, for any purpose [9]. The energy available for conversion mainly depends on the wind speed and the swept area of the turbine blades. The rotational kinetic power of an air mass *m* (kg) that flows at speed *v* (m/s) through an area *A* (m^2) can be derived as follows [10]:

Under constant acceleration, the work accomplished by displacing an object to a distance *d* (m) under the force *F* (Newton) is given in Equation (2-1):

$$Work = E = Fd \tag{2-1}$$

According to Newton's Second Law of Motion [11], the force *F* (Newton) can be expressed in terms of the acceleration *a* (m/s^2) and mass *m* (kg).

$$F = ma \tag{2-2}$$

By combining Equation (2-1) and Equation (2-2), the expression of work is re-written.

$$E = mad \tag{2-3}$$

Using the Third Equation of Motion [11]; the initial velocity, the final velocity, the acceleration of the mass, and the distance are related; where u (m/s) is the initial velocity of the mass.

$$v^2 = u^2 + 2ad \tag{2-4}$$

Since the initial velocity of the mass (wind) is zero, Equation (2-4) simplifies to Equation (2-5).

$$a = \frac{v^2}{2d} \tag{2-5}$$

By substituting (2-5) to Equation (2-3), the equation for kinetic energy of the mass is acquired.

$$E = \frac{1}{2}\, m\, v^2 \tag{2-6}$$

The power P (watts) of the wind is given by the rate of change of energy over unit time. Therefore; applying the definition of power to Equation (2-6), gives Equation (2-7).

$$P = \frac{dE}{dt} = \frac{1}{2}\, v^2 \frac{dm}{dt} \tag{2-7}$$

The mass flow rate through the area A is given in Equation (2-8) where ρ (kg/m^3) is the density and X (m) is the distance.

$$\frac{dm}{dt} = \rho\, A\, \frac{dX}{dt} \tag{2-8}$$

By introducing the definition of velocity *v* as the rate of change of distance and the definition of mass flow rate from Equation (2-8), Equation (2-7) can be simplified to Equation (2-9).

$$P = \frac{1}{2}\,\rho\,A\,v^3 \tag{2-9}$$

The power calculated in Equation (2-9) is the total available kinetic energy in wind per unit of time. The power in the wind is converted into the mechanical–rotational energy of the wind turbine rotor, which results in a reduced speed in the air mass. Therefore, the power in the wind cannot be extracted completely by a wind turbine, as the air mass would be stopped completely in the intercepting rotor area.

The theoretical optimum for utilizing the power in the wind by reducing its velocity was first discovered by Betz, in 1926 [9]. Albert Betz concluded that no wind turbine can convert more than $\frac{16}{27}$ (59.3%) of the kinetic energy of the wind into mechanical energy turning a rotor. In other words, according to Betz, the theoretical maximum power that can be extracted from the wind is given in Equation (2-10).

$$P_{max} = \frac{1}{2}\,\rho\,A\,v^3 * C_{p,max} = \frac{1}{2}\,\rho\,A\,v^3 * 0.59 \tag{2-10}$$

However; when the losses and the other factors (gearbox, bearings, etc.) are taken into account, the theoretical value in Equation (2-10) cannot be reached and the power coefficient needs to be factored. As a result, the extractable power from the wind is generally expressed as Equation (2-11).

$$P = \frac{1}{2}\,\rho\,A\,v^3 * C_p \tag{2-11}$$

where,

C_p is the variable power coefficient.

2.2. Variability and Uncertainty of Wind

Wind energy is a natural resource; it is almost unlimited and free. Apart from that, the most important characteristic of it is the change of wind flow through different time of day, year, season, and height.

Wind speed varies rapidly and frequently within a wide range; therefore, generation of the wind turbines are not precisely predictable; as the output power of a wind turbine is a function of the wind speed in the third degree (Equation (2-11)). As a result, the availability of the electricity generated from wind energy differs fundamentally from that generated conventionally from fossil fuels. This unpredictable characteristic of wind power is different; therefore; its integration leads to some important challenges and additional investments concerning the power system.

As explained by Equation (2-11), the available energy in the wind varies with the cube of the wind speed. Hence; a 10 % increase in the wind speed will result in a 33.1 % increase in the available energy. Therefore, wind speed is the most effective variable in defining the power output. In Figure 2-1, the power curve of a wind turbine [12] is given: As seen the power curve follows the cubical relationship between cut-in wind speed (the speed at which the wind turbine starts to operate) and rated speed (the speed at which the wind turbine generates its maximum output power). The wind turbine usually reaches rated capacity at a wind speed between 12 - 16 m/s depending on the design of the wind turbine. Beyond rated speed, the wind turbine generates the maximum power (rated power) until the wind speed reaches to cut-off speed, after which turbine stops operating. As an example, in Figure 2-1, the power curve of Vestas 112-3.0 MW wind turbine is shown. It can be followed that the cut-in speed of this turbine is 3 m/s, the rated speed is 12 m/s, the cut-off speed is 25 m/s and the rated power is 3 MW.

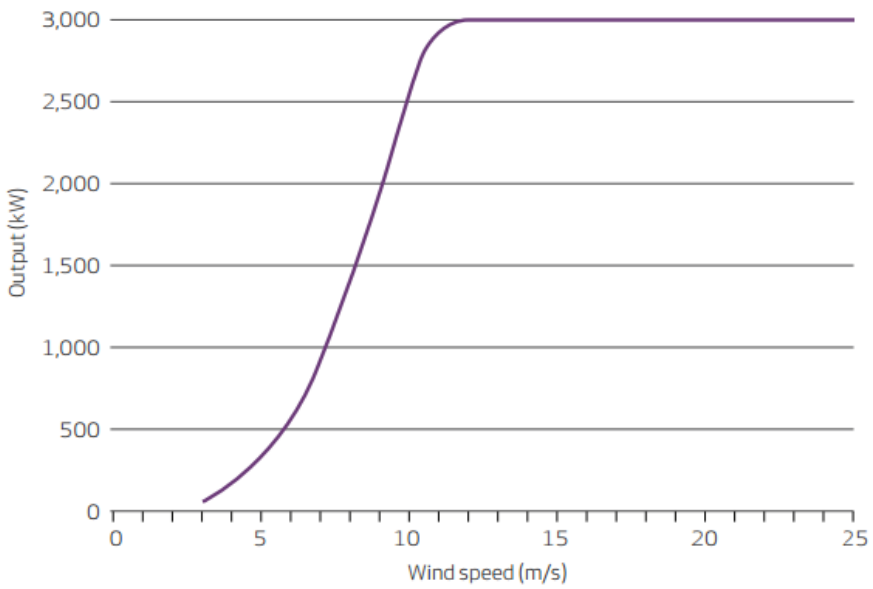

Figure 2-1. Power Curve of Vestas 112-3.0 MW Wind Turbine [12]

Main features of the wind power, namely, variation and fluctuation, have effects on the power system. Short-term variation mainly impacts the formulation of power schedule, the balance of power and determination of needed reserve capacity. Long-term variation determines the credibility of power capacity and transmission investments in the power system.

For the prediction of wind power generated from wind power plants, it is the wind speed variability that leads to the largest generation variations; therefore, it is hard to forecast. However, variations of wind velocity and direction with meteorological conditions are not completely unpredictable.

It is important to predict the generation from wind power plants in order to fulfill the grid dispatching management in the system. There are a lot of methods available, the most commonly used is to rely on 10 minutes average wind speed data, the weather forecast and the data provided by wind power plants (WPP) and make use of a forecasting software to make detailed calculation and forecasts [13] - [14].

In Turkey, in scope of RITM (Wind Power Monitoring and Forecast Centre) [15] project, completed in 2010; short term and medium term wind power forecasts for selected 14 WPPs are computed. The project is intended to include all wind power plants in Turkey in the future; therefore, wind power system monitoring and forecasting systems will be disseminated throughout Turkey. With RITM, it is aimed to fulfill the grid dispatching management and provide large-scale integration of WPPs to Turkish Electricity System. In Figure 2-2, wind power generation forecast and actual generation of 09.12.2013 and 10.12.2013 can be seen. The gap between the predicted and the measured wind power generation could be quite substantial. During the monitored time, the predicted power can be less or higher than the actual generation. In long term planning, forecast errors are not the concern. The behavior of the wind, the overall capacity factor of the power plant and maximum wind power penetration are the main inputs for the long term planning.

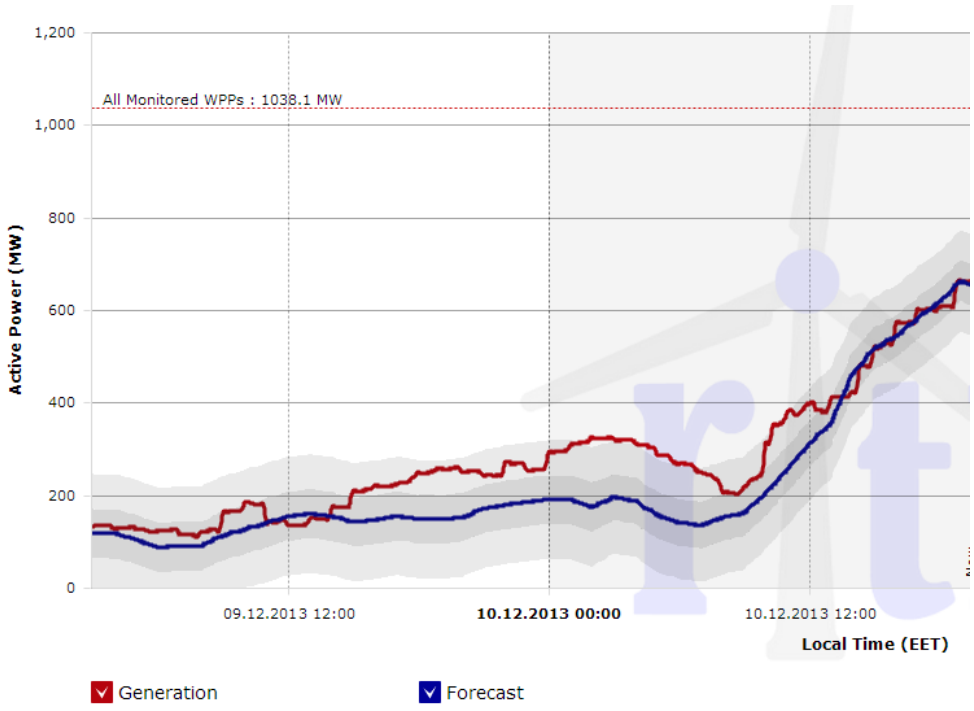

Figure 2-2. Comparison of Wind Power Forecast and Actual Generation (RITM, 09-10.12.2013)

The capacity factor of a power plant is the ratio of its actual output over a period of time to its potential output; if it were possible for it to operate at full nameplate capacity indefinitely. The capacity factor for conventional power plants is typically 40 % to 80 %; whereas, despite the high availability of the wind turbines (98 %), the capacity factor rarely reaches beyond 30 % for onshore wind power and 40 % for offshore wind power [16]. Therefore, one installed megawatt of wind power cannot replace one megawatt of thermal power, and in long term generation planning, this issue should also be considered.

2.3. Impact of Wind Power Generation on Power Systems

The wind power is very important in evolving towards a renewable power generation system. With the wind power becoming an important alternative for the generation of electricity, it is essential to accurately model the effects of wind power on the entire power system.

Integration of the wind generation to the power system is associated with both benefits and costs. The main benefit of the wind power is to reduce the domination of fossil fuel together with lower emissions. As the disadvantage, the capacity value of the wind power generation will be clearly limited; since, it will not be possible to displace conventional generation capacity on a megawatt for megawatt basis [17]. In order to maintain the system security, the installed capacity of generation must be greater than the peak demand due to the unpredictable nature of the wind. In addition, it must be noted that wind turbines are very limited in providing the range of system support services (e.g., voltage and frequency regulation) that are provided by conventional thermal and hydro power plants. This can usually be tolerated at relatively low levels of penetration; but, at the higher levels indicated by the target it will require systematic solutions in order to maintain stability and integrity of the transmission system [18]. In Turkey, the necessary requirements from WPPs are defined in Division 18 of Electricity Market Regulation [19].

It is technically possible to integrate large amounts of the wind power into the power systems, the limits are arising from how much can be integrated at socially and economically acceptable costs [20]. Large penetration of the wind power generation will have strong cost influence; since, other power plants must deliver both the flexibility and reserve necessary to maintain the continuous balance between load and generation. To enable a proper management for large-scale wind power, more flexibility will be needed in the power system. The flexibility could be achieved by flexible generation and demand or sufficient transmission capacities between interconnected areas [18]. As a result, high penetration of wind power has impacts that have to be managed through proper power plant interconnection, integration, transmission planning and system and market operations.

In summary, in a large and well-interconnected system, the limit of the wind energy penetration is economic, not technical. With sufficient resources such as system reserves and backup capacity, the power supply will stay secure even with 100 % wind power. International experiences show that power systems can technically accommodate large shares of wind without disturbing security of supply [21]. For instance, Denmark which has already a wind penetration level about 20 % (share of electricity produced by wind) plans to increase it up to 50 % in 2020 [22].

2.4. Wind Power and Transmission Grid Planning

Proper interconnected transmission grid with a sufficient transmission capacity is the key in successful transmission planning. The impact of wind power on power systems depends on the location of wind power plants relative to the load, and the correlation between the wind power generation and the electricity consumption areas [18].

Integration of the wind power to the system clearly affects the power flow in the network. It may change the power flow direction, reduce or increase power losses and bottleneck situations, especially in grids with high wind power concentration areas where local electricity consumption is low. The general transmission grid

planning consists of three aspects which have to be considered when planning the integration of large amount of wind power into the power system [18]:

- Adequate level of operational security;
- Adequate transmission capacity;
- Functioning of electricity market.

In order to maintain adequate level of operational security and transmission capacity, grid connection becomes very important financial issue for all renewable projects; especially, if the integration of WPPs requires heavy grid reinforcement. Therefore, while allowing the wind power plant connections to the grid, the most suitable locations must be chosen according to the social welfare. In other words, when deciding on the optimal location for the wind power plants, 2 aspects can be considered:

- Siting of new generation where the generation deficiency exists (from Transmission System Operator (TSO) point of view);
- Siting of new generation where wind is favorable (from power plant operator point of view).

The above mentioned two aspects can lead to different siting of WPPs. For instance, for a certain area, if there is a generation deficit and system bottleneck, additional generation will be welcomed from TSO's point of view. However, the wind power in the area should also be worthy to establish WPPs there. Therefore, an optimal capacity should be applied to satisfy both of the parties.

2.5. Utilization of Wind Power in Turkey

In Turkey, local winds are effective; wind is usually stronger in summer and winter and weaker in spring. However, due to the different types of landforms, wind speed

depends also location. Winds are most effective in the west part and sea coasts of Turkey [23].

Ministry of Energy and Natural Resources presented a wind atlas, REPA, showing the variation of wind resources to enlighten the way to the investors [23]. In Figure 2-3, the wind speed variation map of Turkey is presented. High wind speed averages are present in the Aegean, Marmara, and Eastern Mediterranean regions. Therefore; as expected, more than 40 % of the existing wind power plants are in Aegean region, and it is followed by Marmara region with 38 % [24].

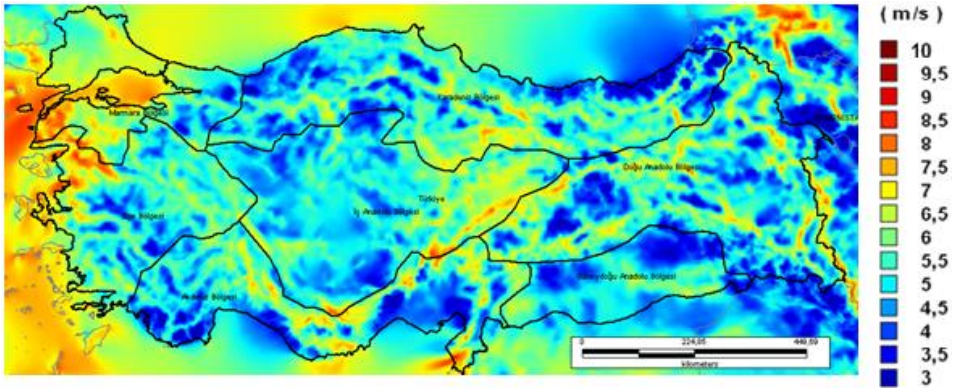

Figure 2-3. Wind Speed Variation in Turkey (100 m. above Ground Level (a.g.l.), REPA)

As Turkey is very rich in renewable potential, the renewable power opportunities have become one of the most important topics. In Turkey, the installed capacity of the wind power increased more significantly starting from year 2007. Figure 2-4 shows the development of the installed wind capacity in Turkey. Total installed capacity of wind power plants represents 4 % of the total capacity, at just above 2.2 GW in March 2013 [24].

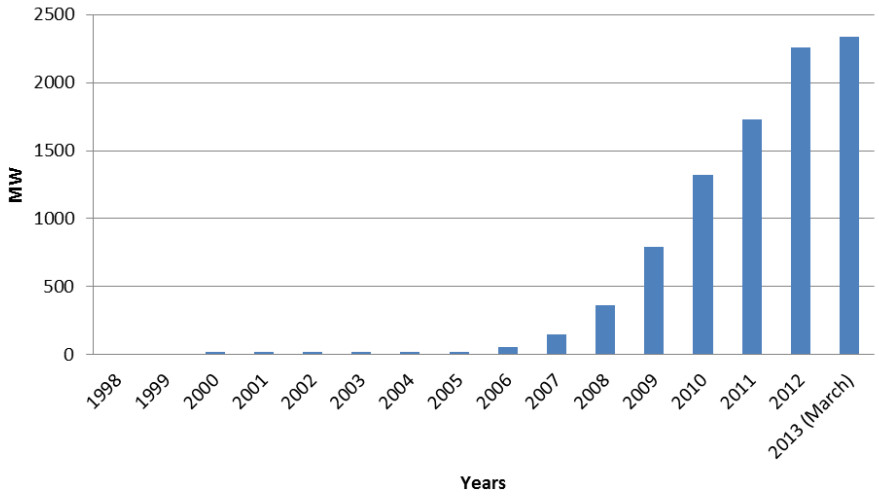

Figure 2-4. Development of Installed Wind Power in Turkey

As the electricity sector is growing steadily with economic growth and population, Turkey is one of the most prominent wind markets in Europe [24]. Many investors would like to invest in Turkey and establish wind power plants. By 2013, there are 261 licensed WPP projects with 10 GW of total capacity. When they are all implemented, 153 of those plants will be connected at 154 kV level; whereas, the others will serve at distribution level [25].

2.6. Future Plans and Obstacles about the Integration of Wind Power to Turkish Grid

By the end of 2012, there are 772 power plants with 57.05 GW of total installed capacity in Turkish electricity network [26]. The transmission system operator, Türkiye Elektrik İletim A.Ş. (TEIAS), owns and regulates the high voltage transmission lines; whereas, at the generation level, there are both private companies and generators owned by the government such as large hydro plants. The share of the fuel types of the installed capacity in Turkey by the end of 2012 are shown in Figure 2-5. The biggest share, 30 % of the installed capacity, belongs to the natural gas power plants. The share of the wind power plants is 4 %.

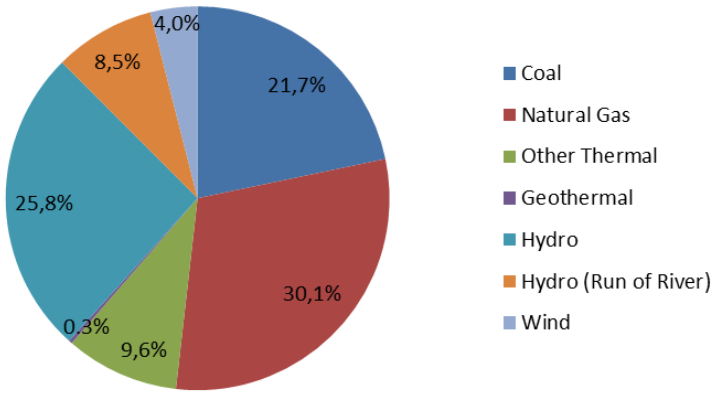

Figure 2-5. Fuel Types of the Installed Capacity of Turkey (2012)

Turkey is a developing country; therefore, the demand for the electricity has been increasing for the past decades except during the economic crises. In 2012, Turkish power system had generated 239.5 TWh of electricity (Figure 2-6). The biggest share of the generation consists of thermal power plants using fossil fuels, coal and natural gas. The peak demand, which was approximately 39 GW in 2012, occurs at summer due to irrigation and the use of air conditioners; however, because of electrical heating, the winter peak is still high. The demands in big cities are considerably high and will continue to grow; therefore, adequate measures should be taken to secure system to serve this increasing demand.

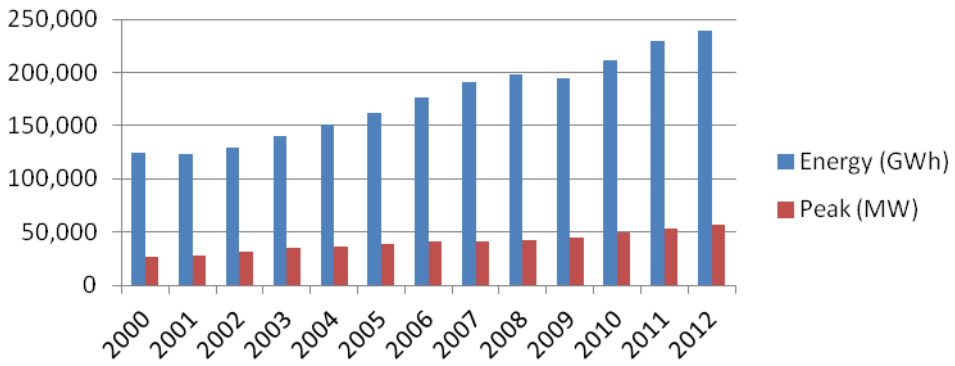

Figure 2-6. Energy Statistics of Turkey

One of the most disturbing features of current power system in Turkey is the huge share of natural gas power plants in the installed capacity and generation. Since, natural gas power plants can be established within a few years, most of the investors prefer to invest in natural gas power plants. However, Turkey has limited natural gas resources; therefore, must import the natural gas from neighboring countries. Especially, in the winter, due to lack of sufficient amount of natural gas, some of the natural power plants cannot operate and this results in an unsecure generation profile. Therefore, increase in the share of natural gas plants will both increase the cost of electricity generation due to imported fuel, as well as due to inadequate supplies, there is always the risk of inadequacy of fuel.

Like all developed countries, Turkish government plans to increase the share of renewable resources in generation. By the government targets for wind energy and the desire of investors to convert potential wind energy resources in Turkey into business opportunities, the installed wind power capacity is expected to continue increasing rapidly. 2010 - 2014 Strategic Plan of the Ministry of Energy and Natural Resources indicates 10 GW of installed WPP capacity as a goal for 2015; furthermore, this strategy paper sets the WPP capacity target as high as 20 GW by 2023 [1].

There are three main difficulties which need to be solved in order for Turkey to achieve its ambitious goal about wind power plants expansion. First of the problems is economic: In order to increase the WPP investments, government increased the feed-in tariffs and it seems they should be further increased [2] to reach the targets in the mid-term. The second and the third problem are related with each other: Investors do not know about the potential wind source locations; as a result, the transmission system operator cannot plan the related necessary investments in order to be able to securely deliver the WPPs outputs.

The increase in share of wind power plants is slow in the recent years and the 20 GW of target in 2023 seems an optimistic value. However, the TSO should plan the transmission system so that it is capable to serve this goal. In addition to that, in

Turkey; since, transmission system operator also announces the available connection capacity for wind power; it can lead and guide power plant investments to optimal places which will not endanger the system security. Up to January 2013, TEIAS had been declaring the possible wind connection capacities by 5 % criteria which stated the total installed power of wind power plants connected to a substation cannot exceed the 5 % of the short circuit MVA of that transformer substation (TS) [27]. At the current time, TEIAS declares the possible investment places regionally and make investment plans in order to ensure the system security [8].

Typically, a transmission investment (cables, overhead lines, substations, etc.) takes longer time to build than a wind power plant [28]. As a result, long term operation plans and transmission system investments of TEIAS should be prepared carefully: While declaring the wind power plant connection capacities, the transmission system operator should figure out the possible locations for the wind power plant investment and prepare different transmission investment plans considering the wind power penetration. These plans should take the point of view of investors and transmission system operator and optimum long term transmission and wind power generation expansion plan should be accomplished. TEIAS announced that transmission infrastructure will be able to deliver an additional 1 GW wind power connection capacity each year starting from 2013 until 2020. In addition, TEIAS has declared that the transmission network will be able to support the “20 GW WPP by 2023” target of Strategy Paper [1].

CHAPTER 3

DETERMINATION OF WIND POWER POTENTIAL IN TURKEY

TUBITAK Marmara Research Center has prepared a database which includes the hourly wind speed, the wind direction, the ambient temperature and the air pressure variations of last 8 years (2005 - 2012) for each 6 km x 6 km area in Turkey. As a result, in the database, there are more than 38000 areas which are represented by their latitude and longitude values. The values in the database are deduced from the satellite data which are purchased from the European Centre for Medium-Range Weather Forecasts (ECMWF) [4].

In this chapter, by using the above mentioned database, the wind power potential in Turkey will be investigated in detail: Weibull parameters of the wind speed, the average wind speed, the wind power density and the capacity factor calculations will be evaluated. In addition, in order to visualize the results geographically, a necessary map transformation will also be applied and the results will be presented via maps.

The process of the investigation of wind power potential in Turkey is summarized in Figure 3-1. For each 6 km x 6 km area in the database, the algorithm inputs the 8 years hourly wind speed, wind direction, pressure and temperature values. Then, using the wind speed and wind direction data, Weibull parameters are calculated using the built-in function '*wblfit*' in Matlab [29] for each direction segment. Using the wind speed values, the seasonal and annual averages are also calculated and

presented via maps. The air density values are calculated using temperature, pressure and constant humidity data; since, air density will be used in order to calculate the wind power density values. After that, wind power density variations are to be calculated using Weibull parameters and the air density values, and again the results are presented via maps. Lastly, the capacity factors are calculated. Since, the capacity factor depends on the turbine selection, 2 different methods are used and the capacity factors are calculated using the power curve of the turbine and Weibull parameters of the wind speed.

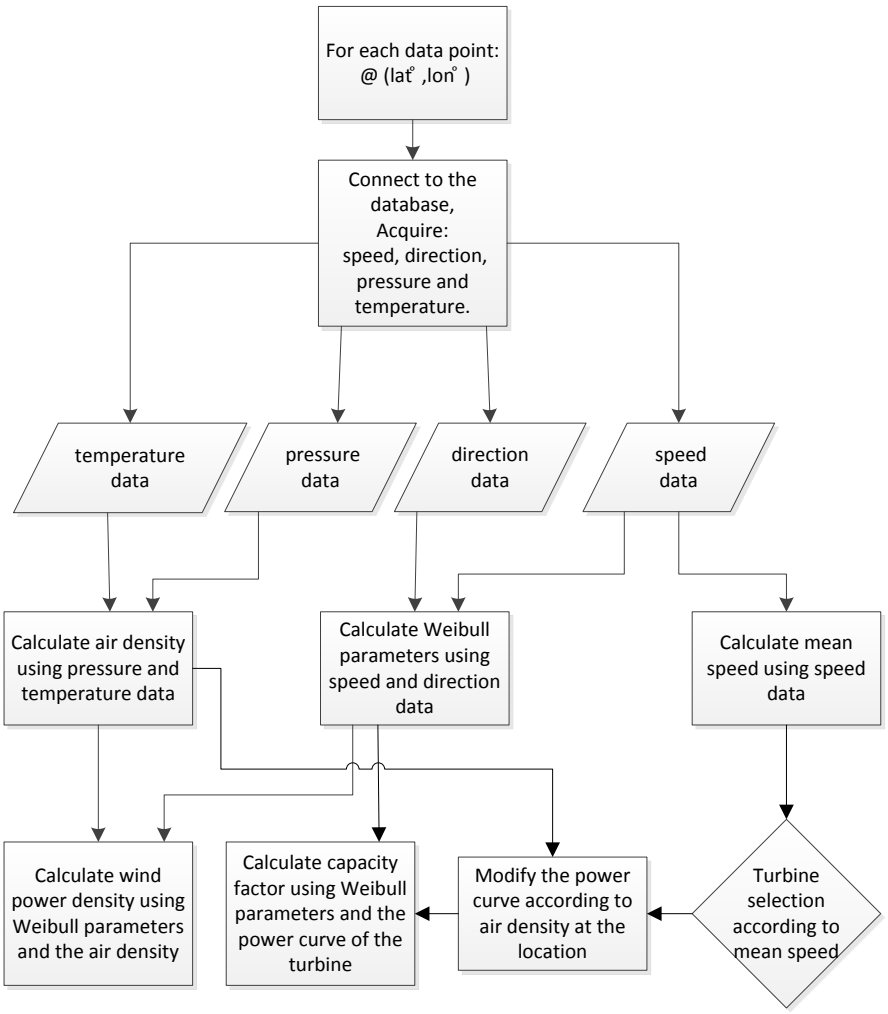

Figure 3-1. The Flowchart of the Process of the Investigation of Wind Potential in Turkey

3.1. Calculation of Weibull Parameters of the Wind Speed

3.1.1. Definition of Weibull Distribution

In studies related to wind, the speed of the wind is taken as a random parameter. The most common distribution function to define the wind speed variation is Weibull distribution function [30]. For the speed *v*, the corresponding Weibull probability density function $f_v(v)$ is defined in Equation (3-1).

$$f_v(v) = b\, a^{-b}\, v^{b-1}\, e^{(-v/a)^b} \tag{3-1}$$

where,

v is the wind speed,

a and *b* are Weibull parameters.

The cumulative distribution function (CDF) of Weibull distribution which represents the probability of wind speed being equal to or smaller than a certain value *V*, is defined as the integration of probability density function (PDF).

$$F_v(V) = \int_0^V b\, a^{-b}\, v^{b-1}\, e^{(-v/a)^b}\, dv \tag{3-2}$$

In order to simplify Equation (3-2), a new integration variable *y* and its derivative *dy* are defined.

$$y = \left(\frac{v}{a}\right)^b \tag{3-3}$$

$$dy = \left(\frac{b\, v^{b-1}}{a^b}\right) dv \tag{3-4}$$

Then, substituting the definition of *y*, the new limits of the integral and the expression for *dv* in terms of *dy* into Equation (3-2) gives the simplified version of cumulative distribution function $F_v(V)$, which gives the probability of speed being smaller than or equal to *V*.

$$F_v(V) = \int_0^{(\frac{V}{a})^b} b\, a^{-b}\, v^{b-1}\, e^{-y}\, \frac{a^b}{(b\, v^{b-1})} dy$$

$$F_v(V) = \int_0^{(\frac{V}{a})^b} e^{-y}\, dy = -(e^{-(\frac{V}{a})^b} - 1)$$

$$F_v(V) = 1 - e^{-(\frac{V}{a})^b} \tag{3-5}$$

In Weibull distribution, *a* is called as the scale parameter; since, when the value of *a* increases for a given value of *b*, the shape of the distribution gets wider. In the definition, parameter *a* has dimensions of velocity. *b* is called as the shape parameter; since, when *b* increases for a given value of *a*, the maximum in the probability density function increases. Parameter *b* is dimensionless. In Figure 3-2 and Figure 3-3, the plots of Weibull distribution for various values of the parameters *a* and *b* are presented.

There are numerous works for calculating Weibull parameters for a particular data [30] - [31]. For the calculation in this study, the built-in Matlab [7] function will be used. In Matlab simulation toolbox, '*wblfit*' [29] function estimates Weibull parameters of the given data. In a similar manner, using '*wblpdf*' [32] and '*wblcdf*' [33] functions, the corresponding probability density function and cumulative distribution function parameters can be calculated.

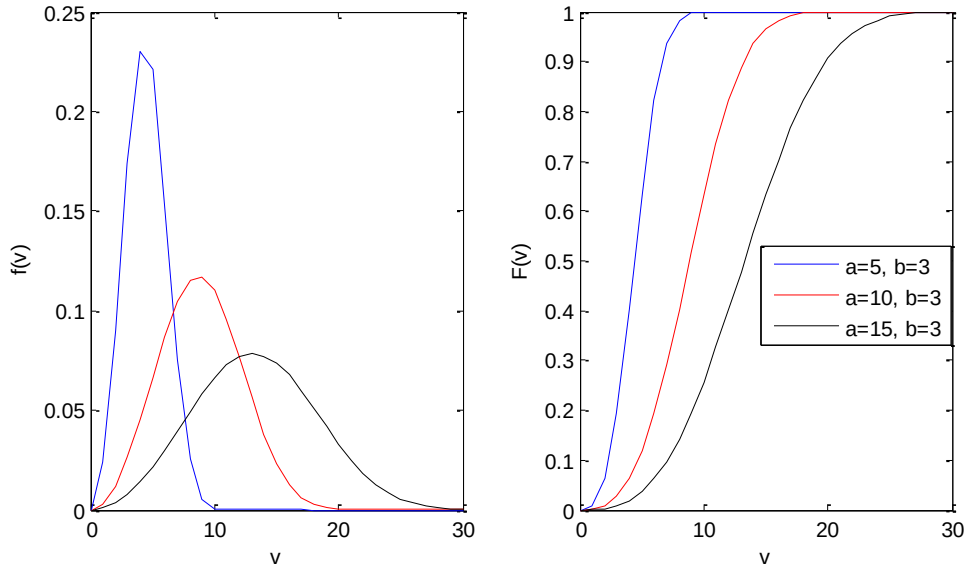

Figure 3-2. Weibull Probability Density and Cumulative Distribution Function for Different Values of *a* (Scale Parameter)

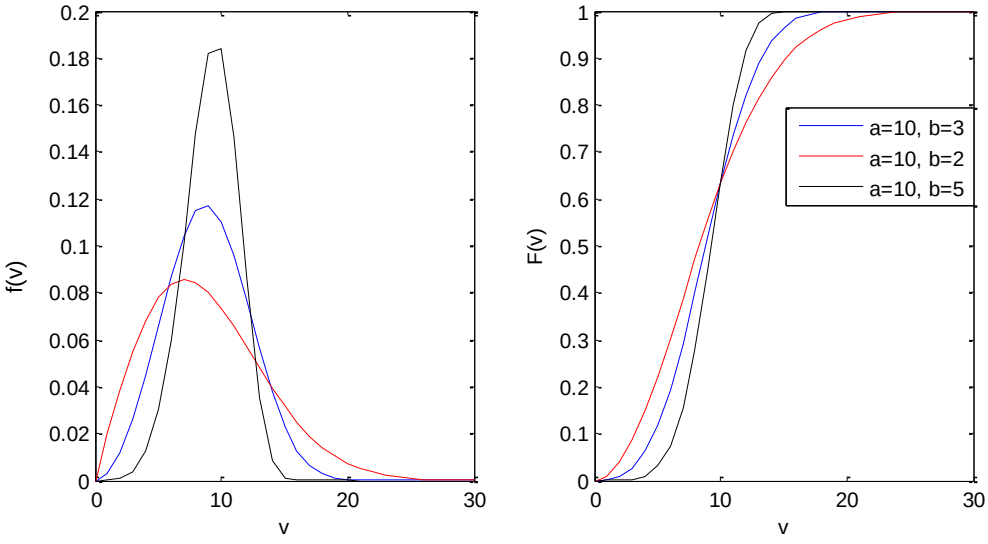

Figure 3-3. Weibull Probability Density and Cumulative Distribution Function for Different Values of *b* (Shape Parameter)

3.1.2. Importance of Wind Direction

In most of the studies, while calculating Weibull parameters of the wind speed variation, the direction of wind is not concerned [34] - [36]. However; the wind speed is correlated with the direction. For instance, wind from a particular direction can be stronger than the other directions; as a result, Weibull parameters in a particular direction and in all directions can be different. Therefore, while deciding on the Weibull parameters of a speed variation, it is essential to consider the wind direction to be accurate [37] - [40]. An example study is established based on Turkish data in order to demonstrate the importance of the wind direction in determining Weibull parameters. From the database, speed variations of the data point with latitude and longitude value 40.0442°, 26.4063° (near Intepe WPP) are acquired and are presented in Figure 3-4.

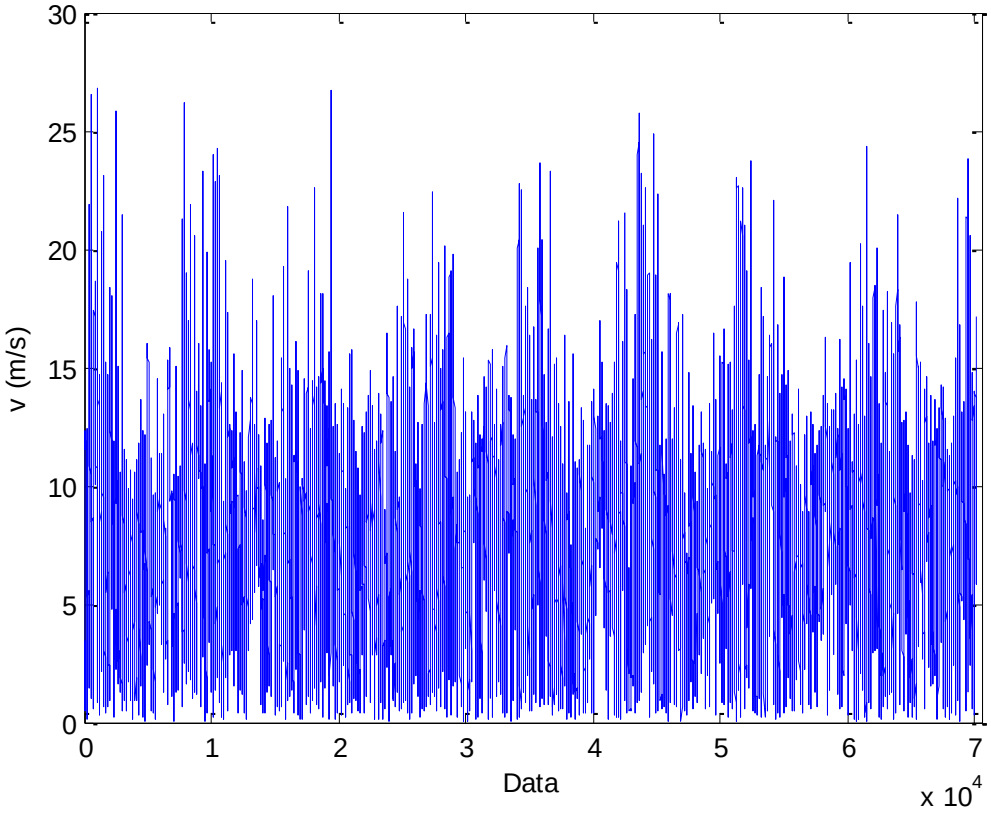

Figure 3-4. The Hourly Speed Variations of Intepe WPP (2005 - 2012)

Since, the data point is chosen to be closer to an actual WPP location; it can be seen from Figure 3-4, the wind speeds are relatively high. When '*wblfit*' function is applied to the speed data, the scale parameter *a* turned out to be 9.06 m/s and the shape parameter *b* turned out to be 2.058.

In Figure 3-5, the actual distribution of the acquired speed data from the database and the fitted Weibull distribution using '*wblfit*' are shown together. The result is satisfactory; since, the distribution function patterns are almost the same. For the mean values of the wind speeds, the mean of the acquired data from the database is calculated as 8.0394 m/s; whereas, the mean of the fitted Weibull distribution turns out to be 8.0258 m/s; yielding a small difference of 0.17 %.

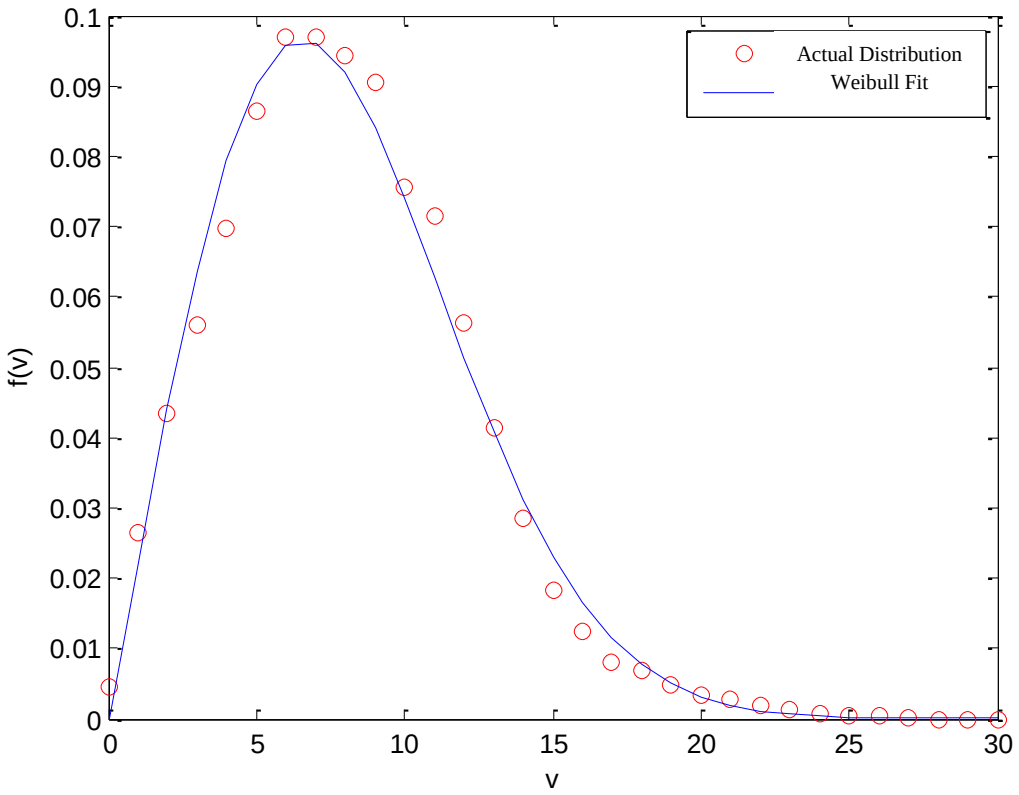

Figure 3-5. Comparison between the PDF of the Actual Distribution and Weibull Fit of the Wind Speed Variation of Intepe WPP

In the demonstration of Intepe WPP; although the direction variation is not used, Weibull fit of the speed variation is found to be quite satisfactory. In the second example, Weibull fit results of the wind speed variation of the data point with latitude and longitude value 36.4731°, 36.2295° (near Belen WPP) is presented. In Figure 3-6, the 8 years of hourly speed variations read from the database are shown.

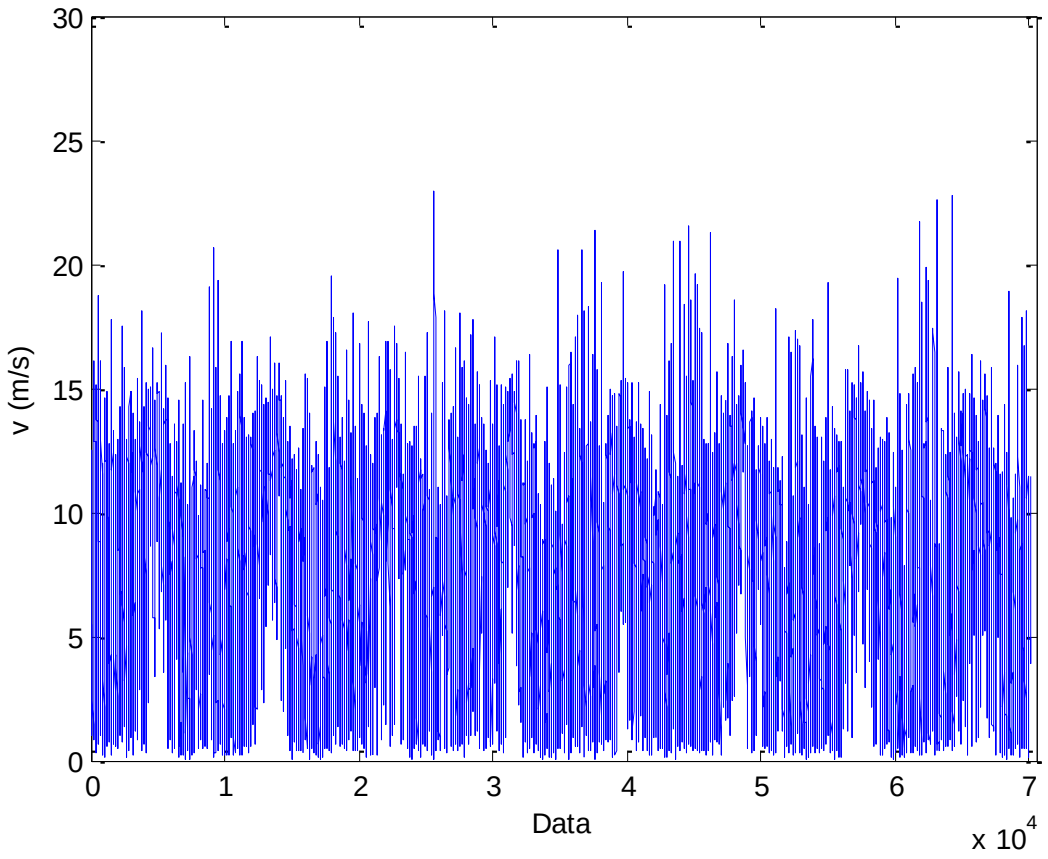

Figure 3-6. The Hourly Speed Variation of Belen WPP (2005 - 2012)

In Figure 3-7, the actual distribution of the read speed data from the database and the fitted Weibull distribution using '*wblfit*' are shown together. When '*wblfit*' function is applied the variation, it is seen that there is a considerable difference between the distribution of the fitted function and the actual data. This is because, at that chosen location, there are more than one dominant wind pattern which blow from different

directions and have different Weibull distributions. As a result; their sum, the speed data regardless of direction, is not a Weibull distribution. Although these kinds of different wind patterns are more common in areas where Monsoon winds are applicable [39], the authorities state that it is more precise to derive Weibull parameters for each direction. The calculated mean speed from database readings is 8.1349 m/s; whereas, from Weibull fit estimation, mean turns out to be 8.0885 m/s. The difference which is calculated approximately as 0.5 % is still not significant. However, the errors will be considerable when calculating the wind power density and the capacity factor; since, Weibull probability density function parameters of the wind speed will directly change the results.

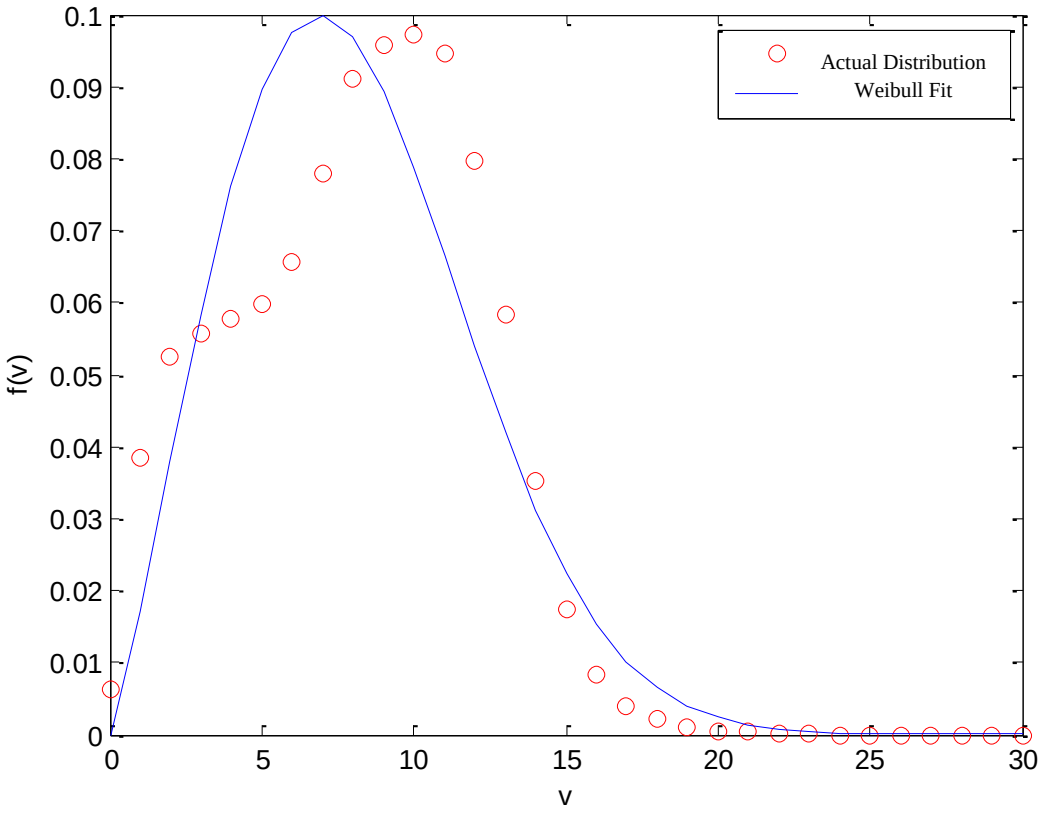

Figure 3-7. Comparison between the PDF of the Actual Distribution and Weibull Fit of the Wind Speed Variation of Belen WPP

3.1.3. Calculation of Weibull Parameters Considering Wind Direction

From the results of Weibull fit demonstrations, for each data location, instead of using only the speed variation when calculating Weibull parameters of the wind, Weibull fit will be accomplished considering both the speed and the direction variations. According to the corresponding directions, the wind speed data will be divided into 12 segments each of which represents 30 degrees. Then, to the constructed wind speed variations according to the direction, Weibull fit is applied and; as a result, for a single data location, 12 different Weibull patterns are calculated. The frequency of these patterns is also calculated for each direction. Figure 3-8 represents the developed algorithm in order to accomplish Weibull fit considering both the wind speed and wind direction variations.

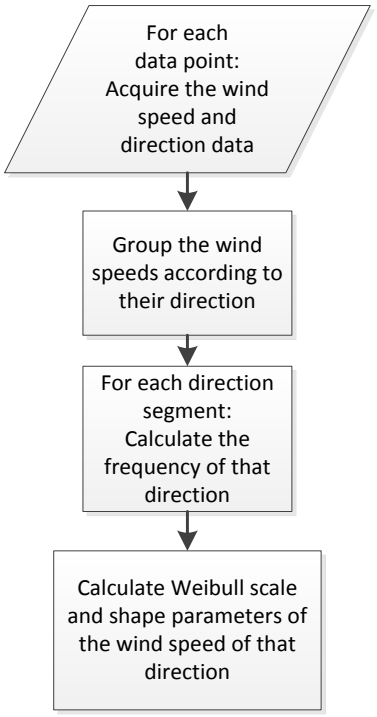

Figure 3-8. Flowchart of the Calculation of Weibull Distribution Parameters Considering the Wind Direction

3.1.4. Example Study: Calculation of Weibull Parameters of Belen WPP Considering the Wind Direction

For Belen WPP, Weibull parameter estimations will be repeated for direction bins of 30 degrees. In Figure 3-9, wind speed and wind direction variations read from the database are shown. It can be followed that, in direction variation, 2 dominant values are present and the corresponding speed values show also different patterns.

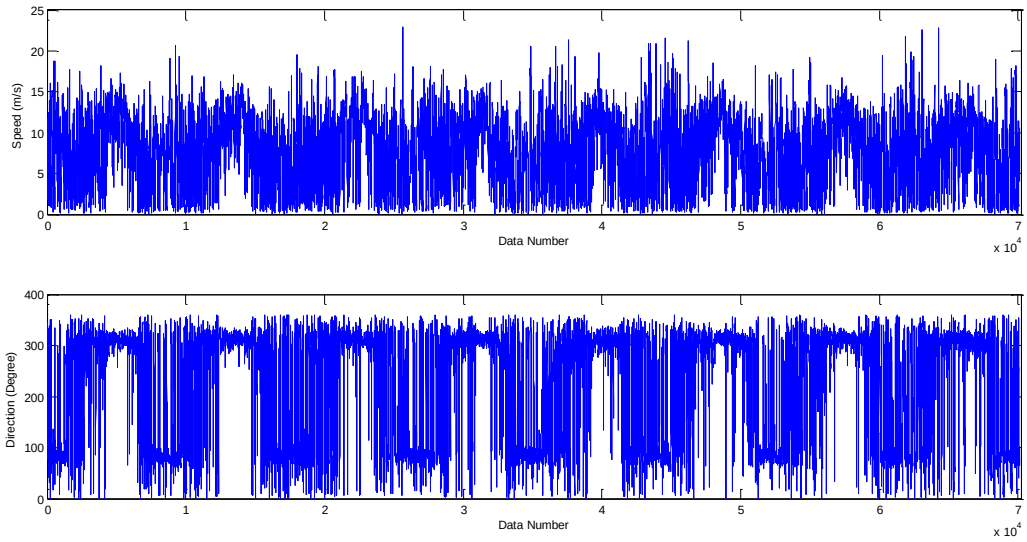

Figure 3-9. The Hourly Speed and Direction Variations of Belen WPP

The algorithm considering the direction while calculating Weibull parameters is applied to the wind speed and direction data of Belen WPP. The comparison between the probability density function of the actual data and Weibull fit is shown in Figure 3-10 and the numerical values are presented in Table 3-1. Although Weibull fit of the data slightly differs between 225 to 285 degrees, the frequencies corresponding to those direction segments are small, so as the overall error. Between 45 to 105, and 285 to 345 degrees, where the frequencies of the wind are higher, the fittings are very accurate.

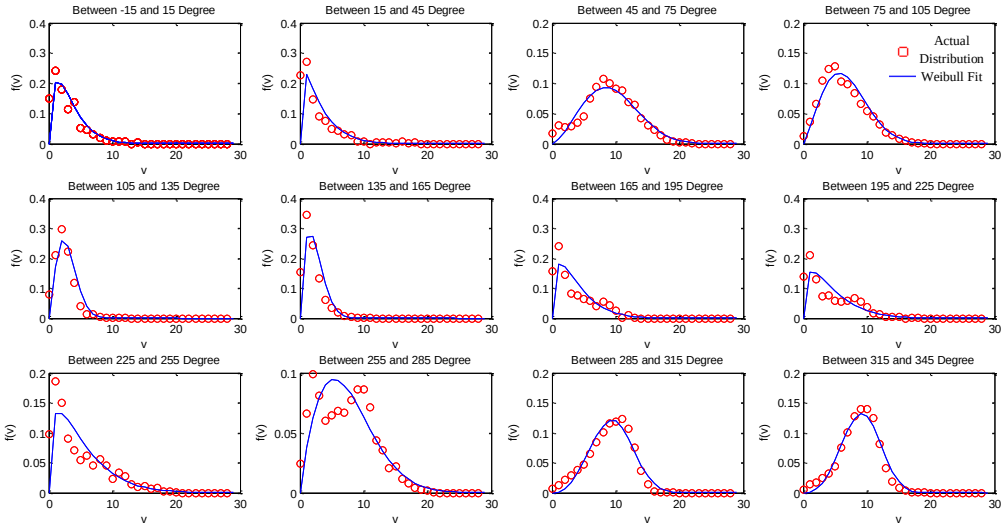

Figure 3-10. Comparison between the PDF of the Actual Distribution and Weibull Fit of the Wind Speed Variations of Belen WPP

Table 3-1. Calculated Weibull Parameters of Belen WPP

Direction Segment (Degrees)	Frequency (%)	Scale Parameter, *a* (m/s)	Shape Parameter, *b*	Mean Speed (m/s)
-15 to 15	0.93	3.54	1.36	3.24
15 to 45	0.68	3.25	1.12	3.12
45 to 75	9.89	10.57	2.44	9.37
75 to 105	17.37	7.66	2.13	6.78
105 to 135	3.34	3.27	1.98	2.90
135 to 175	1.39	2.67	1.64	2.39
165 to 195	1.29	4.08	1.27	3.79
195 to 225	1.37	4.79	1.24	4.47
225 to 255	2.04	5.54	1.24	5.17
255 to 285	7.42	8.49	1.80	7.55
285 to 315	32.61	10.51	3.29	9.43
315 to 345	21.68	10.14	3.49	9.12
			Vmean	8.11

After the satisfactory results, the developed algorithm for Weibull fitting is applied to the all data points in the database and Weibull parameters are calculated for each data point. The deduced Weibull parameters will be used in the wind power density and the capacity factor calculations.

3.2. Calculation of Mean Speed Variations

Before the calculation of the wind power density and the capacity factor, the average wind speed of the data points will be calculated to gain insight about wind patterns in Turkey. The average speed calculation is accomplished annually and seasonally. In order to be correlated with the summer and winter peaks and spring off-peak demands of Turkey, the seasons are defined as follows: Summer: July and August; Spring: April and May; and Winter: December and January. From this point on, this terminology will be used for seasons.

For each data point, the 8 years of hourly wind speed data are read from the database, and the average speeds are calculated annually and seasonally. In Figure 3-11, the histogram of the calculated mean speeds of data points is shown.

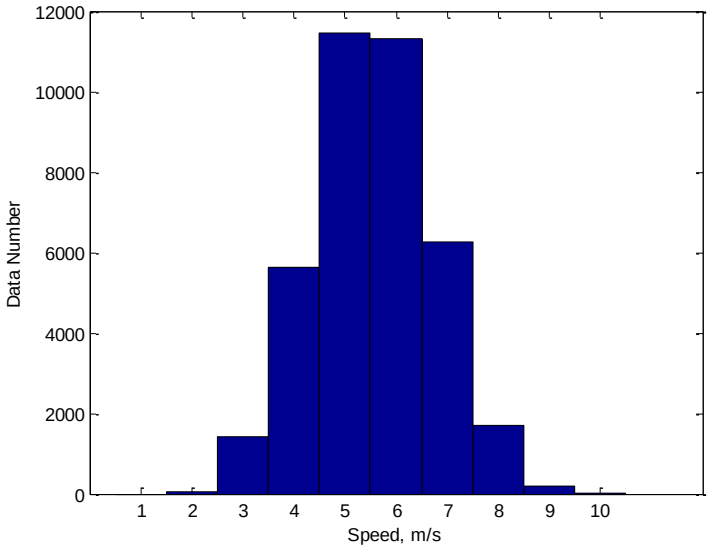

Figure 3-11. Annual Mean Wind Speed Histogram of Turkey

From Figure 3-11, it can be deduced that the average speeds in most of the data points are between 5 and 7 m/s and the mean of the average annual speeds of the data points is calculated as 5.55 m/s. Similarly, seasonal histograms of the data points are calculated and the results are presented in Figure 3-12.

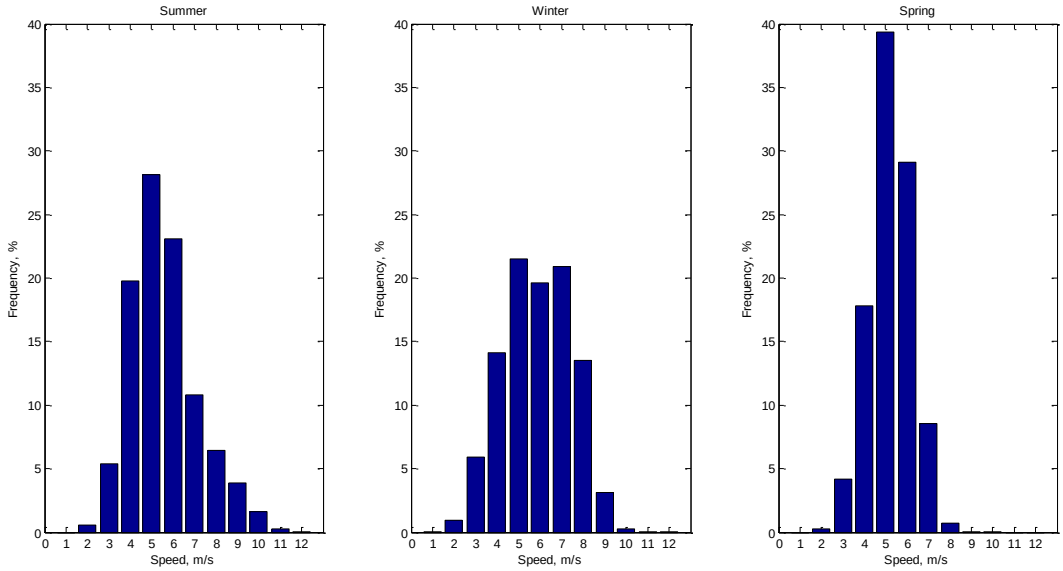

Figure 3-12. Seasonal Mean Speed Histograms of Turkey

From the seasonal plots, one can deduce that, every season the wind patterns are different. In summer, although the frequencies of weak wind speeds are high; there are also strong wind contributions. In winter, the wind is more stable, the frequencies of wind are high between the speeds 5 and 8 m/s. In spring, the wind is weakest. Approximately 60 % of the data points have average wind speed smaller than 6 m/s, which is not favorable for wind power generation. Therefore, in the later analyses where the power densities of wind and capacity factors of the wind power plants are calculated, the spring season is expected to have the lowest values.

3.2.1. Importance of Location

The histogram plots give insight about the general wind characteristic in Turkey; however, the information lacks the whereabouts of the corresponding data point. In other words, the exact location on earth where the speed information belongs to should also be presented. From now on, the necessary map transformation will be applied to the locations of the data points and the results will be visualized on a geographical map.

In the database, the data points are defined by their latitude and longitude values which are not easy to follow. As a result, the outcomes should be visualized by a map for ease and further purposes. A map can be defined as a visual representation of an area. Therefore, the first step before starting the analyses is to prepare the necessary maps.

A map is an image and images can be represented and stored by matrices according to their indices. However, in order to represent and store the results in a matrix, necessary map transformation must be accomplished. A map projection is a systematic transformation of the latitudes and the longitudes of the locations on the surface of a sphere or an ellipsoid into locations on a plane [41]. There are numerous map projections which serves different kind of purposes [42]. In this study, the purpose of visualizing the results in a map is to easily relate the data points with their locations in Turkey. Therefore, Plate Carrée, an easy equidistant transformation is chosen.

3.2.2. Equidistant Map Projection

In equidistant projection, also known as geographical projection, the degrees are converted into X/Y coordinates, pretending the earth is a flat rectangle [42]. The reason to choose this transformation is that it has the obvious advantage of being geometrically simple. However, it is not an accurate representation of the earth. Plate

Carrée, meaning square plane, pretends each 1°x1° segment is a square. The further moved from the equator, the more distortion is present in the shape of the earth.

In particular, Plate Carrée Transformation has become a de facto standard for global raster datasets, such as Celestia and NASA World Wind [43] - [44], because of the particularly simple relationship between the position of an image pixel on the map and its corresponding geographic location on Earth.

The equidistant projection maps meridians to vertical straight lines of constant spacing, and circles of latitude to horizontal straight lines of constant spacing:

$$X = \mu \cos \gamma_1 \tag{3-6}$$

$$Y = \gamma \tag{3-7}$$

where,

μ is the longitude,

γ_1 is the standard parallel where the scale of the projection is correct,

γ is the lattitude,

X is the horizontal position along the transformed map,

Y is the vertical position along the transformed map.

Plate Carrée is the special case of equidistant transformation (Equation (3-6)) where γ_1 is zero. This projection maps X with the value of the longitude and Y with the value of the latitude:

$$X = \mu \tag{3-8}$$

$$Y = \gamma \tag{3-9}$$

X and Y values are directly related with the distances between latitudes and longitudes. The distances between the latitudes are nearly the same (around 111.2

km). However, the length of a degree of longitude depends on the position of the point. The length of a degree of a longitude can be approximated as [45]:

$$\text{Length of a degree of longitude} = \cos\gamma * 111.325 \text{ (km)} \quad (3\text{-}10)$$

This equation is directly related with $\cos\gamma$ factor in equidistant map projection formula (Equation (3-6)) and that's why the projection is named as equidistant.

The data points in the database are approximately 6 kilometers apart from each other. As a result, in the transformed map, a pixel value should map a 6 km x 6 km area. The length of a degree of latitude does not change; therefore; the scaling factor for *Y* points to a degree of latitude can be taken approximately $\frac{6\ km}{111.2\ km}$ and the scaling factor for *Y* values is chosen as 0.053695.

As shown in Equation (3-10) the length of a degree of a longitude depends on the latitude. Therefore, the length of degree of a longitude in Turkey differs depending on the location. Turkey lies between 36° - 42° latitude and 26° - 45° longitude. In the southern point of Turkey at 36°, the length of a degree of a longitude is approximately $111.325 * cos\ 36° \cong 90.06$ kilometers; whereas, in the northern, at 42°, the length of a degree of a longitude is approximately $111.325 * cos\ 42° \cong 82.73$ kilometers making the maximum error in equidistant mapping $\frac{90.06 - 82.73}{90.06} * 100\ \% \cong 8\ \%$ which is acceptable for this study; since, the aim is to visualize the whereabouts of the data point. From the results of these calculations, the scaling factor for *X* to a degree of a longitude is chosen as 0.065798 and a pixel value is made to represent a 6 km x 6 km area.

Other than the scaling factors for the *X* and *Y* values, the latitude and longitude values for the first pixel value should be defined for the transformation. For the latitude, 42.3° and for longitude 25.1° is chosen for the first pixel. The other values are found by linearly scaling using the equation of the transformation. The final

equations of transformation are shown in Equations (3-11) and (3-12) and the transformation is summarized in Figure 3-13.

$$X - 1 = (\mu - 25.1°)\,\frac{1}{0.065798} \tag{3-11}$$

$$Y - 1 = (42.3° - \gamma)\,\frac{1}{0.053695} \tag{3-12}$$

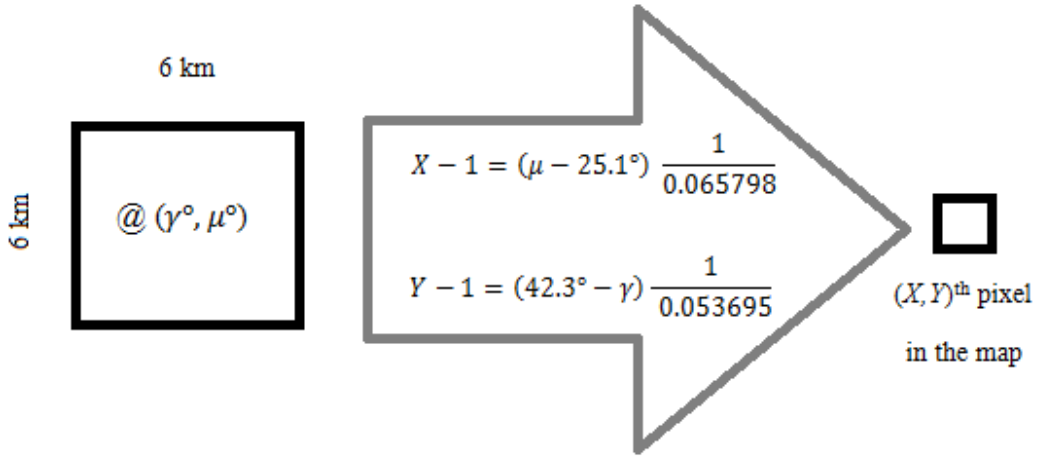

Figure 3-13. The Summary of the Map Transformation

3.2.3. Variation of Mean Speeds on Equidistant Map

In Figure 3-14, the variation of annual wind speed averages of the data points are re-drawn, this time using the geographical coordinate information of the data points and map transformation. As expected, the average wind speeds are high in western parts of Turkey, in Trakya region and in Hatay region. The results are similar with Turkish Wind Atlas (REPA) prepared by Directorate of Renewable Energy [23]; however, that work does not include the wind patterns, in other words, Weibull distribution of the wind. In addition to that, seasonal behaviors are not included.

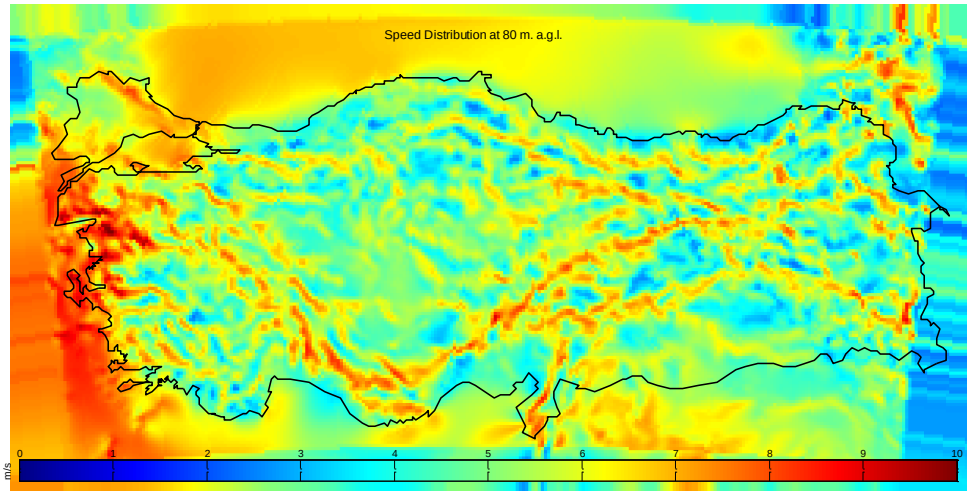

Figure 3-14. Speed Distribution at 80 m. a.g.l. (Annual)

The average speed distributions are also plotted for summer, winter and spring seasons and presented in Figure 3-15, 3-16 and 3-17. In summer, the wind is strong in western areas, near Mersin and Hatay regions of Turkey. Depending on the turbine type, the wind turbines usually start giving their rated power when the wind speed reaches 10 - 12 m/s, meaning that the red areas in the map will likely to have large capacity factors.

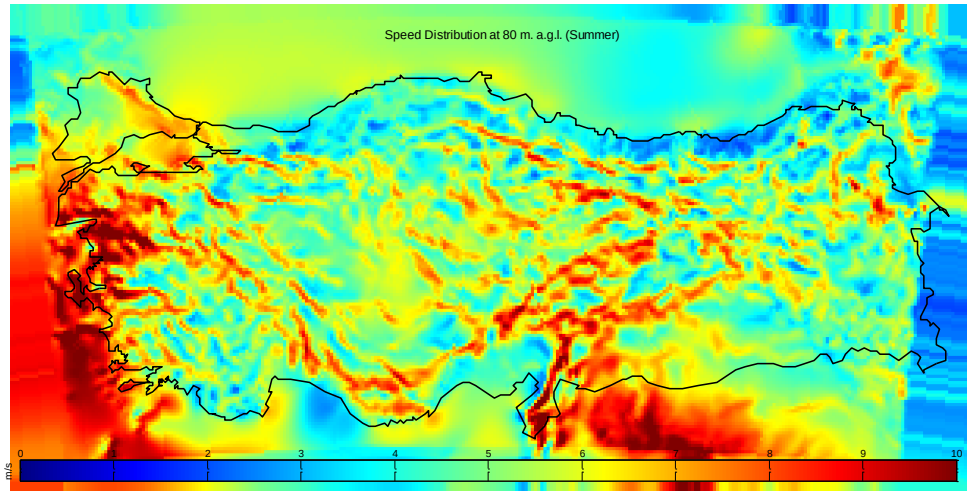

Figure 3-15. Speed Distribution at 80 m. a.g.l. (Summer)

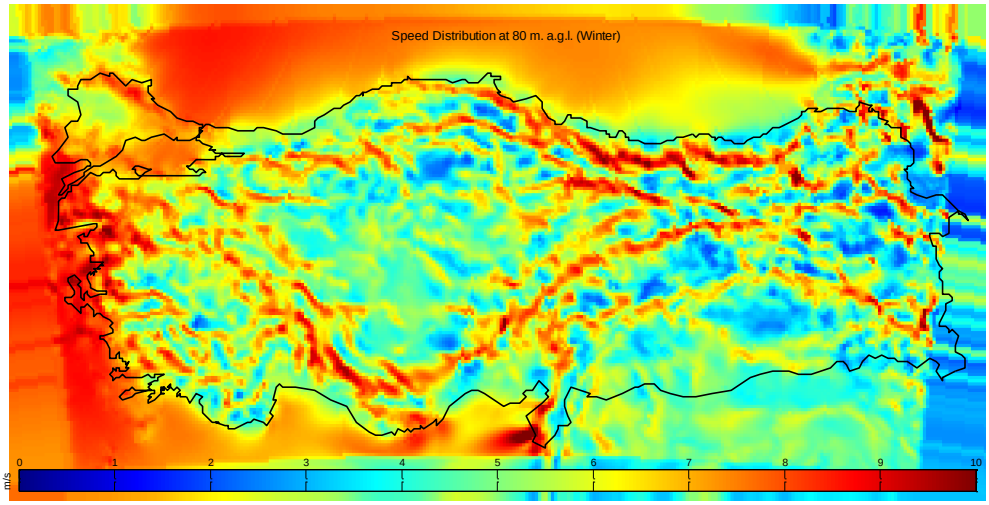

Figure 3-16. Speed Distribution at 80 m. a.g.l. (Winter)

In winter, the average wind speeds are not as high as in summer in western areas; however, wind speeds are still favorable for wind power generation. Hatay, Mersin, Çanakkale, Trakya region and western parts of Turkey are still have high wind speed averages; however, different than the summer season, in winter, considerable strong winds exist in the northern part of Turkey.

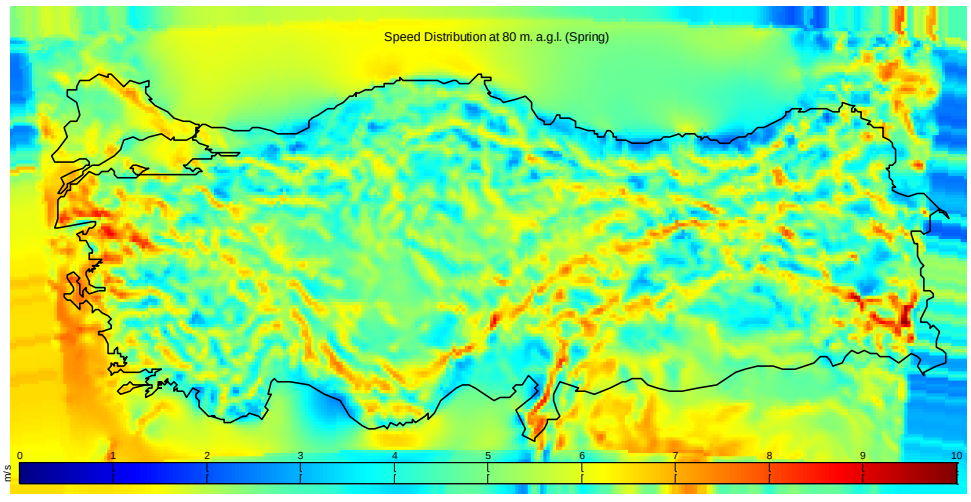

Figure 3-17. Speed Distribution at 80 m. a.g.l. (Spring)

The spring season is the worst season for wind power generation. Usually average wind speeds are lower than 10 m/s, which is not favorable for wind power generation. This will result in lower wind power densities and capacity factors.

As can be followed from the annual and seasonal average speed variation maps, in all three seasons, the wind is favorable in Hatay and Mersin regions in south of Turkey, Izmir, Çanakkale, Balıkesir Region in west of Turkey, which will be the possible places where the investors would like to invest. There is also strong wind in eastern region of Turkey; however, as will be shown in the following chapter, the altitude of some of those places are high and the wind power plants cannot be established after a certain altitude. Therefore, the average wind speed map gives an insight about the favorable places about wind power plants locations; however, it is not sufficient to make investment decisions based on these results only. Then, for next step, the wind power density which is also a gratifying factor to evaluate the wind quality will be calculated.

3.3. Calculation of Wind Power Density Variations

3.3.1. Definition of Power Density in Wind Power Studies

In Chapter 2, it was found that the theoretically available power in the wind can be expressed as:

$$P = ½ \rho A v^3 \quad (3\text{-}13)$$

where,

P = power (W),

ρ = density of air (kg/m^3),

A = Blade sweep area (m^2),

v = wind velocity (m/s).

Wind Power Density (WPD) is defined as the division of power by the cross-sectional area (*A*), then:

$$\text{WPD} = \frac{P}{A} = \frac{1}{2}\,\rho\, v^3 \;\; (\text{W}/m^2) \tag{3-14}$$

It is a calculation relating to the effective force of the wind at a particular location. There are two important points about this expression:

Firstly, the wind power density is proportional to the cube of the wind speed. Therefore, variation of wind speeds directly affects the wind power density. Secondly, by dividing the power by the area, the expression on the right hand side becomes independent of the size of a rotor of wind turbine. In other words, $\frac{P}{A}$ only depends on the density of the air and the wind speed. In fact, there is no dependence on size, efficiency or other characteristics of wind turbines when determining $\frac{P}{A}$. Therefore, $\frac{P}{A}$, in other words wind power density, is a gratifying way to represent the wind characteristics.

3.3.1.1. Need for Air Density Values

In order to calculate the WPD, the wind speed and the air density values are needed for each data point. Wind speed parameters were read from the database and already calculated in the previous section; however, air density values should still be calculated.

Air density can be defined as the mass of a given sample of air, divided by the volume of that sample. At sea level and under standard conditions (temperature of 25 degrees C and pressure of 1 atmosphere), the density of the air is 1.225 kg per m^3 [46]. The database contains the ambient temperature and pressure values of the data points. The air density should be calculated by using these values.

3.3.1.2. Calculation of Air Density Values from Temperature, Pressure and Humidity

The air density of dry air can be calculated from ideal gas law:

$$\rho = \frac{P}{R\,T} \tag{3-15}$$

where,

ρ is the air density (kg/m^3),

P is absolute pressure (Pa),

R is the specific gas constant for dry air (J/(mol*K)),

T is absolute temperature (K).

The air density can be calculated roughly from the ideal gas law, but in the ideal gas law, the effect of humidity is not represented. The air density also depends on the humidity and the average humidity in Turkey is around 60 % (Figure 3-18) which is not negligible [47] - [48].

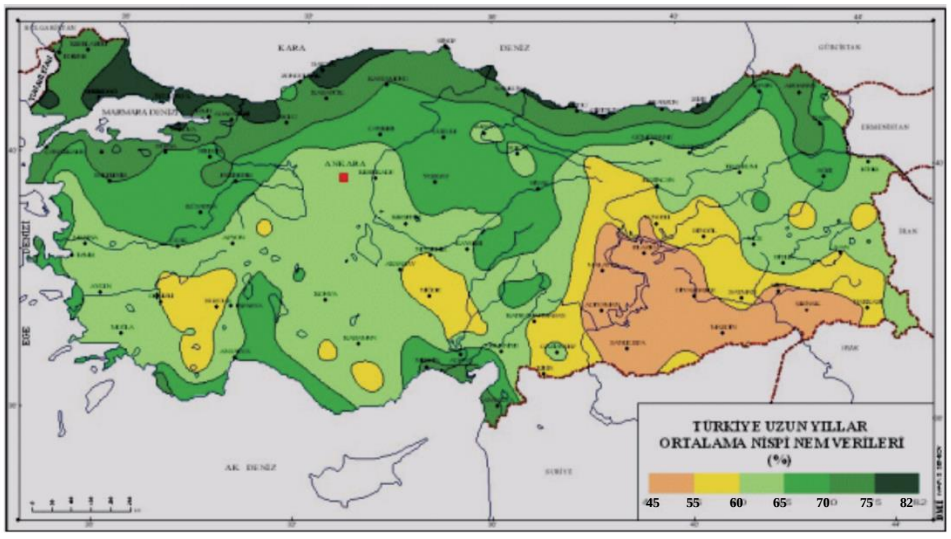

Figure 3-18. Long Term Average Humidity Values in Turkey

From the results of previous section and REPA, it is guessed that wind power integration will be more effective in Çanakkale, Balıkesir, Izmir, Hatay, Mersin, Trakya regions where the humidity levels are above 65 % according to Figure 3-18 which shows the long term average humidity values in Turkey. Therefore, in the calculation of air density, humidity values are taken constant as 67 %.

In order to calculate the air density from pressure, temperature and humidity values, Reference [49] is used and a code that calculates the annual and seasonal air density averages is constructed in Matlab environment. The developed algorithm reads the pressure and temperature values of data points and calculates the average air density values according to Reference [49] annually and seasonally. The methodology will be described below and the flowchart of the algorithm is given in Figure 3-19.

Firstly, the saturation vapor pressure (*psv*) in ambient pressure is calculated as in Equation (3-16) using the average temperature value of the data point:

$$psv = e^{A\,T^2 + B\,T + C + \frac{D}{T}} \quad \text{(Pa)} \tag{3-16}$$

where,

T = Ambient temperature in Kelvin,

A, B, C, D are constants whose values are given as:

$A = 1.2378847 * 10^{-5}$ (K^{-2})

$B = -1.9121316 * 10^{-2}$ (K^{-1})

$C = 33.93711047$

$D = -6.3431645 * 10^{3}$ (K)

Then, calculation of the enhancement factor (*ftp*) at ambient temperature and pressure is taken place according to Equation (3-17) using the temperature and pressure values of the data point:

$$fpt = 1.00062 + (3.14 * 10^{-8})\,P + (5.6 * 10^{-7}) * (t^2) \quad (3\text{-}17)$$

where,

P = ambient pressure (Pa)

t = ambient temperature (C°)

Calculation of the mole fraction of water vapour (xv) is the next step using the decided value of humidity:

$$xv = hr * fpt * psv * (\frac{1}{P}) * (10^{-2}) \quad (3\text{-}18)$$

where,

hr = relative humidity (%).

As the next step, the compressibility factor of the air (Z) is calculated using Equation (3-19):

$$Z = 1 - ((\frac{P}{T}) * (a_0 + a_1 * t + a_2 * t^2 + (b_0 + b_1 * t) * xv + (c_0 + c_1 * t) * (xv^2))) + ((\frac{P^2}{T^2}) * (d + e * (xv^2))) \quad (3\text{-}19)$$

where the values of the constants are given as:

a_0 = 1.58123 * 10^{-6} (K/Pa)

a_1 = -2.9331 * 10^{-8} (1/Pa)

a_2 = 1.1043 * 10^{-10} (1/(K*Pa))

b_0 = 5.707 * 10^{-6} (K/Pa)

b_1 = -2.051 * 10^{-8} (1/Pa)

c_0 = 1.9898 * 10^{-4} (K/Pa)

c_1 = -2.376 * 10^{-6} (1/Pa)

d = 1.83 * 10^{-11} (K^2/Pa^2)

e = -0.765 * 10^{-8} (K^2/Pa^2)

Lastly, using the results of above calculations, the average air density ρ (kg/m^3) is calculated annually and seasonally.

$$\rho = \left(P \frac{Ma}{(Z\ R\ T)} \right) * \left(1 - xv * \left(1 - \frac{Mv}{Ma} \right)\right) \quad (3\text{-}20)$$

where,

R = 8.314510 (Molar ideal gas constant (J/(mol*K))),

Mv = 18.015 * 10^{-3} (Molar mass of water vapor (molecular weight of water) (kg/mol)),

Ma = 28.9635 * 10^{-3} (Molar mass of dry air (kg/mol)).

The flowchart of the work accomplished to calculate the air density values is shown in Figure 3-19.

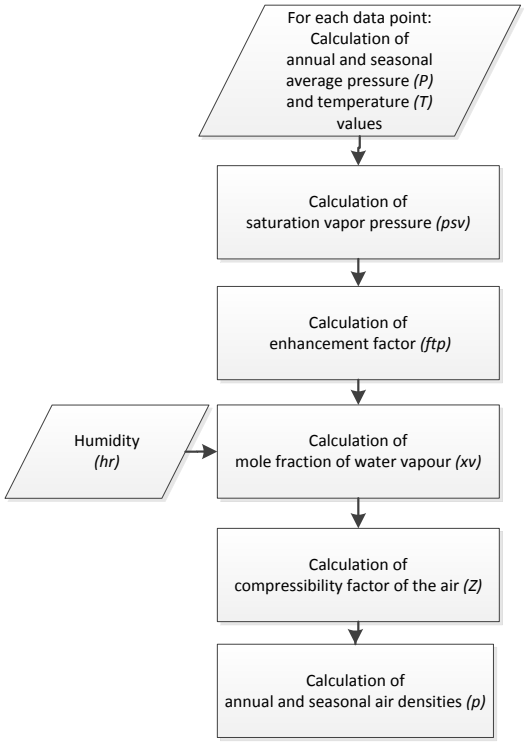

Figure 3-19. Flowchart of the Calculation of the Air Density

In this thesis, only the result of annual average air density variation will be given; since, the seasonal air density calculations follow the same methodology. For annual average air density calculations; the humidity (Figure 3-18), the temperature (Figure 3-20) and the pressure (Figure 3-21) variations from the database are used as inputs, and by the explained methodology in Figure 3-19, the annual average air density values are calculated for each data point.

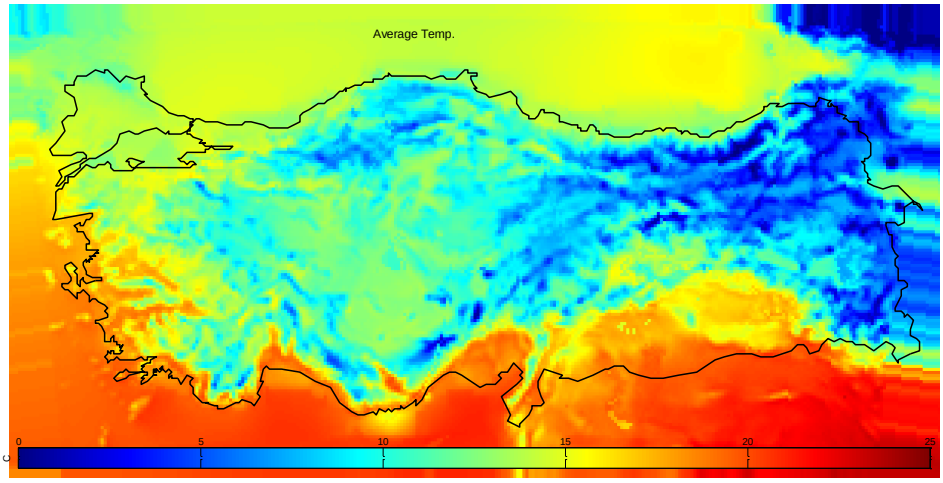

Figure 3-20. Average Temperature Variations (Annual)

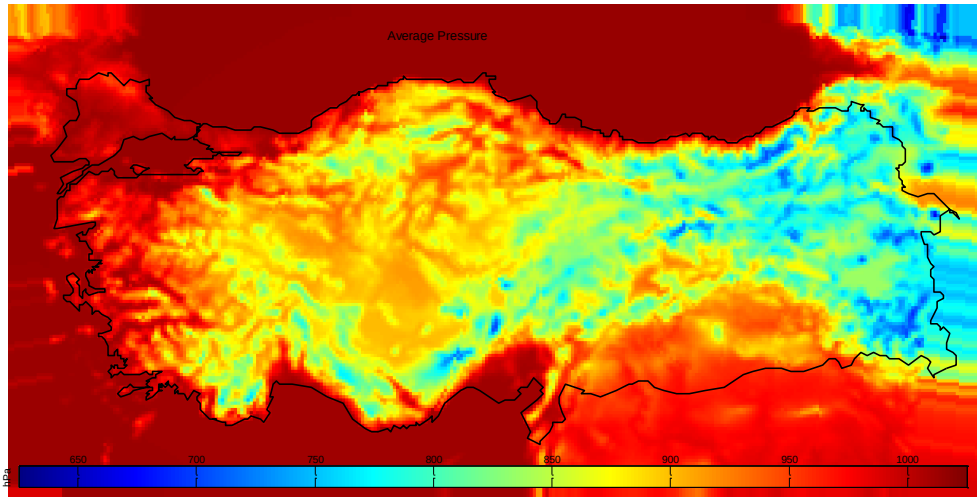

Figure 3-21. Average Pressure Variations (Annual)

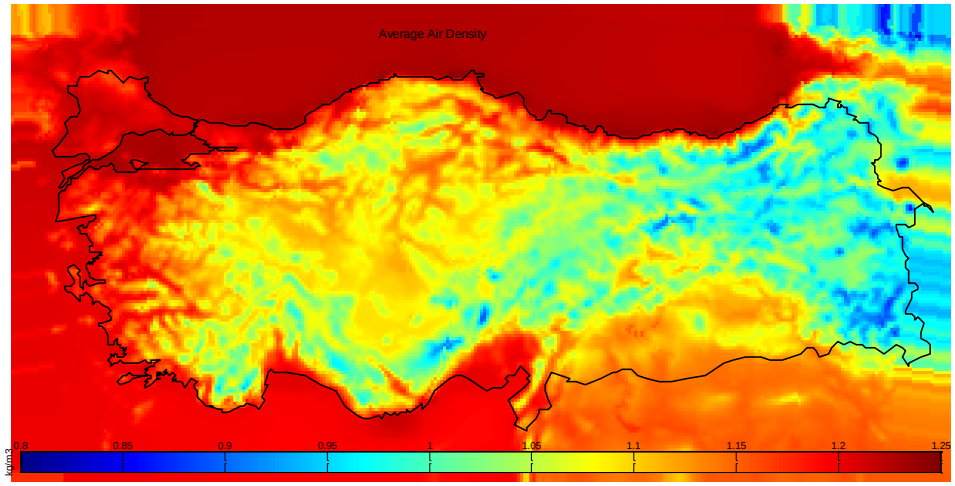

Figure 3-22. Average Air Density Variations (Annual)

As expected, the temperature values are higher at the southern regions and the sea coasts of Turkey, and the temperature values are lowest at the east of Turkey. Similarly, pressure values are higher in sea coasts of Turkey. The calculated annual average air density values are shown in Figure 3-22. The air density are related with the pressure and inversely related with the temperature. The calculated air density values are higher on the sea coasts and lower in east of Turkey.

3.3.2. Calculation of Wind Power Density from Weibull Parameters

After calculation of air densities, the definition in Equation (3-13) can be used to calculate the wind power density. The wind power density is related with the cube of the wind speed; then, the random variable in the definition is the cube of wind speed v^3. Therefore, the mean of the wind power densities can be defined as:

$$\left(\frac{P}{A}\right)_{mean} = ½\ \rho\ (v^3)_{mean} \quad (\mathrm{W/m^2}) \tag{3-21}$$

Since, the probability density function is known for wind speed v, from the expected value theorem [50], the mean of the cube of the wind speed can be determined:

$$(v^3)_{mean} = \int_0^{\infty} v^3 \; f_v(v) \; dv \tag{3-22}$$

where,

$f_v(v) = \; b \; a^{-b} \; v^{b-1} \; e^{(-v/a)^b}$, is Weibull probability density function of the wind speed.

Inserting the definition of Weibull probability density function to Equation (3-22), it becomes:

$$(v^3)_{mean} = \int_0^{\infty} v^3 \; b \; a^{-b} \; v^{b-1} \; e^{(-v/a)^b} \; dv \tag{3-23}$$

Introducing Equation (3-23) to the definition of wind power density (3-21); Equation (3-24) is obtained:

$$\left(\frac{P}{A}\right)_{mean} = \frac{1}{2} \; \rho \; \int_0^{\infty} v^3 \; b \; a^{-b} \; v^{b-1} \; e^{(-v/a)^b} \; dv \tag{3-24}$$

In order to simplify Equation (3-24), change of variables will be used and a new variable *t*, and its derivative *dt* are defined:

$$t = \left(\frac{v}{a}\right)^b \tag{3-25}$$

$$dt = b \; \frac{v}{a^b}^{\,b-1} \; dv \tag{3-26}$$

Lastly, using the definition of the new variable and its derivative, Equation (3-24) is re-written in terms of new variable and simplified.

$$\left(\frac{P}{A}\right)_{mean} = \frac{1}{2} \; \rho \; \int_0^{\infty} (a \; t^{\frac{1}{b}})^3 \; b \; a^{-b} \; (a \; t^{\frac{1}{b}})^{b-1} \; e^{\left(-a \; t^{\frac{1}{b}}/a\right)^b} \; a \; \frac{1}{b} \; t^{\frac{1}{b}-1} \; dt$$

$$\left(\frac{P}{A}\right)_{mean} = \frac{1}{2}\ \rho\ \int_0^{\infty} a^3\ t^{\frac{3}{b}}\ b\ a^{-b}\ a^{b-1}\ t^{\frac{b-1}{b}}\ e^{-t}\ a\ \frac{1}{b}\ t^{\frac{1-b}{b}}\ dt$$

$$\left(\frac{P}{A}\right)_{mean} = \frac{1}{2}\ \rho\ \int_0^{\infty} a^3\ \ e^{-t}\ t^{\frac{3}{b}}\ dt \tag{3-27}$$

Equation (3-27) can further be simplified using the definition of the gamma function $\mathrm{r}(z)$ [51]. The gamma function is defined in Equation (3-28).

$$\mathrm{r}(z)\ =\ \int_0^{\infty} e^{-t}\ t^{z-1}\ dt \tag{3-28}$$

When z = $1 + \frac{3}{b}$, Equation (3-28) becomes:

$$\mathrm{r}(1 + \tfrac{3}{b}) = \int_0^{\infty} e^{-t}\ \ t^{\frac{3}{b}}\ dt \tag{3-29}$$

By introducing Equation (3-29) to Equation (3-27), the final equation of wind power density is obtained:

$$\left(\frac{P}{A}\right)_{mean} = \frac{1}{2}\ \rho\ \ a^3\ \mathrm{r}(1 + \tfrac{3}{b}) \tag{3-30}$$

where,

a is the scale parameter (m/s),

b is the shape parameter of the corresponding Weibull probability density function of wind speed,

ρ is the air density of the point where the wind speed data are taken (kg/m^3),

$\mathrm{r}(.)$ is the gamma function.

Weibull parameters of the wind speeds of each direction segment and the air density averages of the data point are already calculated in the previous sections. Therefore, Equation (3-30) can be used to calculate the wind power density of each direction

segment of the data point. Then, the average wind power density of the data point is calculated using the frequency and wind power density of each direction segment:

$$WPD = \frac{1}{100} \sum_{i=1}^{12} WPD(i)\, Fr(i) \tag{3-31}$$

where,

i represents the direction segment (30°),

$WPD(i)$ is the wind power density of the i^{th} segment calculated from Equation (3-30),

$Fr(i)$ is the frequency of the i^{th} segment (in %).

The flowchart of the designed algorithm to calculate average wind power density of the data points is shown in Figure 3-23.

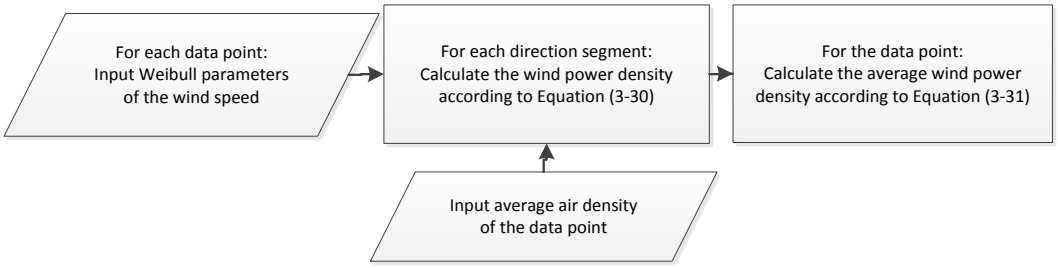

Figure 3-23. Flowchart of the Calculation of Wind Power Density

3.3.3. Variation of the Wind Power Densities on Equidistant Map

Using the developed algorithm in Figure 3-23 for the calculation of the average wind power density values, the annual variations are calculated and shown in Figure 3-24.

As expected, the wind power density has similar properties with the speed variation map (Figure 3-14). The wind power densities are highest and vary between 900 and 1250 W/m^2 in Çanakkale, Balıkesir and Izmir regions. There are also high wind power density values in north of Antalya and Hatay regions. In north of Trakya region, the wind power density values vary between 300 and 500 W/m^2.

The mean wind power densities are also calculated for summer, winter and spring seasons. In the speed variation maps, the average speeds are found to be high in summer and winter periods; therefore, in these seasons, the wind power densities are also expected to be high. From Figure 3-25, which shows the wind power density distributions in summer season, it can be seen that in Balıkesir, Çanakkale, Izmir and Hatay regions, there are locations where wind power densities are higher than 1500 W/m^2.

In winter, the air density values are found to be the highest; therefore, they make a positive contribution to the wind power density values. Figure 3-26 shows the wind power density variation in winter season. It can be seen that, in addition to the locations which have large wind power density values in summer season, there are high wind power densities in Trakya and Mersin Regions and north of Turkey in winter season.

In spring, the speed distribution of the wind was found to be lowest; therefore, it is expected to have low wind power densities. In Figure 3-27, the wind power density variation of spring season is shown. It is seen that, only in a few locations, the wind power densities reach values larger than 500 W/m^2. As seen from the seasonal maps, the wind power density distribution varies significantly from season to season which shows the importance of presenting the seasonal results.

Besides the average speed and the wind power density distribution of the area, the capacity factor of the probable wind power plant is a parameter that indicates economically feasible areas for a wind power plant establishment by the investor. As

a result, in the following section, the capacity factors of the probable investments will be calculated and the capacity factor variation maps will be presented.

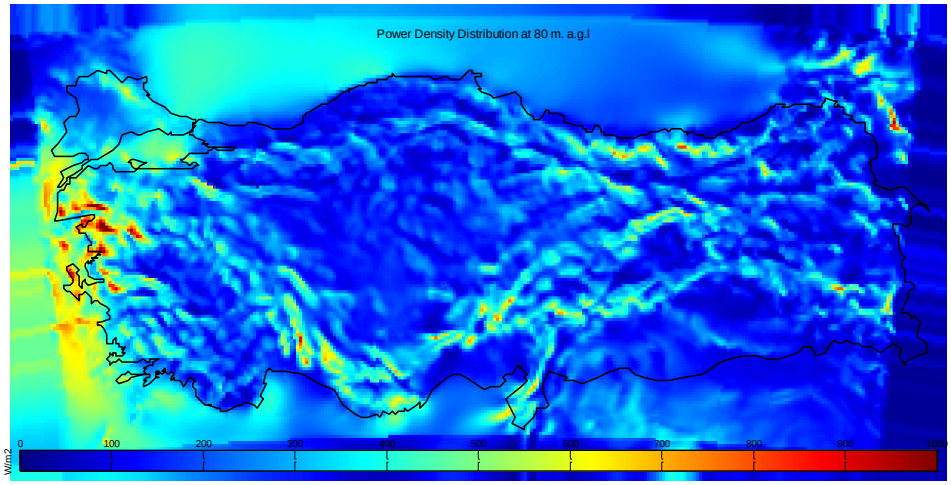

Figure 3-24. Wind Power Density Variation at 80 m. a.g.l. (Annual)

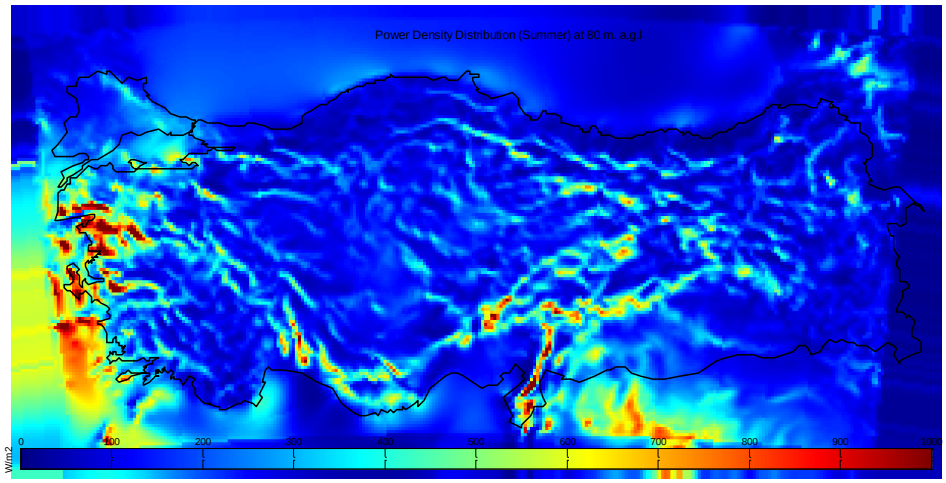

Figure 3-25. Wind Power Density Variation at 80 m. a.g.l. (Summer)

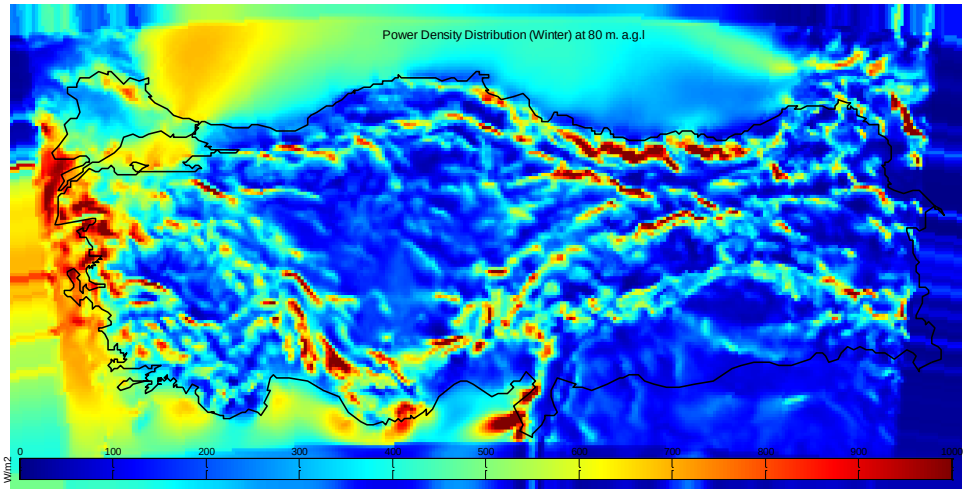

Figure 3-26. Wind Power Density Variation at 80 m. a.g.l. (Winter)

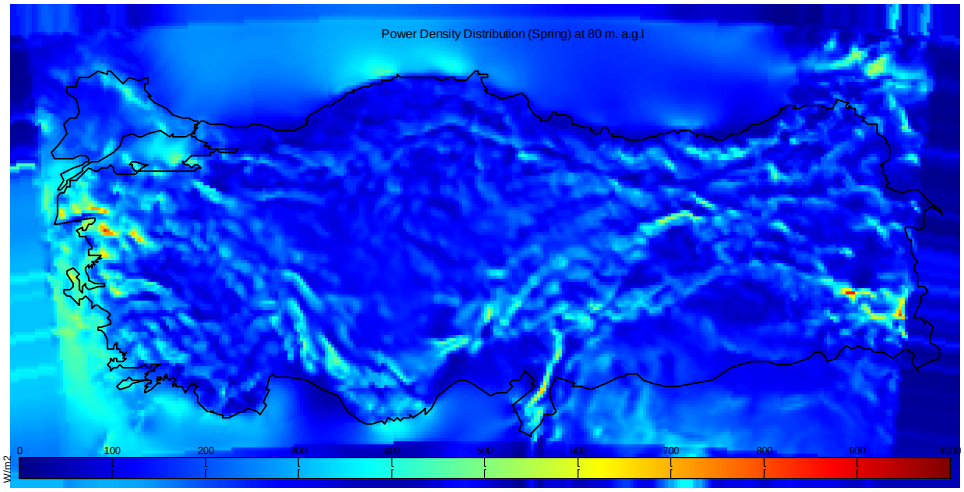

Figure 3-27. Wind Power Density Variation at 80 m. a.g.l. (Spring)

3.4. Calculation of Capacity Factor Variations

The capacity factor of a power plant is the ratio of its actual output over a period of time, to its potential output if it were possible for it to operate at full nameplate capacity indefinitely [16]. To calculate the capacity factor (CF), the total amount of

energy the plant produced during a period of time is divided by the amount of energy the plant would have produced at full capacity:

$$CF = \frac{Generation}{(Installed\ Capacity * Number\ of\ Operating\ Hours)} * 100\% \quad (3\text{-}32)$$

Capacity factor of a wind power plant generally can vary between 20 – 40 % [16]. It can be less; however, in that case, it will not be feasible to establish a power plant due to economic reasons.

3.4.1. Importance of Turbine Selection

In order to derive the capacity factor, the power generation must be calculated. Therefore, the turbine of the wind power plant must be selected. In wind power plants, the wind turbine selection should be accomplished after careful investigation of the location of the power plant; therefore, all investors should conduct measurements on the site. Indeed, the wind speed measurement for one year is a must in order to apply for a wind power plant generation license in Turkey [52]. According to the result of these measurements, the most appropriate turbine must be selected.

The International Electro-Technical Commission (IEC) creates and publishes standards for wind turbines among other electrical and electronics equipment. In those standards, turbine classes are determined by three parameters: The average wind speed, the extreme 50 year gust and the turbulence [53]. Classification from the extreme 50 year gust and the turbulence is beyond the scope of this work. In previous section, the average wind speed variation is calculated; therefore, this parameter will be used for the wind class definition. In Table 3-2, the IEC definition of the wind turbine class according to the wind speed is shown.

Vestas wind turbines are widely used in WPPs of Turkey [24] and the datasheets of the wind turbines can be easily found online. Therefore, in this study, the power

curves of Vestas V90 wind turbines will be used according to recommended wind classes. For Class 1 V 90-3MW, for Class 2 V90-1.8 MW and for Class 3 V90-2 MW turbine will be used according to the user reference in the website [6].

Table 3-2. Definition of the Wind Turbine Class

Wind Turbine Class	I	II	III
v_{ave}: average wind speed at hub-height (m/s)	10.0	8.5	7.5

Figure 3-28 shows the power curves of the selected wind turbines. For all wind turbines, the cut-in speed, after which the turbine starts generating power, is 4 m/s and the cut-off speed, above which the turbine cannot operate normally and stops generating power, is 25 m/s. However, their maximum output power; therefore, the speed at which the turbine reaches the maximum power is different, leading to different capacity factors for each turbine.

As different turbine selection can lead to different capacity factors; while the capacity factors of the wind turbines are calculated, 2 cases will be investigated: In the first case, it will be assumed that the turbine will be selected according to the definition of the IEC (Table 3-2). In the second case, the same wind turbine will be selected regardless of the speed and the calculation of the capacity factor will be repeated. Although the second case will not represent the reality, it can give better realization of wind speed.

When calculating the wind power, the wind power was defined as Equation (3-33):

$$P_{wind} = \frac{1}{2} \rho \, A \, v^3 * C_p \tag{3-33}$$

where,

ρ (kg/m^3) is the air density.

From Equation (3-33), it can be followed that, the power in the wind depends on the wind speed and the air density. Therefore, the power curves of the wind turbines must also be dependent on the air density. The wind turbine manufactures also supply the power curves of the wind turbines for different air densities. In Figure 3-29, the variations of the power curve for different air densities are shown. As can be seen, the output power, so the capacity factor of the wind turbine, increases with the increasing air density. Therefore, the variation of power curves of the wind turbines for different air densities will be taken into account while the capacity factors of the wind power plants are calculated.

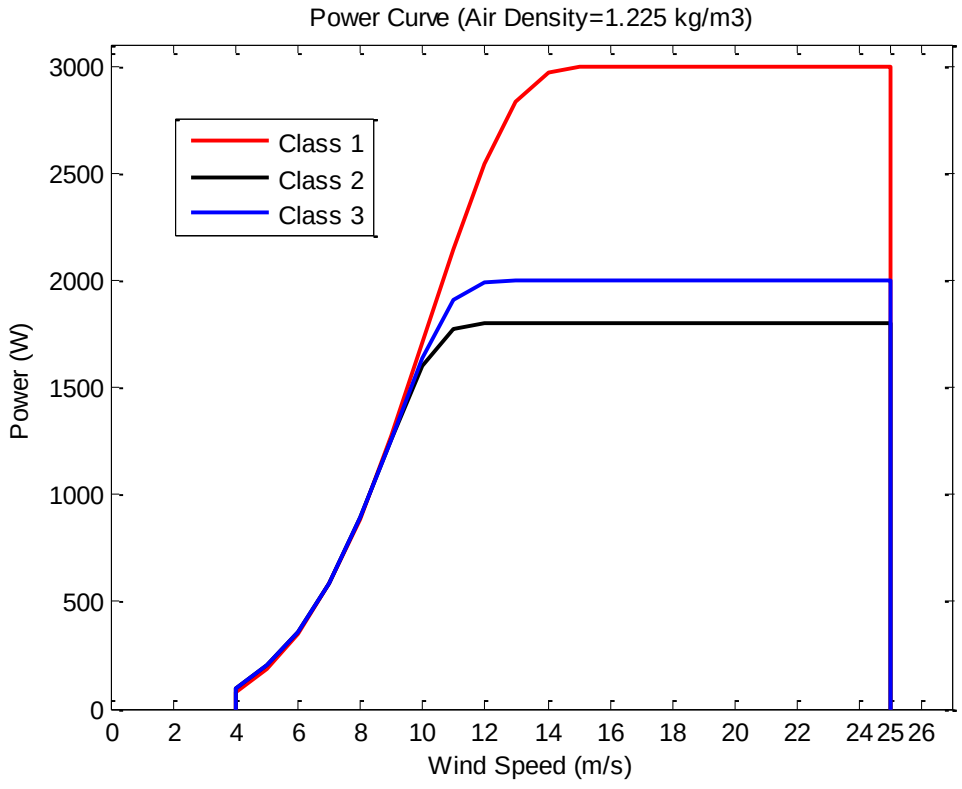

Figure 3-28. Power Curves of the Selected Wind Turbines (Air Density =1.225 kg/m^3)

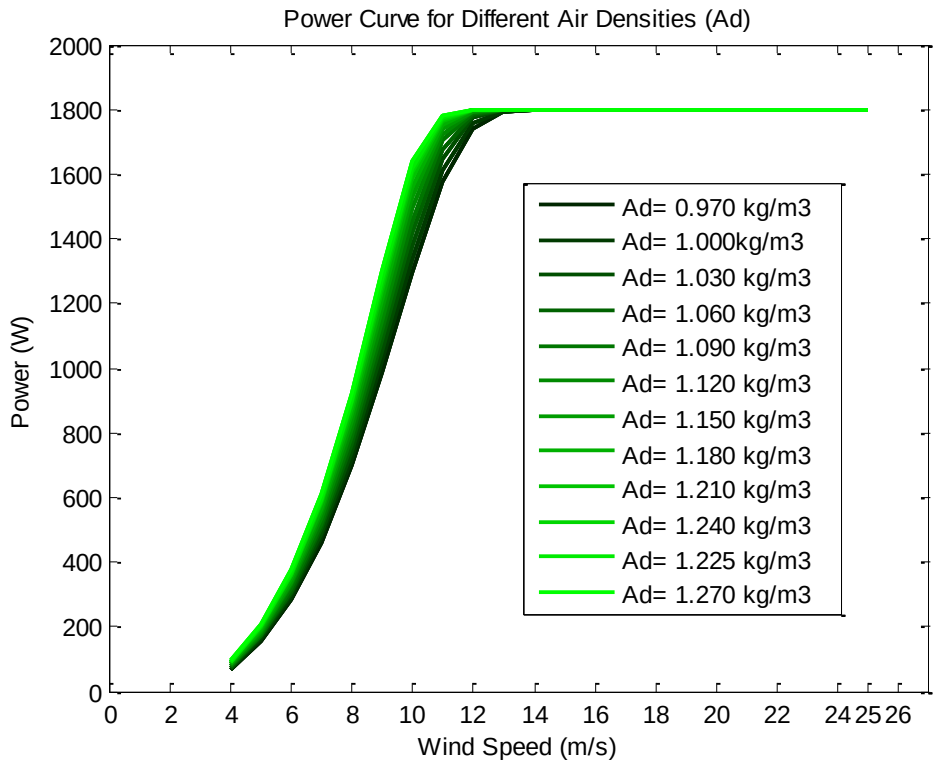

Figure 3-29. Variations of the Power Curve of V90-1.8 MW Turbine for Different Air Densities

3.4.2. Calculation of the Capacity Factor from CDF of the Generated Power

In order to calculate the capacity factor of wind power plant, the duration of working hours and the generated power must be known. Weibull parameters of the wind speed, calculated in previous sections, will be used to calculate the cumulative distribution function of the generated power for each data point. Then, the capacity factors will be calculated using the cumulative distribution function of the generated power.

The cumulative distribution function of wind speed v is defined in Equation (3-34), where the right-hand side represents the probability that the random variable v taking a value less than or equal to V [54].

$$F_v(V) = Probability(v \leq V) \tag{3-34}$$

The CDF of a continuous random variable *v* can also be expressed as the integral of its probability density function, $f_v(v)$, as follows:

$$F_v(V) = \int_{-\infty}^{V} f_v(t)\, dt \tag{3-35}$$

The probability density function parameters of the wind speed for each direction segment were calculated in the previous sections. In addition, the relation between the wind speed and the generated power is also defined by the power curves of the wind turbines. Therefore, the cumulative distribution function of the generated power can be calculated, so that the generation duration curve of the WPP to calculate the capacity factor can be obtained.

The relation between the generated power and the wind speed is defined by the power curve (*PC*) of the wind turbine.

$$p = PC(v) \tag{3-36}$$

where,

p is the generated power (W),

$PC(.)$ is the power curve of the wind turbine,

v is the wind speed (m/s).

Between the cut-in and cut-off speeds, the power curve is linear and one to one; as a result, inverse of the power curve can be taken:

$$v = PC^{-1}(p) \tag{3-37}$$

The cumulative distribution function of generated power is defined as the probability of random variable *p*, being smaller than a certain value *P*:

$$F_p(P) = Probabilty(p \leq P) \tag{3-38}$$

The relation in Equation (3-36) can be used to define the random variable *p*; then, Equation (3-38) becomes:

$$F_p(P) = Probabilty(PC(v) \leq P) \tag{3-39}$$

According to Equation (3-37), $PC(v) \leq P$ can also be expressed as $v \leq PC^{-1}(P)$; then, the expression (3-39) becomes:

$$F_p(P) = Probabilty(v \leq PC^{-1}(P)) \tag{3-40}$$

The right hand side of Equation (3-40) also defines the CDF of the random variable *v* according to Equation (3-34).

$$F_p(P) = F_v(PC^{-1}(P))$$

$$F_p(P) = F_v(V) \tag{3-41}$$

where,

$P = PC(V)$ between cut-in speed $\leq V \leq$ cut-off speed.

For the speeds outside the cut-in speed and the cut-off speed, the wind turbine does not work; therefore, the generated power is zero. Then, probability of generated power to be zero is defined as the sum of probability of speed being smaller than the cut-in speed and probability of speed being larger than the cut-off speed:

$$F_p(0) = Probability\,(P \leq 0) = Probability\,(P = 0)$$

$$F_p(0) = Probability\,(v < cut\text{-}in\ speed) + Probability\,(v > cut\text{-}off\ speed)$$

$$F_p(0) = F_v\,(cut\text{-}in\ speed - \varepsilon) + 1 - F_v(cut\text{-}off\ speed) \quad (3\text{-}42)$$

where,

ε defines a very small positive small number.

In this study, the cut-in speeds of the selected wind turbines are 4 m/s and the cut-off speeds are 25 m/s; then, the cumulative distribution function of generated power will be defined in two parts:

When the speed is smaller than the cut-in speed (4 m/s) or larger than the cut-off speed (25 m/s); the generated power is zero; therefore, the probability of the generated power being zero can be found by adding the probability of each case:

For $P = 0$,

$$CDF_p(0) = CDF_v(4 - \varepsilon) + 1 - CDF_v(25) \quad (3\text{-}43)$$

When the speed is between the cut-in speed (4 m/s) and the cut-off speed (25 m/s), the relation between the generated power and the velocity is one to one. Therefore, the above-mentioned change of variables in Equation (3-41) can be adopted. However, the probability of generated power being zero due higher speeds must be added to the relation:

$For\ P > 0$,

$$CDF_p\,(P) = Probability\,(p \le P)$$

$$CDF_p\,(P) = Probability\,(PC(v) \le P) + 1 - CDF_v(25)$$

$$CDF_p\ (P)\ = Probability\big(v \le PC^{-1}(P)\big) + 1 - CDF_v(25)$$

$$CDF_p(P) = CDF_v(V)\ +\ 1 - CDF_v(25)\ \ where\ P = PC(V) \tag{3-44}$$

From the cumulative distribution function of the generated power, it is easy to find the capacity factor. CDF of the generated power is deduced from annual speed distribution and the power curve of the wind turbine. Therefore, having the probability as 1 corresponds to the total time in the time scale. When the generated power with respect to probability (time) is integrated, the total generation is found. Then, using Equation (3-32), capacity factor can be calculated:

$$Capacity\ factor = \frac{1 - \int_{P=0}^{Pmax} CDF_p(P)}{(Pmax\ *\ 1)} *\ 100\ \% \tag{3-45}$$

Lastly, from the calculated capacity factors for each direction segment, the average capacity factor (CF) of the data point is found by using Equation (3-46).

$$CF\ = \frac{1}{100}\ \sum_{i=1}^{12} CF(i)\ Fr(i) \tag{3-46}$$

where,

i represents the direction segment (30°),

CF(i) is the capacity factor of the i^{th} segment calculated using Equation (3-45),

$Fr(i)$ is the frequency of the i^{th} segment (in %).

The algorithm for the capacity factor calculation is developed in Matlab environment and the flowchart is shown in Figure 3-30.

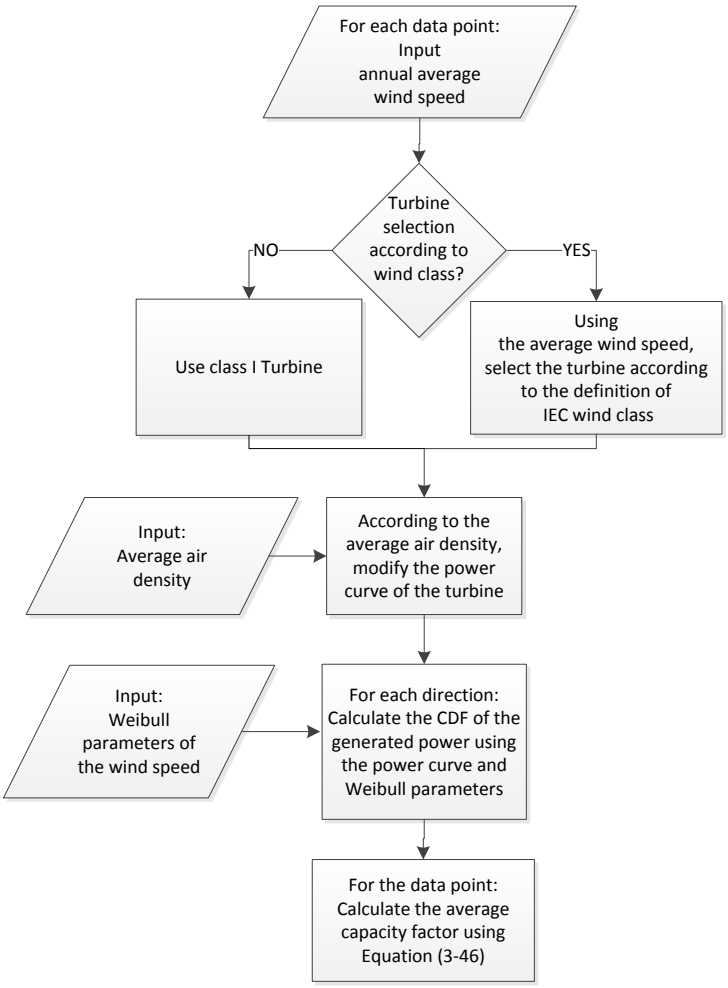

Figure 3-30. Flowchart of the Capacity Factor Calculation

3.4.3. Example Study: Calculation of the Capacity Factor of Belen WPP

In order to demonstrate the developed algorithm for the capacity factor calculation, the average capacity factor of Belen WPP will be calculated. Weibull parameters of the wind speed variation of the data point with latitude and longitude value 36.4731°, 36.2295° (near Belen WPP) were calculated in the previous sections and are presented in Table 3-3. The average wind speed at the specified data location is 8.11 m/s. Then according to Table 3-2, class II wind turbine will be selected.

Table 3-3. Summary Table for Speed and Direction Variation and Weibull Fit Parameters of Belen WPP

Direction Segment (Degree)	Frequency (%)	Scale Parameter *a* (m/s)	Shape Parameter *b*	Mean Speed (m/s)
-15 to 15	0.93	3.54	1.36	3.24
15 to 45	0.68	3.25	1.12	3.12
45 to 75	9.89	10.57	2.44	9.37
75 to 105	17.37	7.66	2.13	6.78
105 to 135	3.34	3.27	1.98	2.90
135 to 175	1.39	2.67	1.64	2.39
165 to 195	1.29	4.08	1.27	3.79
195 to 225	1.37	4.79	1.24	4.47
225 to 255	2.04	5.54	1.24	5.17
255 to 285	7.42	8.49	1.80	7.55
285 to 315	32.61	10.51	3.29	9.43
315 to 345	21.68	10.14	3.49	9.12
			Vmean:	8.11

Using the definition of Weibull probability density function of wind speed ($f_v(v)$) in Equation (3-1), for each direction segment, $f_v(v)$ is calculated for the speeds between 0 and 26 m/s and shown in Figure 3-31.

The cumulative distribution function of each direction, which shows the probability of speed *v* being smaller or equal to a certain value *V*, is also calculated according to Equation (3-5) and shown in Figure 3-32.

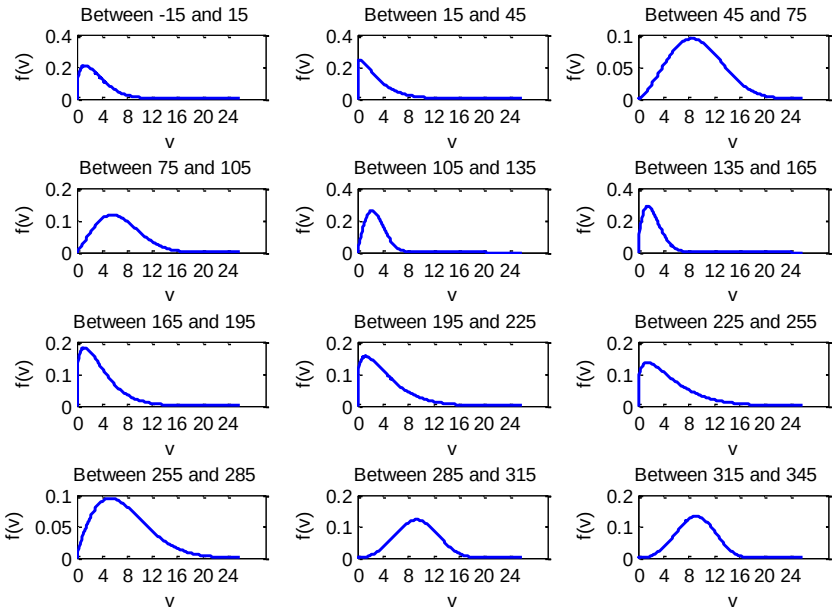

Figure 3-31. Probability Density Functions of the Wind Speed in each Direction Segment of Belen WPP

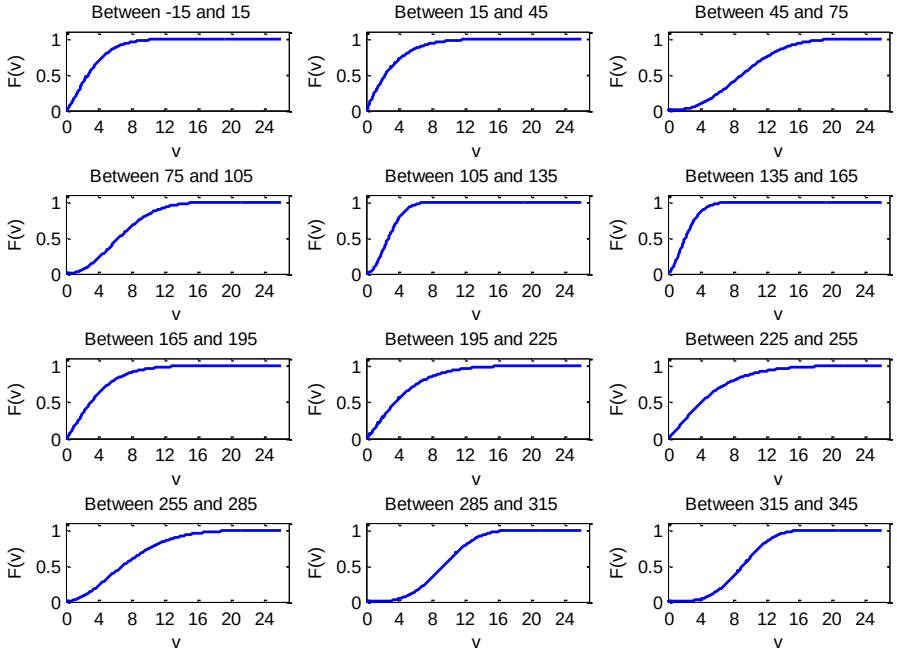

Figure 3-32. Cumulative Distribution Functions of the Wind Speed in each Direction Segment of Belen WPP

The annual average air density of the point is calculated as 1.1243 kg/m^3; then, the power curve of the class II wind turbine at that air density, which will be used to define the $p = PC(v)$ relation, is shown in Figure 3-33.

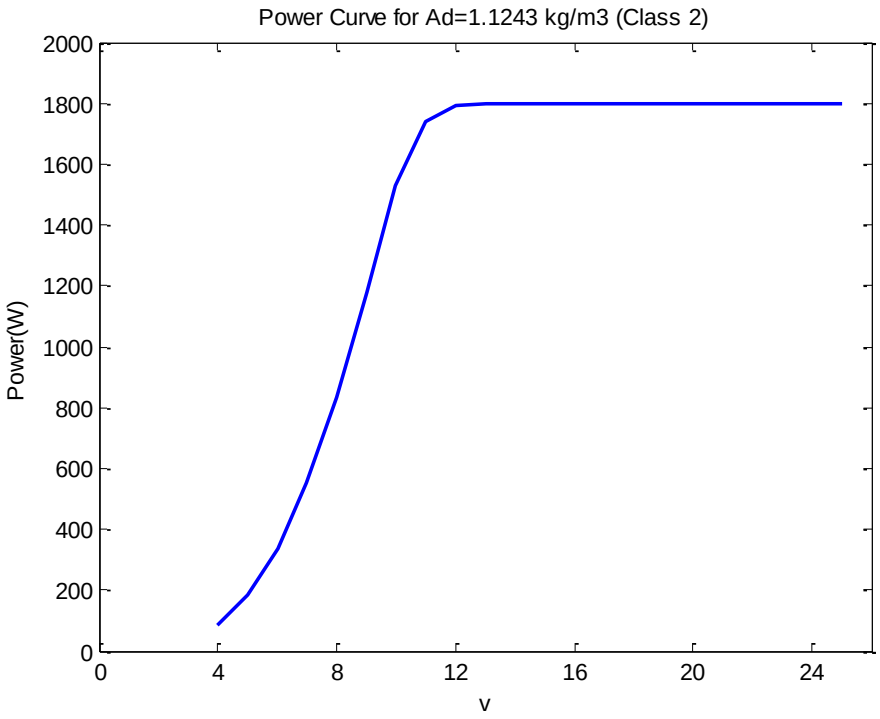

Figure 3-33. Power Curve of the Class II Turbine (Ad=1.1243 kg/m^3)

Using Equations (3-43) and (3-44), the cumulative distribution functions of generated power for each direction segment of Belen WPP are calculated and are shown in Figure 3-34. When the cumulative distribution functions in Figure 3-34 are investigated, the corresponding wind speed variations can also be deduced. For instance, in the 1st, 2nd, 5th and 6th segments, the probabilities of generated power being zero are very close to 1; meaning that, in the wind speed distributions, most of the speed values should be below cut-in speed. When Weibull density functions of the speed segments in Figure 3-31 are investigated; it can be seen, that is the case. In contrast, when the cumulative distribution functions of generated power in the 3rd,

11^{th} and last direction segments are investigated, it is guessed that the speed distributions should yield high wind speeds which are favorable for generation. When Figure 3-31 is investigated, this is actually the case.

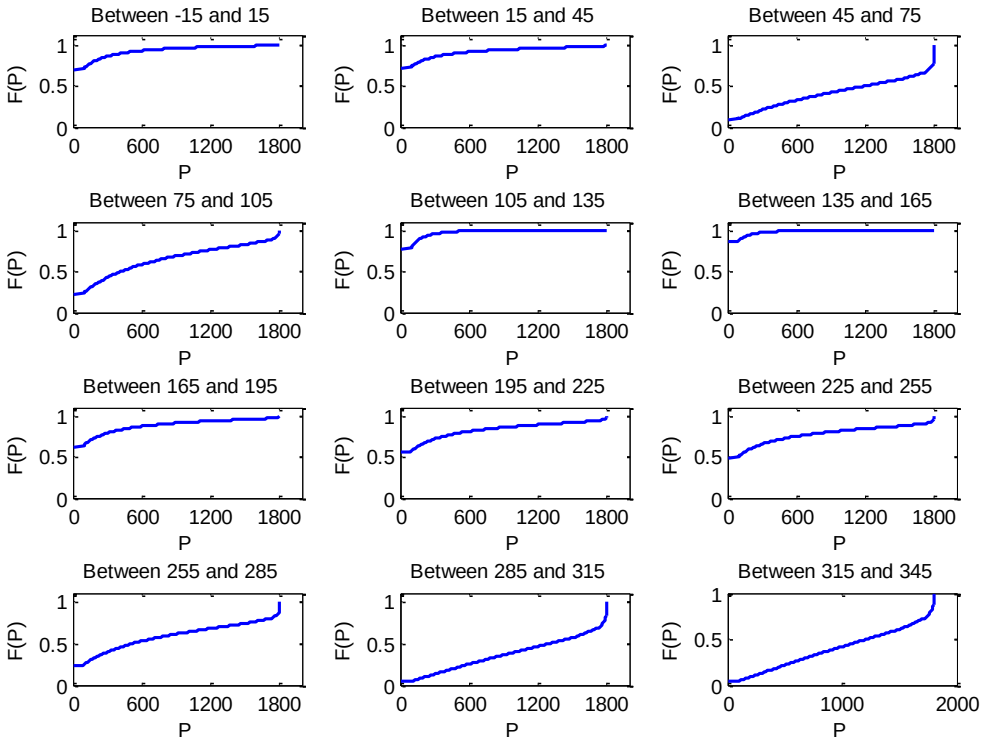

Figure 3-34. Cumulative Distribution Functions of Generated Power of Belen WPP (Class II Turbine)

In Figure 3-35, the generation duration curves of each direction segments are presented. The area under the curves gives the total generation over the time period, and dividing it with the maximum power output of the turbine, 1800 W, will give the capacity factor. The calculated capacity factors according to Equation (3-45) are given in Table 3-4.

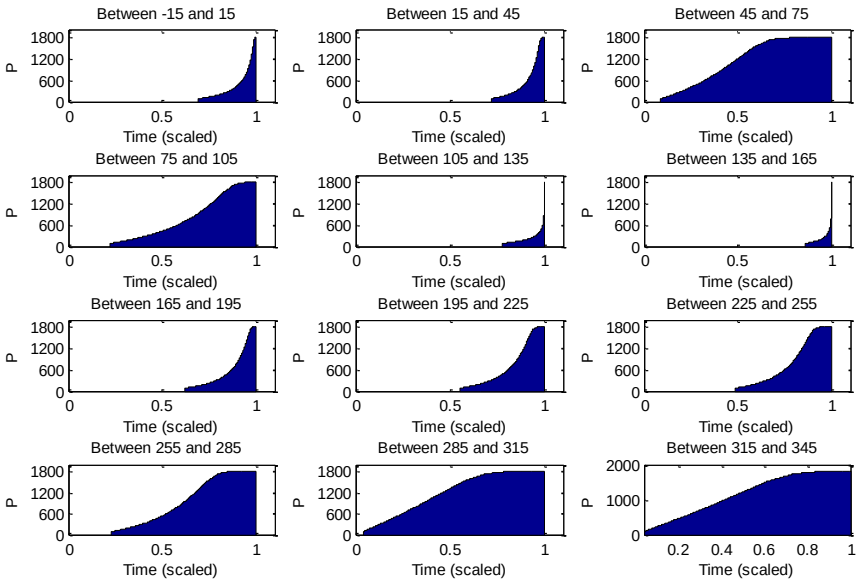

Figure 3-35. Generation Duration Curves of Belen WPP (Class II Turbine)

Table 3-4. Capacity factor of Belen WPP (Class II Turbine)

Direction Segment (Degree)	Frequency (%)	Mean Speed (m/s)	Capacity Factor (%)
-15 to 15	0.93	3.24	7.73
15 to 45	0.68	3.12	8.73
45 to 75	9.89	9.37	59.94
75 to 105	17.37	6.78	36.28
105 to 135	3.34	2.90	2.83
135 to 175	1.39	2.39	1.81
165 to 195	1.29	3.79	12.40
195 to 225	1.37	4.47	17.74
225 to 255	2.04	5.17	23.00
255 to 285	7.42	7.55	42.46
285 to 315	32.61	9.43	64.46
315 to 345	21.68	9.12	62.34
		Average Capacity Factor:	51.03

The annual average capacity factor of the data point (Belen WPP) is calculated as 51.03 % which is a very high number. From Figure 3-35, it can be followed that, although the contribution to power generation from 5th and 6th direction segments are very low; especially, in the 3rd, 11th and 12th direction segments, the power generations are very high, yielding very high capacity factors in those direction segments.

Although according to the definition of the wind class, the appropriate wind turbine for the data point is class II; many power plant investors prefer to use class I turbines; since, it is less expensive. Therefore, while calculating the capacity factor; the calculation will also be conducted by class I turbine selection for all places.

For Belen WPP, the average air density was 1.1243 kg/m^3; then, the power curve of class I turbine at that air density, which will be used to define $p = PC(v)$ relation, is shown in Figure 3-36.

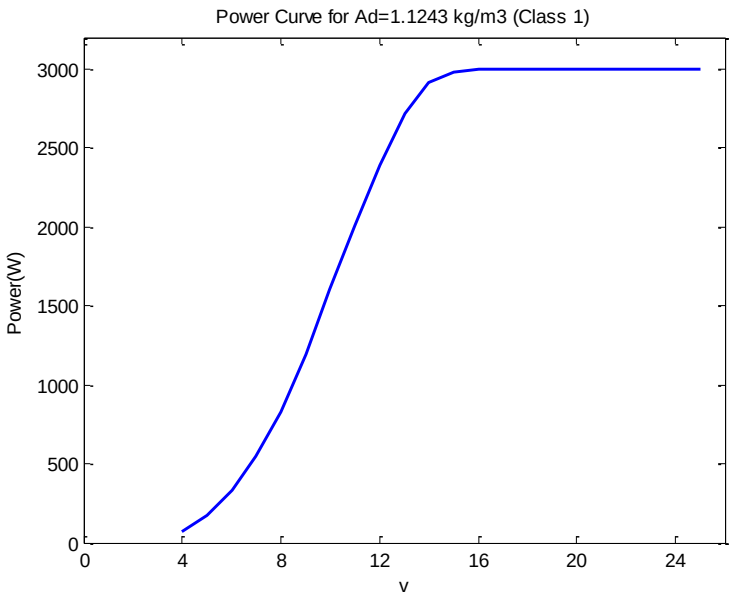

Figure 3-36. Power Curve of the Class I Turbine (Ad=1.1243 kg/m^3)

The cumulative distribution functions of the generated power are calculated using Equation (3-43) and (3-44) for each direction segment and shown in Figure 3-37. In Figure 3-37, it can be seen that, in the 1st, 2nd, 5th and 6th direction segments, the probability of generated power being zero is larger than 0.5, which will yield low capacity factors.

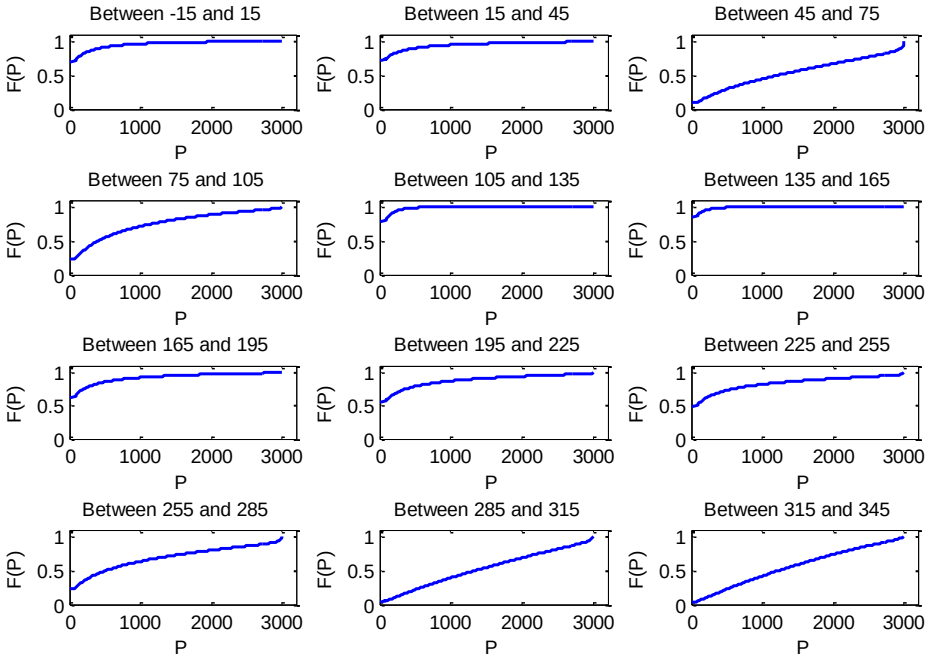

Figure 3-37. Cumulative Distribution Functions of Generated Power of Belen WPP (Class I Turbine)

When the cumulative distribution function of the power generation is integrated with respect to scaled time axis, it will give the total generation. Dividing the total generation by *Pmax* (3000 W) will give the capacity factor. The generation duration curves of the direction segments are presented in Figure 3-38 and the numerical values of capacity factors are given in Table 3-5.

The capacity factor of Belen WPP using class I turbine is calculated as 37.37 % which is considerably less than the calculated capacity factor using class II turbine. The results show that the capacity factor is directly related with the turbine selection. Proper and correct selection of turbine class for a specific location can increase the capacity factor.

The actual capacity factor of Belen WPP in 2012 calculated as 35 % according to RITM data [15]. The actual turbines in Belen WPP are class I; therefore, results of the work accomplished and the actual readings from the power plant can be said to be very similar.

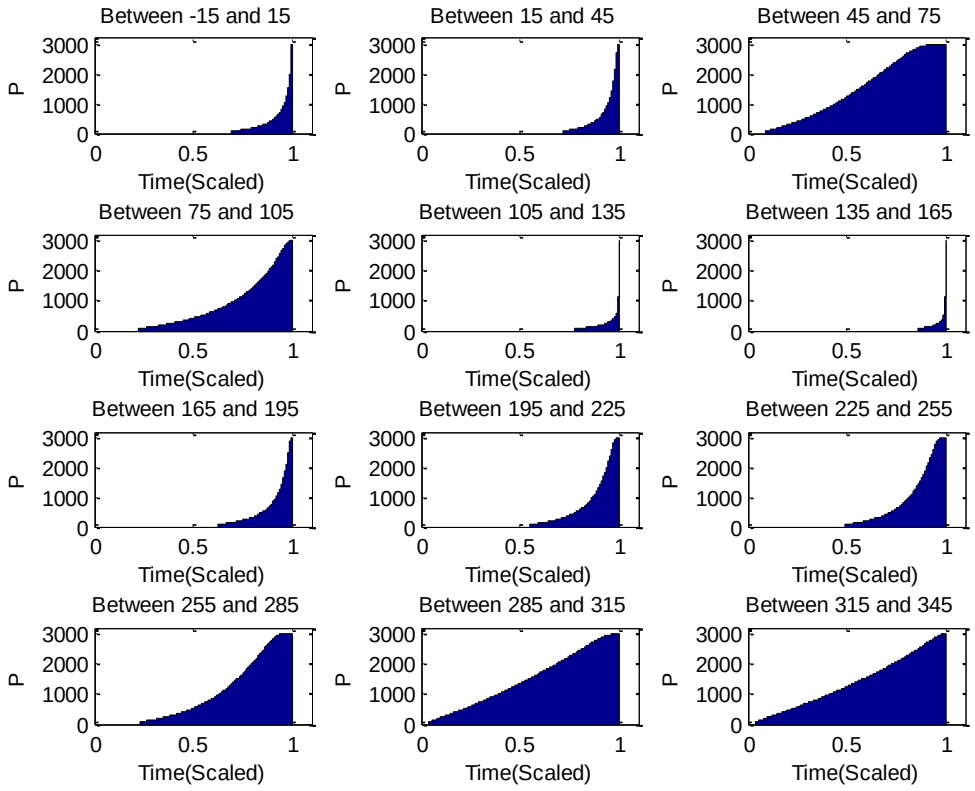

Figure 3-38. Generation Duration Curves of Belen WPP
(Class I Turbine)

Table 3-5. Capacity Factors of Belen WPP for Class I and Class II Turbines

Direction Segment (Degree)	Frequency (%)	Capacity Factor Class I (%)	Capacity Factor Class II (%)
-15 to 15	0.93	4.83	7.73
15 to 45	0.68	5.79	8.73
45 to 75	9.89	46.45	59.94
75 to 105	17.37	25.07	36.28
105 to 135	3.34	1.62	2.83
135 to 175	1.39	1.04	1.81
165 to 195	1.29	8.26	12.4
195 to 225	1.37	12.43	17.74
225 to 255	2.04	16.76	23.00
255 to 285	7.42	31.85	42.46
285 to 315	32.61	47.77	64.46
315 to 345	21.68	44.8	62.34
Average Capacity Factor:		37.37	51.03

3.4.4. Variation of Capacity Factors on Equidistant Map

The capacity factors of all data points in the database are calculated according to Equation (3-46). One thing to notice is that, while calculating the capacity factor in this work, losses in the power plant such as transformer and cable losses and internal needs of the plant are not considered. In addition to that, the annual capacity factor decreases due to turbine unavailability such as maintenance. Therefore, the practical capacity factors can be less up to 7 to 10 % from the calculated theoretical values. However, in the resultant maps, this decrease in the capacity factor is not included and the calculated theoretical values are directly represented; since, the losses can vary for different connections and assumptions may lead errors.

The resultant map of capacity factor variation for class I turbines is shown in Figure 3-39; whereas, the resultant map of capacity factor for turbine selection according to wind class definition (Table 3-2) is shown in Figure 3-40.

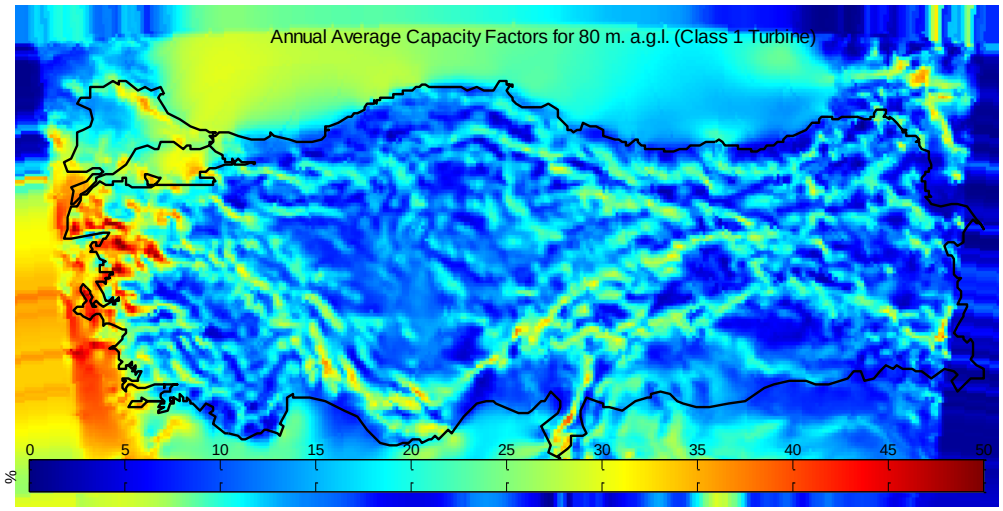

Figure 3-39. Capacity Factor Variations at 80 m. a.g.l.
(Class I Turbine) (Annual)

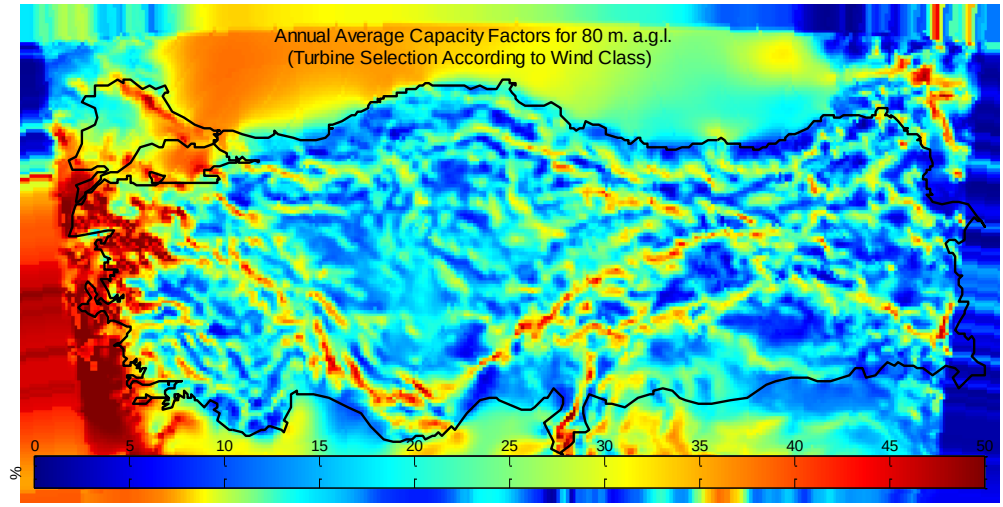

Figure 3-40. Capacity Factor Variations at 80 m. a.g.l.
(Turbine Selection according to the Definition of Wind Class) (Annual)

In both of these figures, it can be seen that, in Çanakkale, Balıkesir, Izmir and Hatay regions, there are places with very high capacity factors. In addition, from the comparison of two figures, it can be deduced that, the selection of turbine directly affects the capacity factor. Since class II and class III turbines are more efficient than class I turbines, Figure 3-40 has higher capacity factors than Figure 3-39.

The seasonal capacity factors are also calculated for class I turbine and shown in the following figures. In summer season (Figure 3-41), in Çanakkale, Izmir, Balıkesir, Trakya and Hatay regions, there are areas which have capacity factors larger than 60 %. However, in other regions, the capacity factors vary between 15 - 25 %, which are around average.

In winter season (Figure 3-42), the capacity factors in Çanakkale, Balıkesir, Hatay and Izmir regions are smaller than the summer season; however, in other regions, the capacity factors are higher than summer season. Since, the air density values are largest in winter season, this also have a positive contribution on the capacity factors.

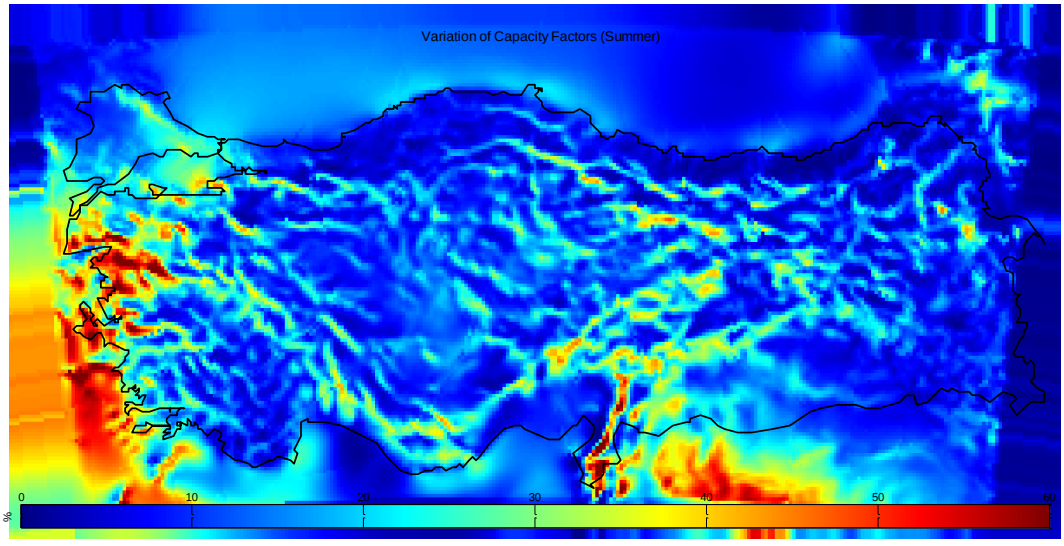

Figure 3-41. Capacity Factor Variations at 80 m. a.g.l.
(Class I Turbine, Summer Season)

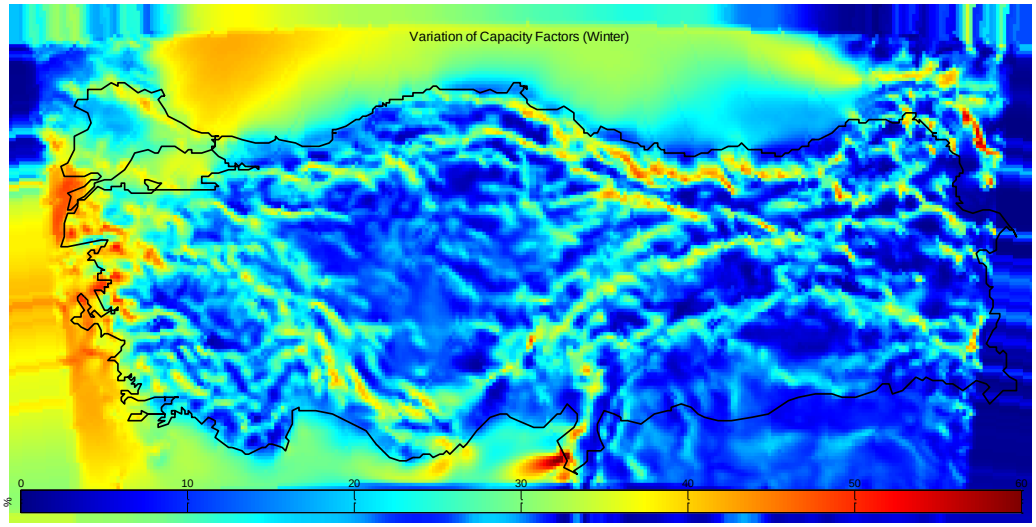

Figure 3-42. Capacity Factor Variations at 80 m. a.g.l.
(Class I Turbine, Winter Season)

Spring season has the lowest values of the capacity factors (Figure 3-27); however, the capacity factors in Çanakkale, Balıkesir, Izmir and Hatay regions are still more than 40 %.

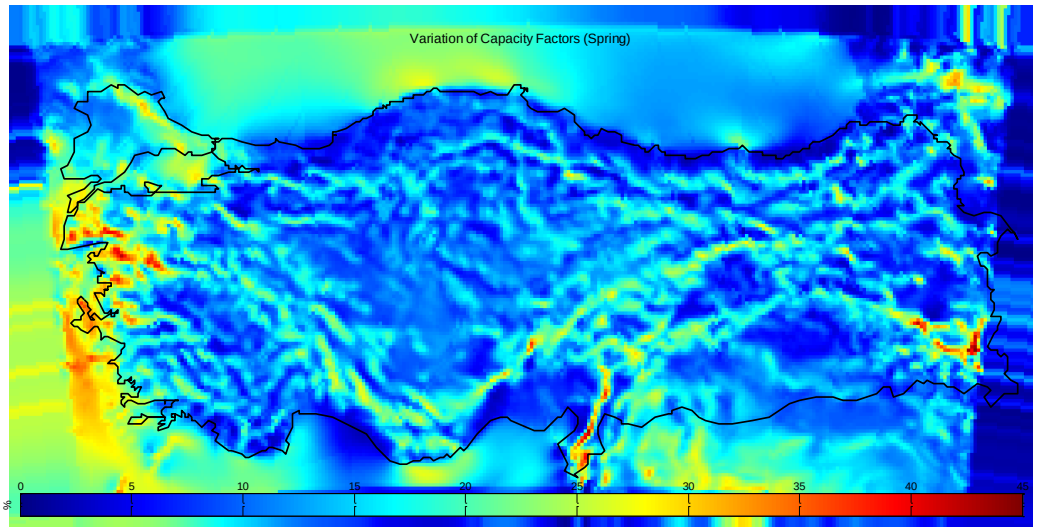

Figure 3-43. Capacity Factor Variations at 80 m. a.g.l.
(Class I Turbine, Spring Season)

For all data points in the database, the wind power potential; namely, the average wind speed, the wind power density and the capacity factor of WPPs are analyzed. In the following section, the numerical results from this study will be compared with the actual measurement data of Yahyalı WPP.

3.5. Comparison of the Results of the Calculations with the Actual Measurement Data

The wind speed and the wind direction variations of Yahyalı WPP are monitored in scope of RITM project. In this section, the actual measurement data of Yahyalı WPP during 2012 summer period will be compared with the results of the work accomplished in this chapter.

In the scope of RITM project, the wind speed and the wind direction variations of Yahyalı WPP (which is at latitude: 38.0413°, and longitude: 35.5340°) were recorded for every 10 minutes in 2012 summer season at 80 meters above ground level (a.g.l.). In Figure 3-44, the measured speed variations in 2012 July and August are shown. It can be followed that the wind is usually strong. The average of the measured wind speed during this period is calculated as 7.94 m/s which is indeed a favorable value for wind power generation.

The direction of the wind is also recorded and shown in Figure 3-45. It can be concluded that, in summer, there exists 2 directions which are dominant: Most of the wind is blowing between -15 and 15 degrees and between 315 and 345 degrees.

From the wind speed and wind direction variations, it is sometimes possible to comprehend their relation; however, for a better understanding, a different algorithm which will show the wind speed and direction in the same plot must be designed. Therefore, in order to visualize the relation between the wind speed and direction, the wind rose algorithm in reference [55] is modified: The designed procedure inputs the wind speed and corresponding direction values and creates a summary table which includes the histogram of wind speed for each 30°. In addition, Weibull parameters

of the wind speed are calculated. Then, according to the frequencies of the direction segments and histogram of wind speeds, wind rose is plotted. In Figure 3-46, the output of the designed procedure; namely, wind rose plot, for the speed (Figure 3-44) and direction (Figure 3-45) inputs is shown.

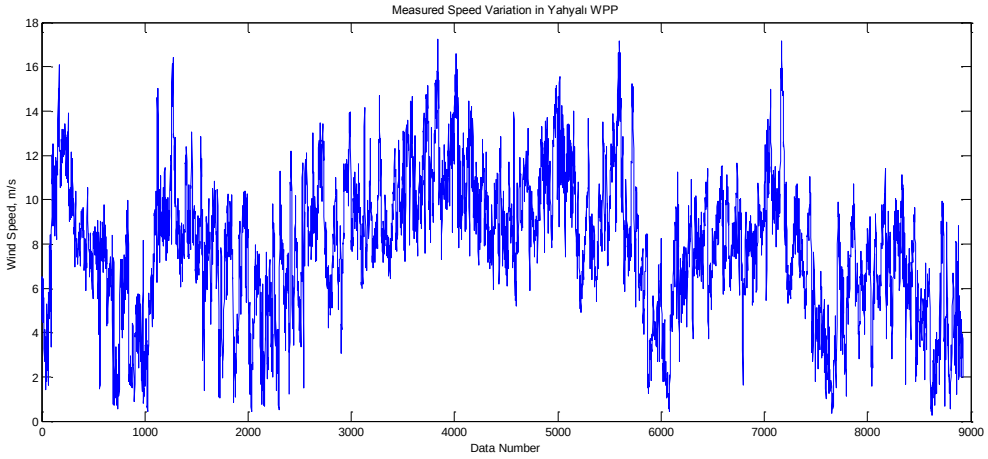

Figure 3-44. Measured Wind Speed Variation of Yahyalı WPP in July and August, 2012 (80 m. a.g.l.)

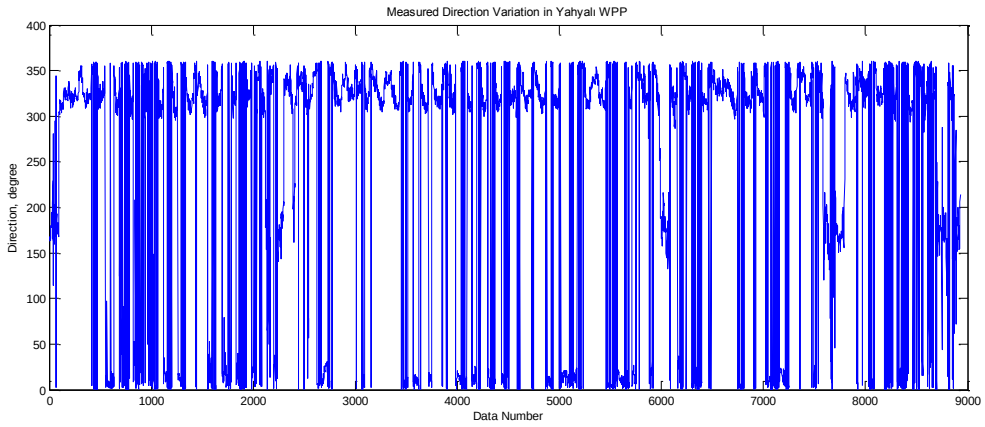

Figure 3-45. Measured Wind Direction Variation of Yahyalı WPP in July and August, 2012 (80 m. a.g.l.)

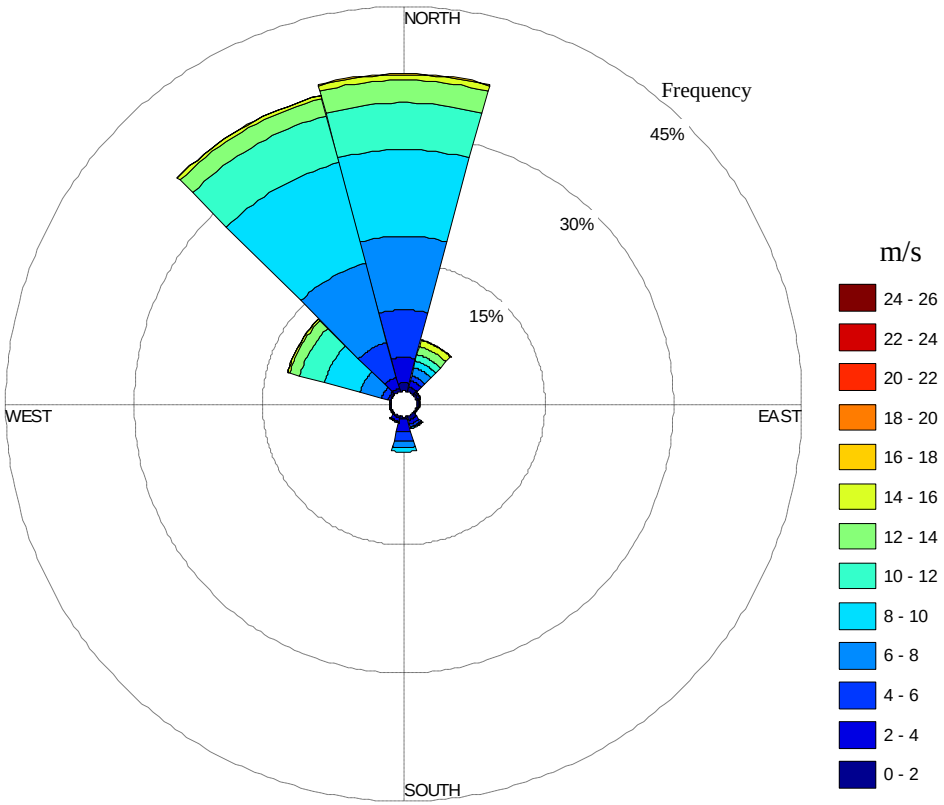

Figure 3-46. Wind Rose Plot of Yahyalı WPP
(Measured Data in July and August, 2012, 80 m. a.g.l.)

As it was inherently deduced from the wind speed and direction variations, the wind rose of Yahyalı WPP clearly shows that, the wind is dominant in 2 directions. However, with the wind rose plot, it can also be seen that, there is also strong but not frequent wind between 15 and 45 degrees. Therefore, it is easier to follow the wind patterns by wind rose.

The designed procedure also outputs a summary table which shows the histogram of the wind speeds according to their directions. Weibull parameters of each direction segment are also calculated. The summary table is shown in Table 3-6 and the comparisons between the histogram of the measured wind speed and Weibull fit are given in Figure 3-47. Between -15 and 45 degrees, and 285 and 345 degrees; the wind is usually strong and their Weibull scale parameters *a* are larger than 8.0 m/s.

When the frequencies of these strong wind patterns are investigated, it can be seen that they add up to 92 %. It means that, besides these directions, the wind blow is not frequent. This was also seen from the wind rose plot. The average wind speed is calculated as 7.94 m/s.

Table 3-6. Summary Table of the Developed Procedure for Yahyalı WPP (Measured Data in July and August, 2012)

Direction Segment (Degrees)	Frequency (%)	Mean Speed (Actual Data) (m/s)	Mean Speed (Weibull Fit) (m/s)	Scale Parameter *a* (m/s)	Shape Parameter *b*
-15 to 15	37.18	7.96	7.95	8.91	2.93
15 to 45	6.31	8.56	8.54	9.63	1.99
45 to 75	0.53	2.48	2.49	2.81	1.94
75 to 105	0.38	2.10	2.11	2.34	1.53
105 to 135	0.20	1.48	1.49	1.65	1.51
135 to 175	1.56	3.74	3.76	4.20	1.63
165 to 195	4.16	4.80	4.81	5.43	2.32
195 to 225	0.82	3.03	3.04	3.43	2.13
225 to 255	0.21	3.28	3.29	3.70	1.79
255 to 285	0.17	2.90	2.91	3.28	1.90
285 to 315	12.58	9.13	9.09	10.03	3.99
315 to 345	35.92	8.30	8.28	9.17	3.70
	Vmean:	7.94	7.93		

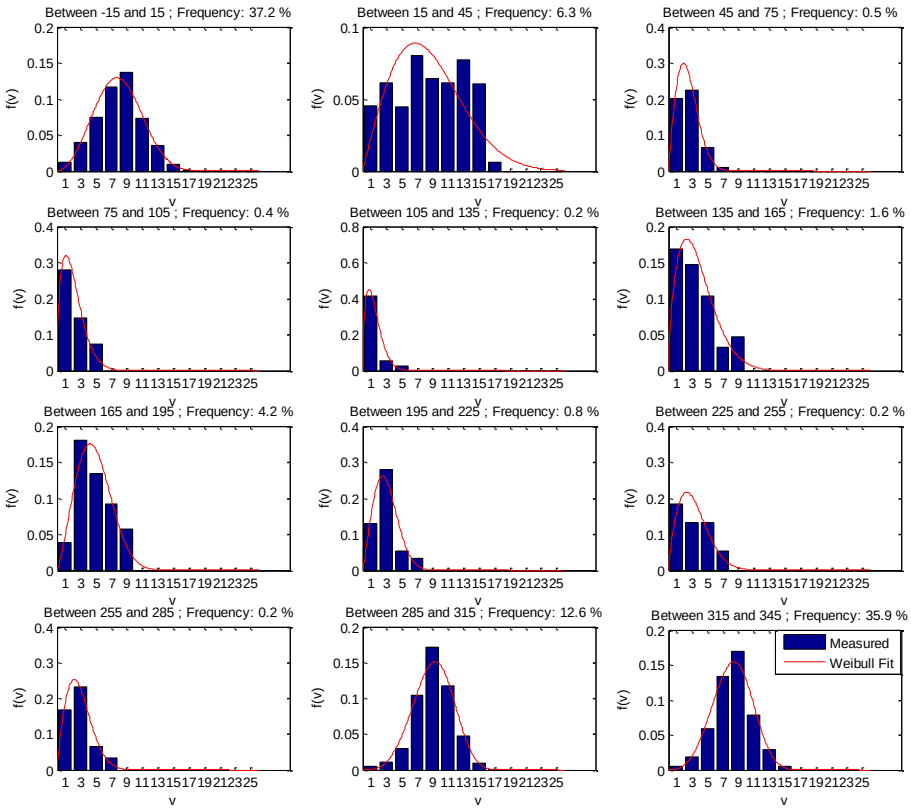

Figure 3-47. Comparison between the PDF of the Actual Variation and Weibull Fit of the Wind Speed of Yahyalı WPP (Measured Data in July and August, 2012)

The calculations from the measured speed and direction data of Yahyalı WPP will be compared to the calculations from the database values. The nearest point to Yahyalı WPP has the coordinates of latitude and longitude 38.0421°, 35.5010°. From the database, the 8 years hourly summer wind speed and direction variations of the corresponding data point are read and shown in Figure 3-48.

Summer wind speed average of hourly data of 8 years is calculated as 7.15 m/s from the database values. It can be seen that the estimated direction values in the database follows a similar pattern with measured direction (Figure 3-45). The developed procedure, wind rose, is applied to the 8 years of summer data and the resultant wind rose plot is presented in Figure 3-49. From the wind rose, it can be seen that, most of the wind blows between -15 and 15 degrees and 315 and 345 degrees. The

comparisons between the histogram of the wind speed and Weibull fit of the speed are also calculated and given in Figure 3-50.

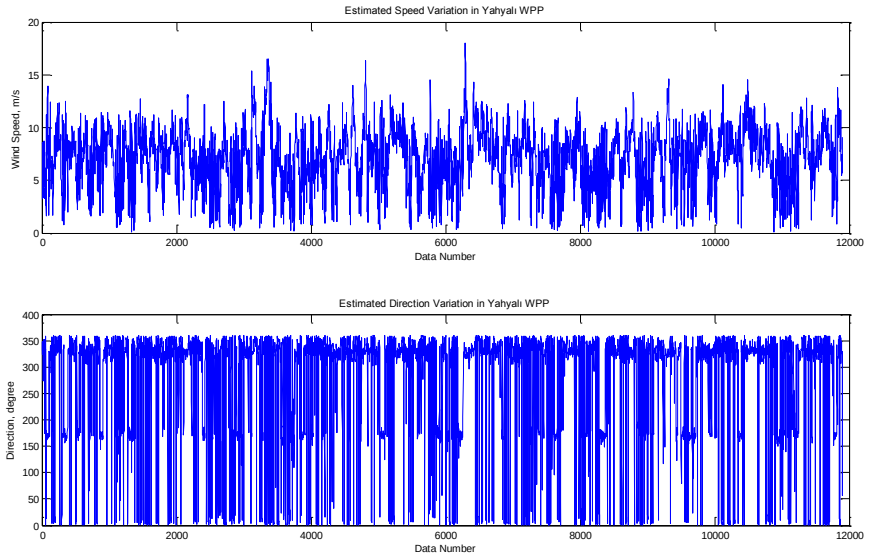

Figure 3-48. Summer Wind Speed and Direction Variations of Yahyalı WPP (80 m. a.g.l.) (Estimated Data of Summer Season for 8 Years)

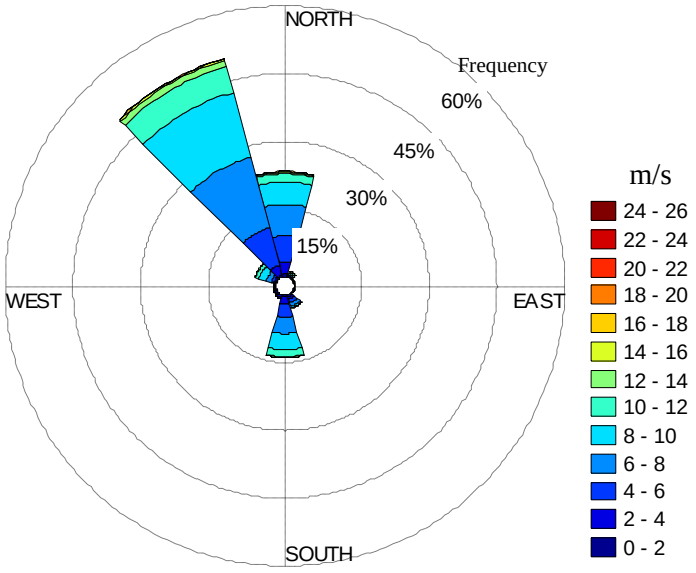

Figure 3-49. Wind Rose Plot for Yahyalı WPP (Estimated Data of Summer Season for 8 Years)

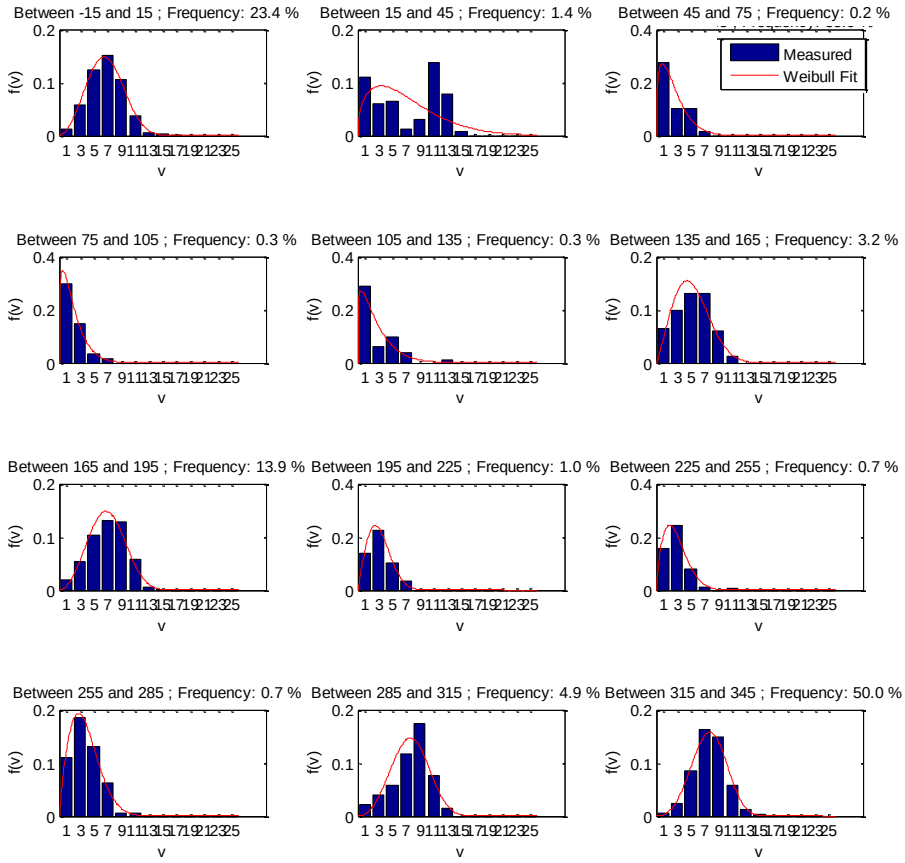

Figure 3-50. Comparison between the PDF of the Actual Variation and Weibull Fit of the Wind Speed of Yahyalı WPP (Estimated Data of Summer Season for 8 Years)

From the histogram of the estimated wind speeds which are read from the database, it can be seen that strong winds are between -15 and 45 degrees, and 285 and 345 degrees which is similar with the measured data. In Table 3-7, the numerical values of the wind rose are presented and it can be seen that the percentages of those strong winds add up to 80 %.

The calculated frequency, the mean speed, and Weibull parameters of the database values and the measured data for summer period are shown in Figure 3-51, 3-52, 3-53 and 3-54.

Table 3-7. Summary Table of the Developed Procedure for Yahyalı WPP

(Estimated Data of Summer Season for 8 Years)

Direction Segment (Degree)	Frequency (%)	Mean Speed (Actual Data) (m/s)	Mean Speed (Weibull Fit) (m/s)	Scale Parameter *a* (m/s)	Shape Parameter *b*
-15 to 15	23.37	6.76	6.75	7.58	2.84
15 to 45	1.41	7.21	7.16	7.88	1.43
45 to 75	0.24	2.49	2.50	2.71	1.31
75 to 105	0.25	2.02	2.02	2.15	1.21
105 to 135	0.34	2.71	2.73	2.86	1.14
135 to 175	3.20	5.24	5.23	5.90	2.19
165 to 195	13.89	6.98	6.97	7.81	2.94
195 to 225	1.02	3.16	3.16	3.57	2.02
225 to 255	0.67	2.87	2.87	3.22	1.72
255 to 285	0.68	3.77	3.77	4.24	1.86
285 to 315	4.91	7.70	7.66	8.55	3.23
315 to 345	50.03	7.72	7.69	8.55	3.50
	Vmean	7.15	7.14		

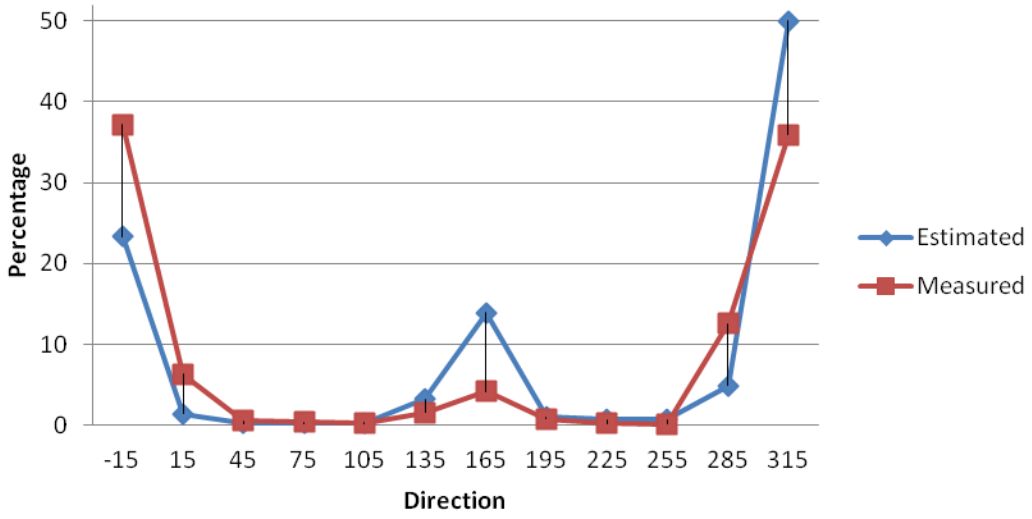

Figure 3-51. Comparison of Frequency Variations

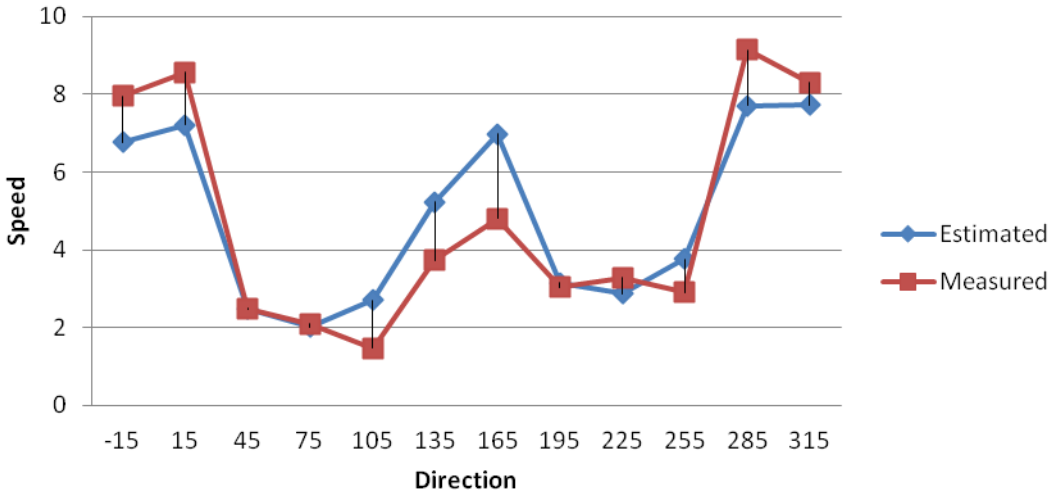

Figure 3-52. Comparison of Mean Speed Variations

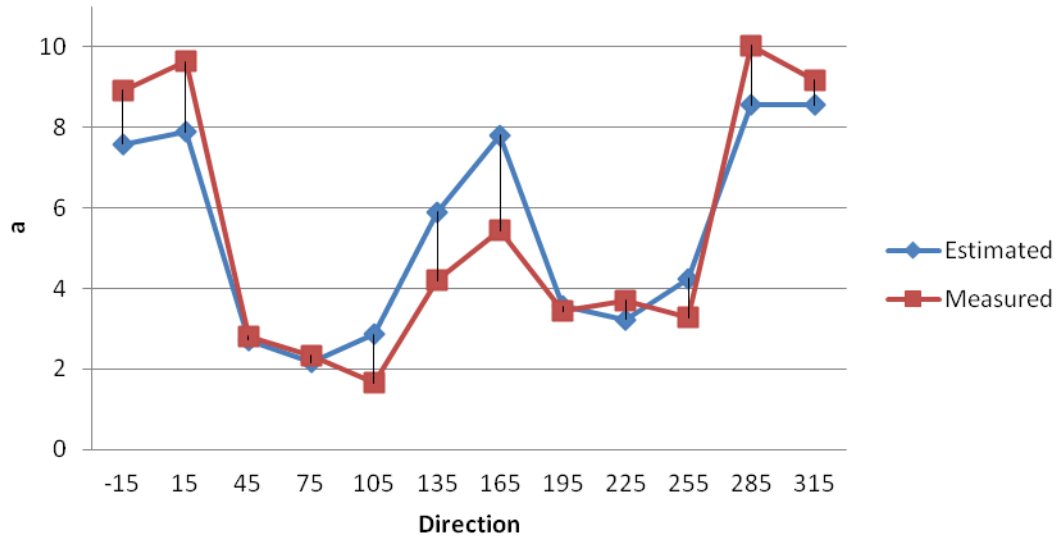

Figure 3-53. Comparison of Weibull Scale Parameter Variations

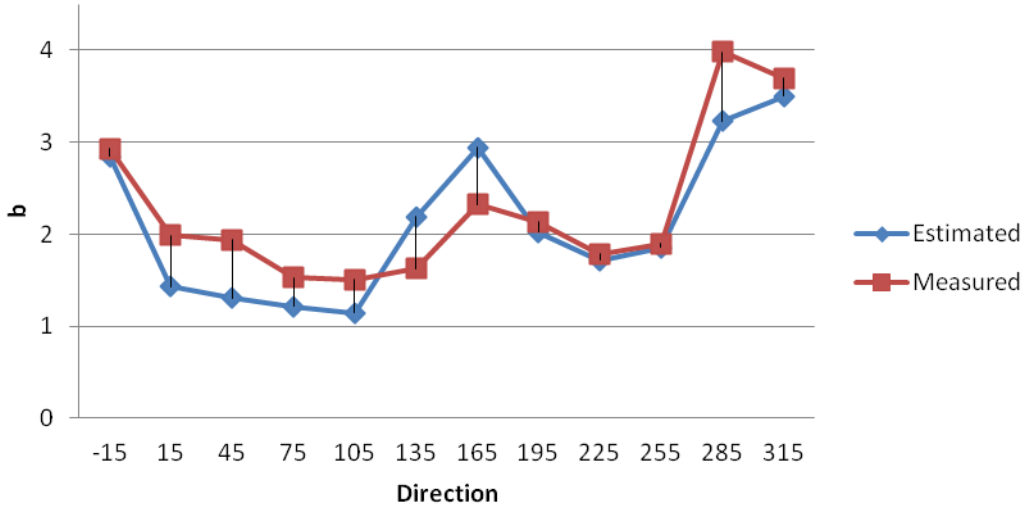

Figure 3-54. Comparison of Weibull Shape Parameter Variations

From the comparison plots of the estimated values from the 8 years of past data and the measured data for summer 2012, it is seen that, the work accomplished in this study is able to identify the wind speed variations and frequency patterns satisfactorily. However, in order to fully compare the measured and the estimated values, it is not sufficient to use only one year data. Small differences between the measurements and the estimated values from the database may occur due to the following reasons: Since, the estimated values from the database represent 6 km x 6 km areas; the measured values from actual WPP location may be larger. In addition, when more data are present in Weibull parameter calculations, the more accurate Weibull fitting of the speed variation can be accomplished. Therefore, there can be fitting errors when Weibull fit is applied to a one year summer data. Lastly, due to the imperfection of the measurement devices, there can be measurement errors in the speed and direction: Especially, in the consecutive directions segments, a small misread can lead the speed variation to be in another segment. Therefore, the slight differences can be observed due these reasons. However, in the long term analyses, the difference is expected to be smaller.

The average summer air density of Yahyalı WPP is calculated as 1.0036 kg/m^3 by using the air density algorithm. Then, using the formula in Equation (3-30), the wind power densities are calculated for each direction segment and the results are shown in Table 3-8 and Figure 3-55. It can be followed that the calculated wind power density values show similar patterns.

Table 3-8. Wind Power Density Calculation for Estimated and Measured Values

Direction Segment (Degree)	Estimated Data: 8 Years Summer Average		Measured Data: 2012 Summer	
	Frequency (%)	Power Density (W/m^2)	Frequency (%)	Power Density (W/m^2)
-15 to 15	23.37	224.35	37.18	358.25
15 to 45	1.41	537.98	6.31	599.47
45 to 75	0.24	26.72	0.53	15.34
75 to 105	0.25	16.21	0.38	12.47
105 to 135	0.34	44.87	0.20	4.51
135 to 175	3.20	125.48	1.56	64.65
165 to 195	13.89	240.71	4.16	93.51
195 to 225	1.02	29.92	0.82	25.28
225 to 255	0.67	26.92	0.21	38.67
255 to 285	0.68	55.37	0.17	24.96
285 to 315	4.91	304.52	12.58	466.32
315 to 345	50.03	297.49	35.92	361.84
WPD:		262.35		364.97

Using Equation (3-31), the mean wind power density is calculated as 262.35 W/m^2 from the database estimated values and as 364.97 W/m^2 from measured data of 2012 summer season. The calculated mean wind power densities differ by 28 %; however, since, the measured data belong to only one year and the estimated data are the

average of 8 years, the difference is acceptable. It means that, last year, the wind speeds are larger than the average values. In addition, the differences can be resulted from the previously stated reasons when calculating Weibull parameters. In the long term, the average wind power density will become closer to the calculated value from the database.

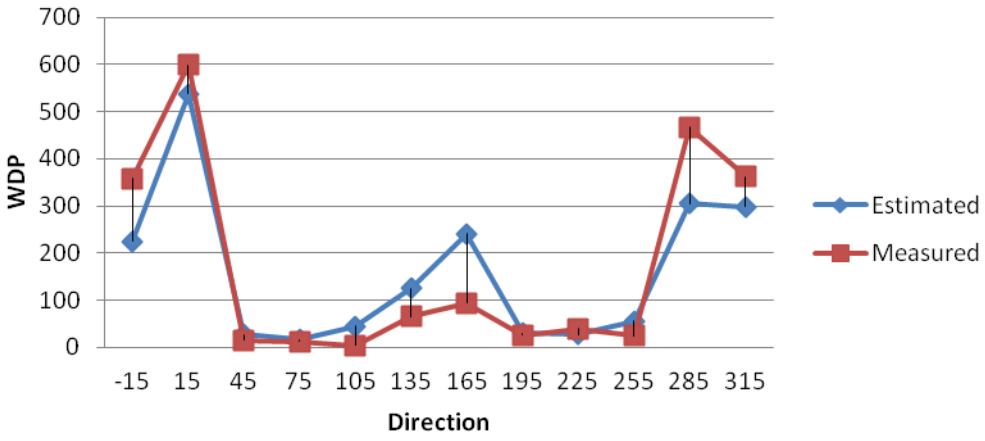

Figure 3-55. Comparison of Wind Power Density Variations

Lastly, the capacity factors of Yahyalı WPP are calculated for class I turbine using Equation (3-45). The numerical results are shown in Table 3-9 and in Figure 3-56. The capacity factor is calculated as 23.22 % from the database values; whereas, the capacity factor of the measured data is calculated as 30.44 %. As stated previously, comparison of short term variations can lead to this difference. In long term calculations, the difference is expected to be smaller; but, still, the patterns in directions segments were able to be recognized.

This completes the analyses accomplished about the determination of the wind power potential in Turkey. In the next chapter, the integration of wind power to Turkish grid will be analyzed using the results of this chapter and the optimal locations of wind power plants which lead maximum wind power generation in Turkey will be determined.

Table 3-9. Capacity Factor Calculation for Estimated and Measured Values of Yahyalı WPP

Direction Segment (Degree)	Estimated Data: 8 Years Summer Average		Measured Data: 2012 Summer	
	Frequency (%)	Capacity Factor (%)	Frequency (%)	Capacity Factor (%)
-15 to 15	23.37	20.07	37.18	30.20
15 to 45	1.41	26.62	6.31	36.17
45 to 75	0.24	1.94	0.53	0.72
75 to 105	0.25	1.07	0.38	0.63
105 to 135	0.34	3.42	0.20	0.10
135 to 175	3.20	10.98	1.56	5.30
165 to 195	13.89	21.54	4.16	8.10
195 to 225	1.02	2.00	0.82	1.53
225 to 255	0.67	1.82	0.21	2.90
255 to 285	0.68	4.46	0.17	1.58
285 to 315	4.91	26.97	12.58	39.74
315 to 345	50.03	26.80	35.92	32.00
CF:		23.22		30.44

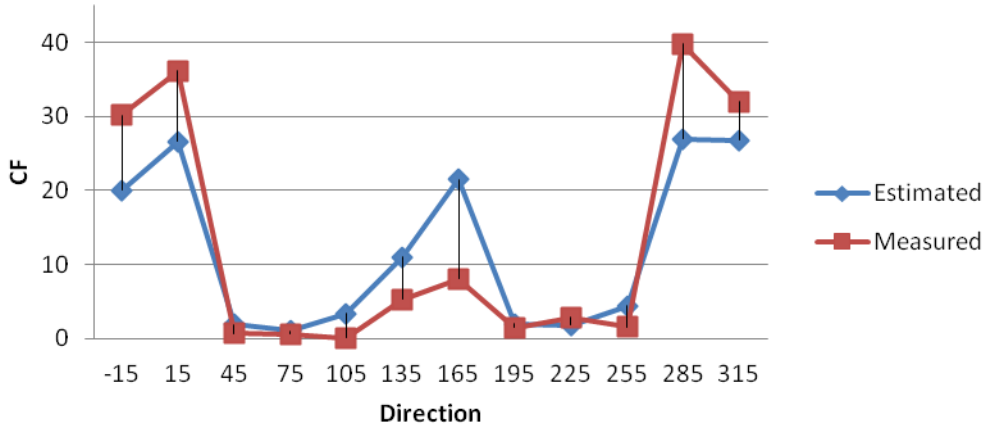

Figure 3-56. Comparison of Capacity Factor Variations

CHAPTER 4

DETERMINATION OF OPTIMAL WIND POWER PLANT LOCATIONS IN TURKEY

The maps that define wind power characteristics in Turkey; namely, the average wind speed, the wind power density and the capacity factors of the probable power plants were presented in the previous chapter. In this chapter, first, these data will be merged with the altitude and urban data of Turkey in order to eliminate locations where WPPs cannot be established. Then, using the coordinates of Turkish HV transformer substations (TS), substations which are suitable for WPP connection will be selected and the probable connection substation for each feasible location for WPP establishment will be found. Lastly, 2017 expected summer peak data of Turkish electricity network is prepared and an optimization problem is solved to determine the optimum wind power plant locations which maximize the annual wind energy production while satisfying the total wind capacity targeted. In the optimization problem, the linear programming optimization method is used with the DC load flow linear equations. In addition, as the constraints in the optimization problem, the thermal constraints from the thermal limits of the transmission elements are taken into consideration, as well as the regional constraints from the regional wind power connection capacities declared by TEIAS are used as inequality constraints.

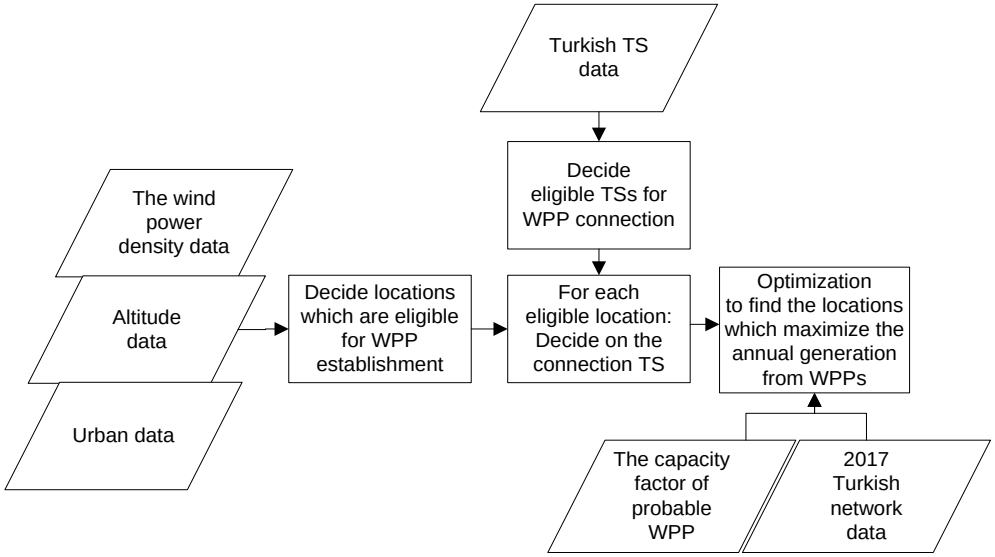

Figure 4-1. Summary of the Work Accomplished about the Determination of Optimal WPP Locations

4.1. Determination of Locations Suitable for Wind Power Plant Establishment

From investor's point of view, the most important criterion to decide on the wind power plant location is the promising wind characteristic. However, it is not possible to establish a wind power plant at every promising site. There are some additional restrictions which can be economic or geographic. Economic reasons could be the lack or difficulty of transportation to the site, the land cost or the distance to the electrical grid; whereas, geographic factors can be the site being close to the city centers or forested areas, having high altitude or being close to airports and so on. Indeed in Turkey, for wind power plants to have a generating license, investors have to submit an Environmental Impact Assessment (ÇED) showing that the wind power plant to be established will not result in any harm to the nature and environment [56]. Therefore, there are many criteria other than wind itself. For transmission planning, the system operator should be prepared for these uncertainties, and plan the necessary investments to cover most of the possibilities. However, it is also a must to narrow down possibilities in order not to come up with over investment.

In this work, four criteria will be used in order to locate the possible locations for new wind power plants:

Firstly, the candidate areas will be selected according to quality of wind: The annual average wind speed value is an agreeable indicator; however, it does not include the speed variation, so the wind power potential cannot be guessed. For capacity factor, and power density values, it is possible to relate the values with the wind power generation. The power density is said to be the most revealing variable in energy [57] also in the wind energy; since, it both includes the effect of Weibull parameters and it is independent of the turbine selection. Therefore, as the first elimination criterion, it will be assumed that from investors' point of view, places which have wind power densities smaller than 200 W/m^2 (approximately 7 m/s in terms of average wind speed) will not be feasible to establish power plants and they will be eliminated. Later, in the optimization part, capacity factors will be used to locate the most appropriate locations to maximize the annual wind energy production. In Figure 4-2, the histogram of the calculated wind power densities of data points in Turkey in Chapter 3 is shown. From Figure 4-2, it can be followed that nearly 51 % of the data points have smaller wind power density values than 200 W/m^2.

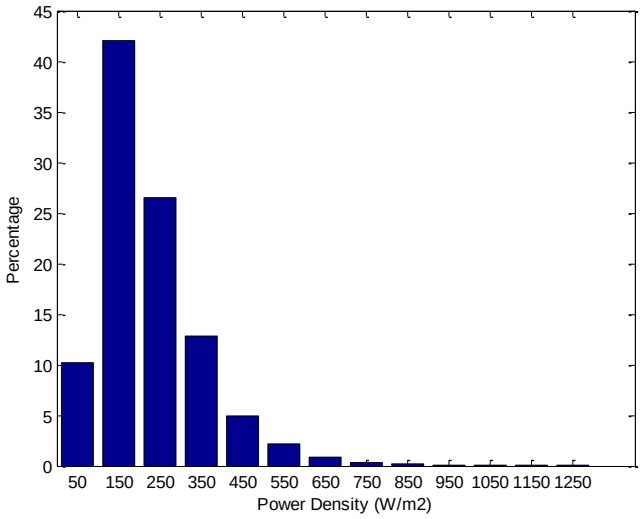

Figure 4-2. Histogram of the Calculated Wind Power Densities in Turkey

Figure 4-3 shows the elimination procedure of the places where the wind power density values are smaller than 200 W/m^2 (gray areas). The white areas are the places where the power density being equal to or larger than 200 W/m^2 criteria are satisfied.

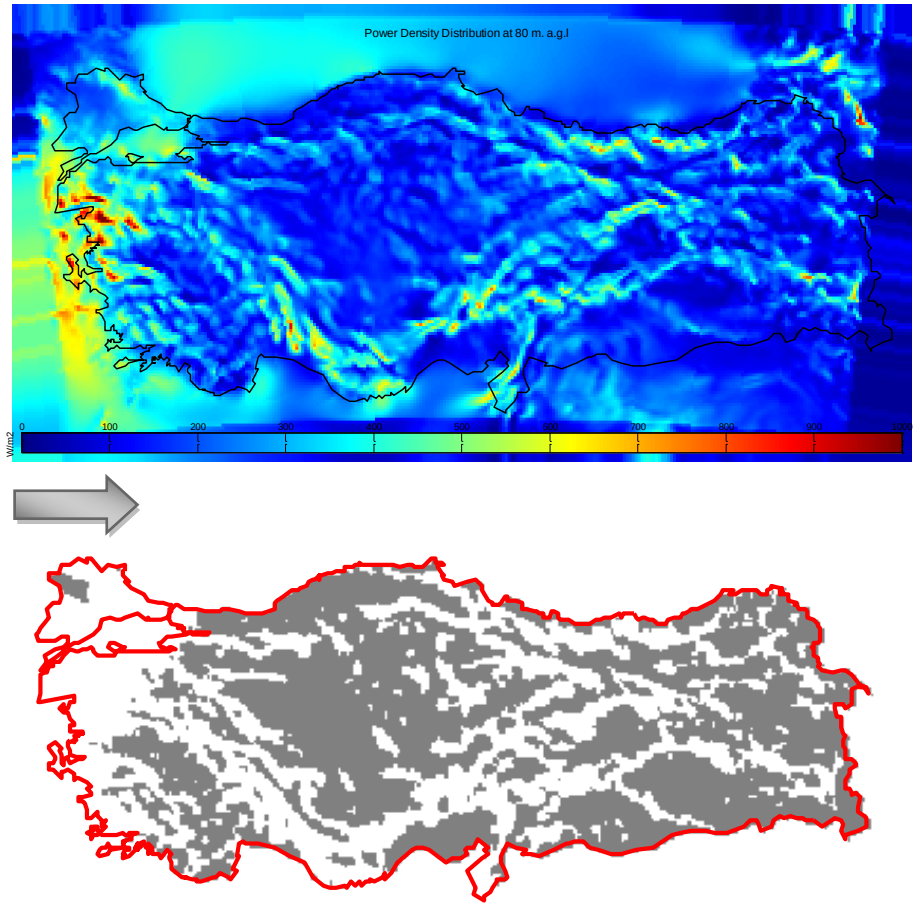

Figure 4-3. Elimination of Locations where Wind Power Density Values are Smaller than 200 W/m^2

As the second elimination criterion to locate the infeasible locations, places near urban areas should be found. For this purpose, using Google Earth [58], REPA [23] and the related list from EPDK [59], the cities in Turkey are investigated one by one and more than 100 places corresponding to existing urban areas are selected as not suitable for wind power plant establishment. The selected areas contain city centers,

airports, lakes, dams, and some large natural forested areas. Figure 4-4 shows the places which are eliminated due to geographic reasons.

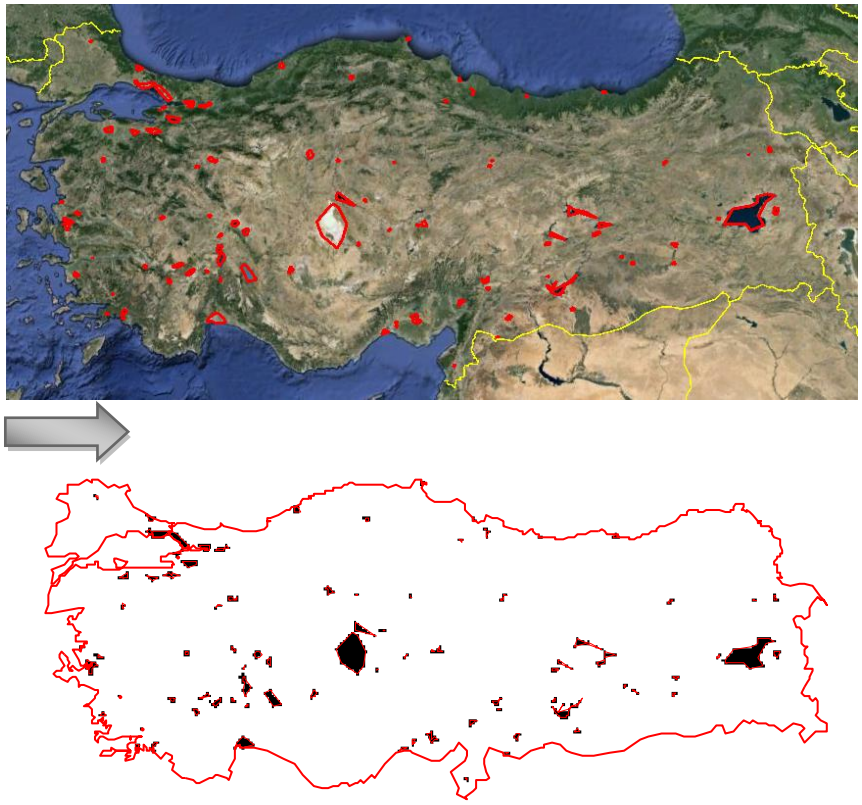

Figure 4-4. Elimination of Locations which are not Suitable for WPP Establishment due to Geographic Reasons

The next criterion that will be used to find the infeasible locations is the elevation of the area. The air density decreases with the increasing elevation so as the wind power density and the capacity factor. In addition, as the elevation increases, the transportation to the site gets difficult and the slope of the site may become high which makes the wind power plant establishment impossible. For this purpose, altitude of each data point is downloaded from the database and the ones which have altitude higher than 2000 meters are eliminated. Figure 4-5 shows the elimination procedure of the places which have altitude higher than 2000 meters. Since, a data

points represent a 6 km x 6 km area, the calculated altitude cannot represent the altitude of the whole area; instead, the altitude of nearest location to the data point will be used for the calculations.

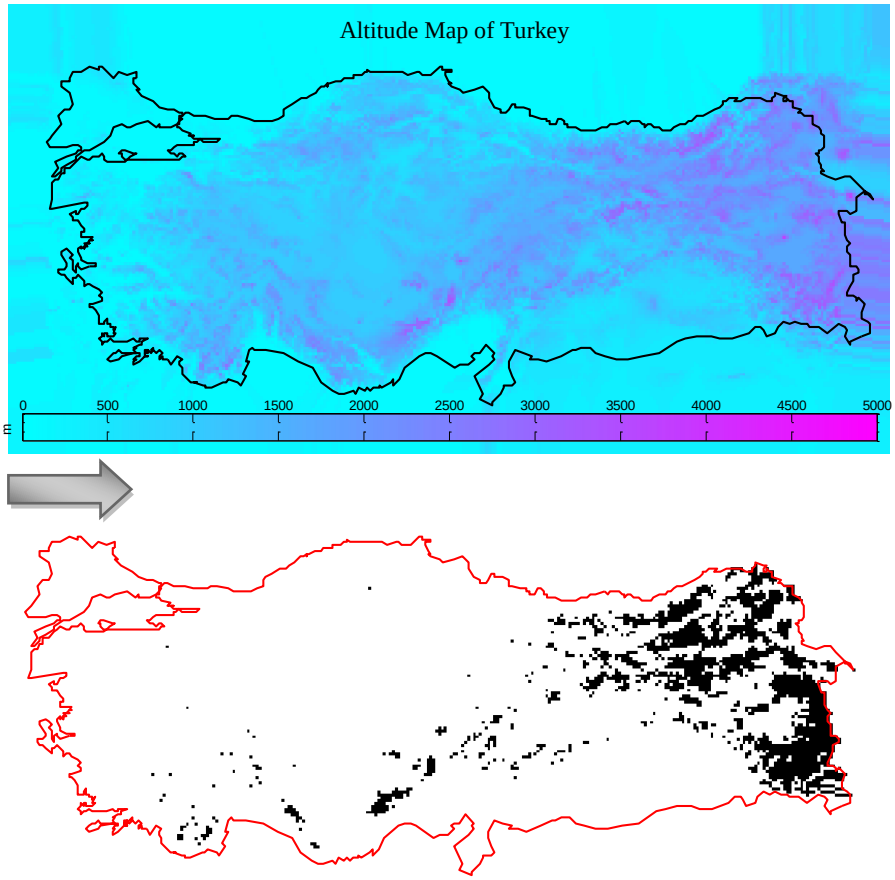

Figure 4-5. Elimination of Locations with Altitude above 2000 Meters

As the last elimination criterion to find the infeasible locations, the places of the existing WPPs and the licensed WPPs will be used. Generally, the wind turbines are placed by 3 - 10 rotor diameters apart [60] - [61]. For instance, the rotor diameter of a Vestas V90 turbine (3 MW) is 90 meters; therefore, the placing can be between 270 meters to 900 meters which will limit the maximum number of wind turbines in an area. Therefore, it will be assumed that, the data points corresponding to the places of

the existing and the licensed WPPs on the transmission level are not suitable for additional new WPP investments. According to the above mentioned assumption, Figure 4-6 shows the elimination procedure of these places.

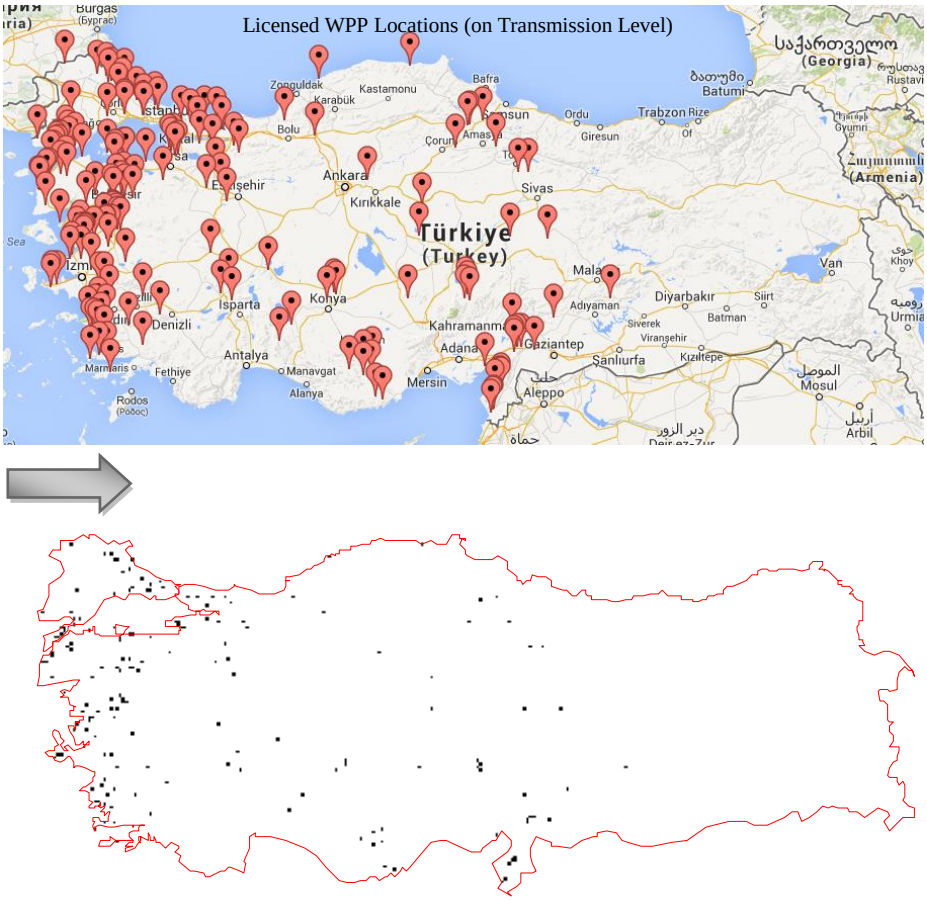

Figure 4-6. Elimination of Licensed WPP Locations

Using these four criteria, the areas which are not suitable for new wind power plant establishment can be obtained. The flowchart which shows the elimination procedure of the infeasible data points is shown in Figure 4-7 and the resultant map according to these assumptions is presented in Figure 4-8, in which the places where wind power plants can be installed (white areas, 10096 onshore data points) are shown. In Turkey, special permissions are needed to establish wind power plants onto areas

where forested, agricultural and mine potential nearby [56]; therefore, areas suitable for actual implementation are less than the locations given in Figure 4-8. However, a more detailed study is beyond the scope of this thesis and the rules change from area to area; therefore, it is not included.

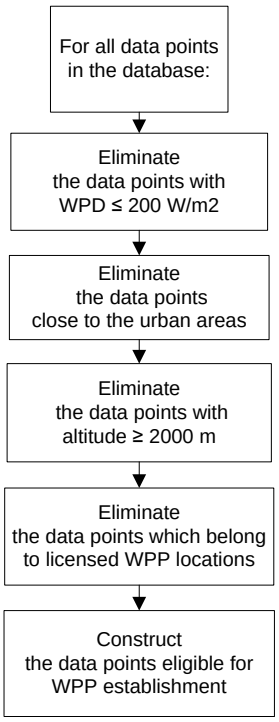

Figure 4-7. Flowchart of the Elimination Procedure for Infeasible Locations

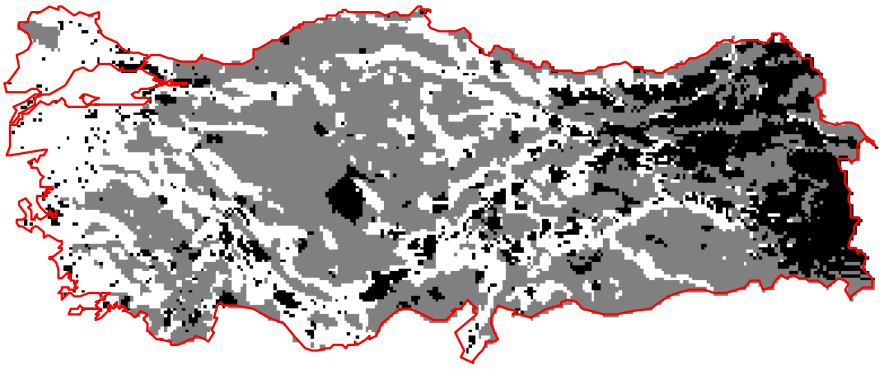

Figure 4-8. Locations which are not Suitable for WPP Establishment

4.2. Determination of Transformer Substations Suitable for Wind Power Plant Connection

The probable WPP locations are decided by the above mentioned procedure. Then, next thing to do is to decide the available transformer substations for wind power plant connection and prepare a possible connection list of eligible TSs. For this purpose, TS data of Turkey will be used. In addition to the transformer substations which are in service, TEIAS announced 7 planned HV transformer substations for WPP connection (Figure 4-9), where the wind is very promising [62]. Therefore, these substations must also be included for the substation list.

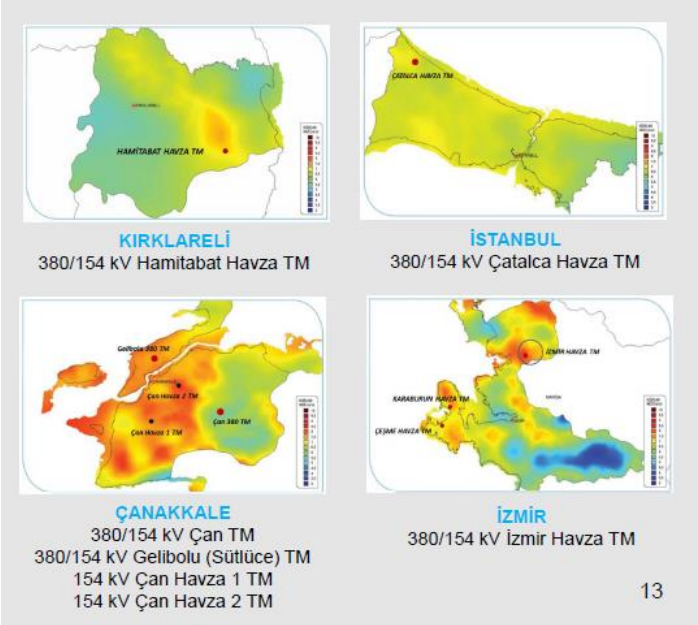

Figure 4-9. Planned HV Transformer Substations for WPP Connection

In Turkey, most of the wind power plants are radial connected to nearest available 154 kV substations. Therefore, in this work, it will be assumed that the wind power plants will be connected to the nearest 154 kV transformer substation (TS) if it is available. To decide whether a TS is available for wind power plant connection, 3

criteria will be checked. Firstly, if TS is too close to the city centers, it will not be possible to connect to that TS by overhead lines. Therefore, it will be infeasible to consider that possibility and these TSs will be eliminated from the possible connection list. For instance, in Figure 4-10, European part of Istanbul is shown. It is evident that, it will be infeasible to consider that a WPP to connect Bağcılar (GIS), Bahçelievler (GIS), Davutpaşa, Topkapı and Sağmalcılar TSs. However, a WPP can connect to Ikitelli, Atişalani, and Küçükköy TSs because they are not in city center and connections by overhead lines can be accomplished.

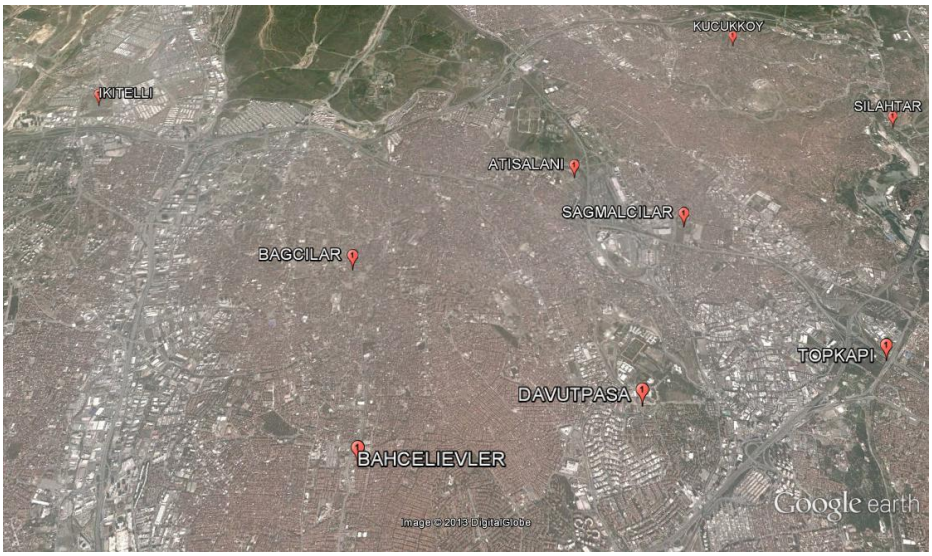

Figure 4-10. The TSs in European Part of Istanbul

Secondly, substations of some large natural gas, coal and hydro power plants will be eliminated from the list of eligible TS. However, small plant substations will not be eliminated; since, connections can be accomplished as the case in Figure 4-11. It can be seen that Gök R-2 WPP will be connected to Soma-A (Coal PP). Similar connections can be seen with Sayalar, Geres and Gök R-1 WPPs.

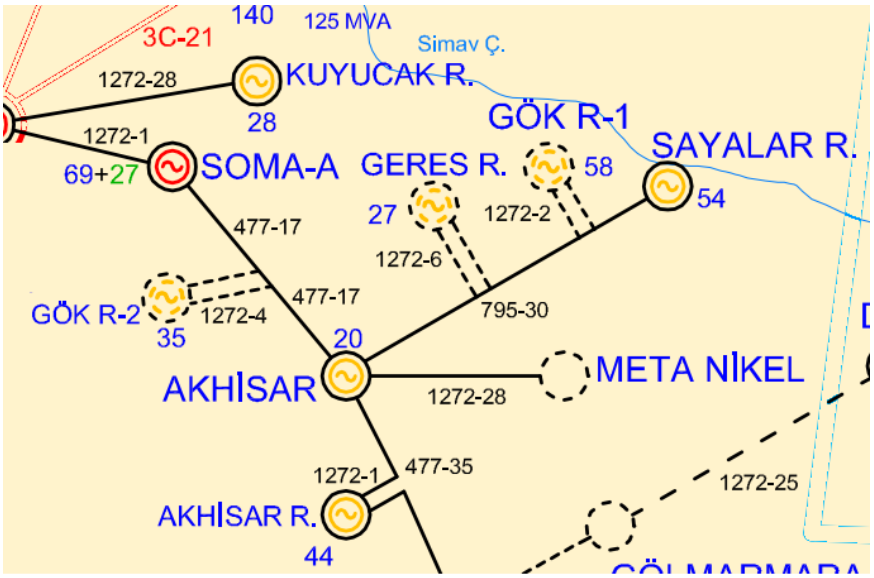

Figure 4-11. Connections of Different WPPs in Turkey

Last elimination will be to check whether the TS is a GIS (Gas Insulated Substation). The GISs are preferred mostly in city centers, if there is no sufficient space for a transformer substation and it can be assumed that WPP connection to these substations will be impossible.

By the end of 2012, there are 903 transformer substations in Turkey and by above assumptions, it can be stated that connections to 216 of them are not feasible. The remaining 687 of the substations can be said to be feasible substations for WPP connection. In addition to that, the announced 7 substations are added to the probable substation list, so in total 694 TSs are obtained (Figure 4-12).

As stated before, in this work, it will be assumed that, the WPPs will connect to nearest eligible transformer substations. Therefore, for each data point in Turkey, the nearest feasible substation is found and the data point is assigned with it. Figure 4-13 shows the flowchart of the work accomplished to find the connection substation of each probable wind power plant.

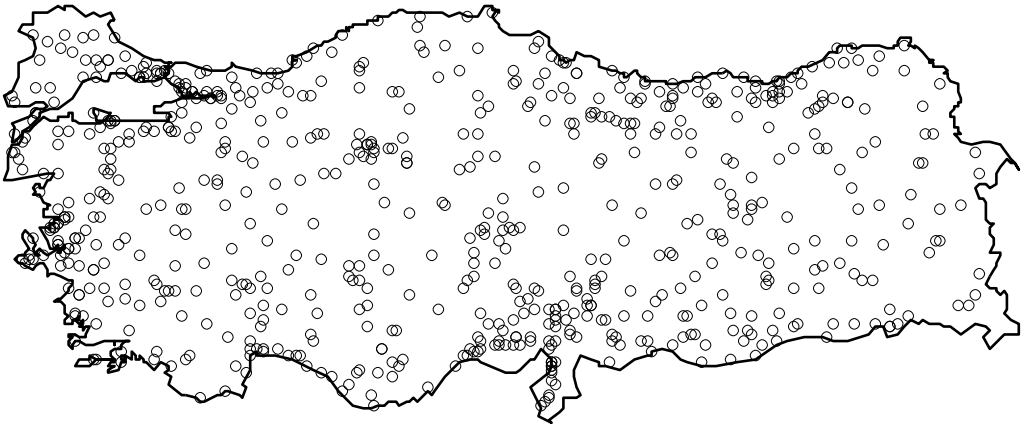

Figure 4-12. Eligible Transformer Substations for WPP Connection in Turkey

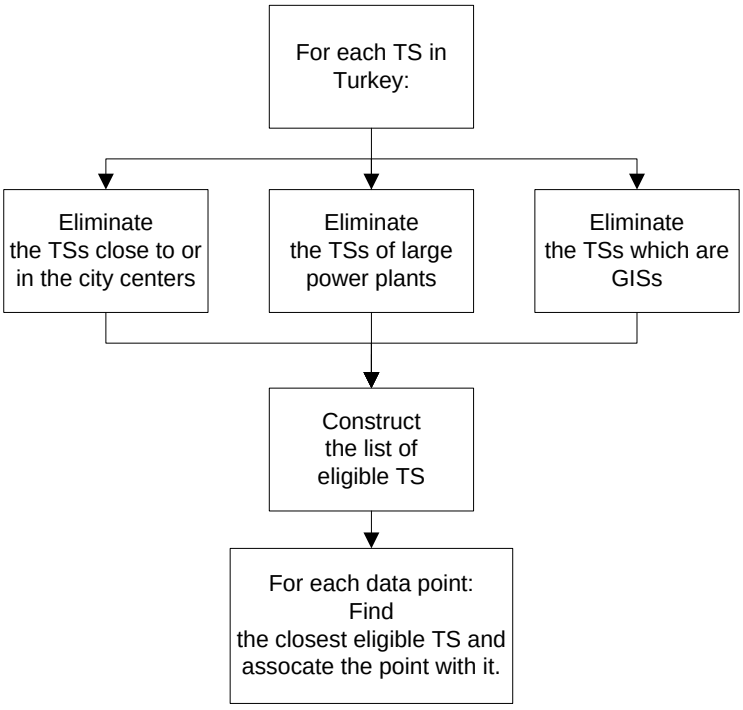

Figure 4-13. Flowchart of the Work Accomplished about Finding the Connection TSs of WPPs

4.3. Regional Wind Power Connection Capacities declared by TEIAS

Besides the wind power plants which already have generating licenses from EMRA, as of November 2013, TEIAS announced additional 3 GW of wind power connection capacity in different regions of Turkey [8]. The announced capacities are shown in Figure 4-14 and numerical values are given in Appendix A. The previously found eligible locations will be merged with these regional capacity limits in the optimization part in order to find the optimal locations for WPP establishment in Turkey.

Figure 4-14. Regional Wind Power Connection Capacities declared by TEIAS

After preparing the needed data about the parameters of the wind and the locations of WPPs, the next step is to formulate an optimization problem in order to determine the optimum locations which maximize the annual wind energy production. 2 cases will be studied about the determination of the optimal locations of WPPs: In Case 1, the locations of new WPPs will be constrained by the announced regional wind connection capacities by TEIAS and in Case 2, the locations will be selected disregarding the capacities announced by TEIAS in order to find the best locations

for WPP establishment in Turkey and lead the way for investors to understand the wind power potential in Turkey. For each case, DC load flow equations together with linear programming will be used.

4.4. Investigation of Optimal Locations for WPP Establishment

It is shown in the previous chapter that the power contribution from wind power plants is lowest in spring season and highest in summer and winter seasons. The peak demand of Turkey occurs in summer season [63] and in addition, the thermal capacity of the transmission elements is lowest in summer season. As a result, the expected summer peak data of 2017 will be used for analyses.

4.4.1. Constructing the Network Data for the Expected Summer Peak of 2017

In order to simulate the system, the electricity network data of the year 2017 should be constructed. For this purpose, the demand forecast and the generation dispatch of the peak hour will be accomplished. Then, for the preparation of network data, the existing system data will be merged with the investment plan of the TSO to construct the electricity network in 2017.

4.4.1.1. Generation Dispatch

In order to decide on the maximum allowable wind penetration to the system, the most important input is the contribution of the already built generation in the dispatch. At the end of 2012, the installed capacity of Turkey is approximately 57 GW. A typical generation curve of Turkey is given in Figure 4-15, which is indeed the generation curve of summer peak of 2012 [63]. Since, most of the installed capacity in Turkey consists of thermal units, the biggest share in daily generation is also from thermal power plants.

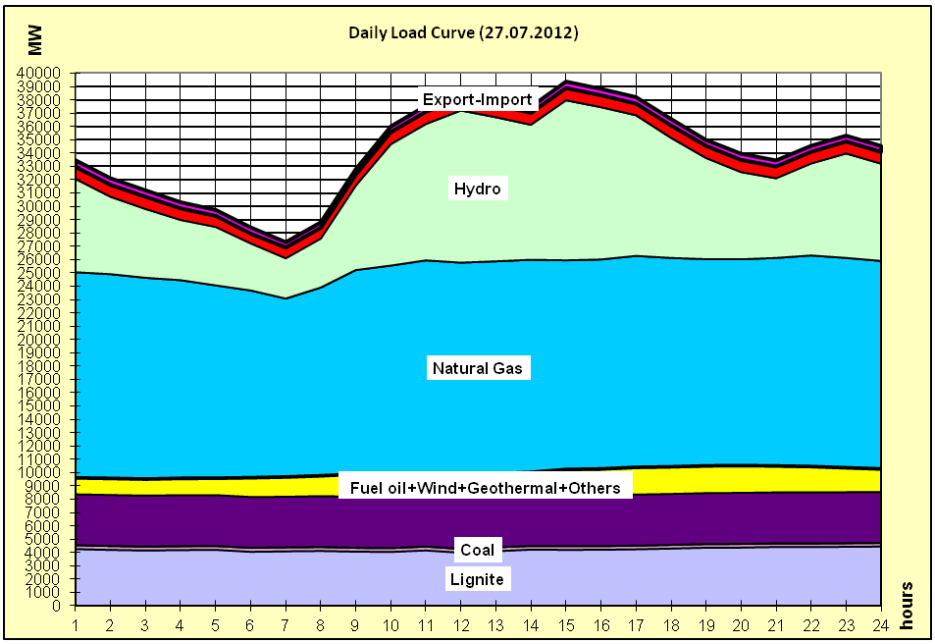

Figure 4-15. Generation Curve for Summer Peak of 2012 (27.07.2012)

As known, electrical energy consumption is not constant, in other words, at certain times of the day, peak demand takes place; whereas, especially during the night hours (base load level), the energy consumption goes down. As the demand for electricity changes, the outputs of the generators can change or new generators can be dispatched. Therefore, a realistic generation dispatch scenario must be prepared. In order to find out the probable outputs of the existing generators and create a realistic generation dispatch scenario for summer peak of 2017, the generation data of summer peaks between 2007 and 2011 are examined: The generators are divided into 7 categories by their fuel type and their most probable utilization factors at summer peak are found.

Coal-Fired Thermal Power Plants (Coal / Imported Coal / Lignite)

Coal-fired thermal power plants work as independent base load power plants (Figure 4-15, Figure 4-16). From Figure 4-16, which shows the utilization factors of the coal-fired thermal power plants between summer peaks of years 2007 – 2011, it can be

seen that the average utilization factor of coal power plants is found to be around 60 – 70 %. Therefore, in the dispatch, it is reasonable to take the utilization factor of those thermal plants as 65 %.

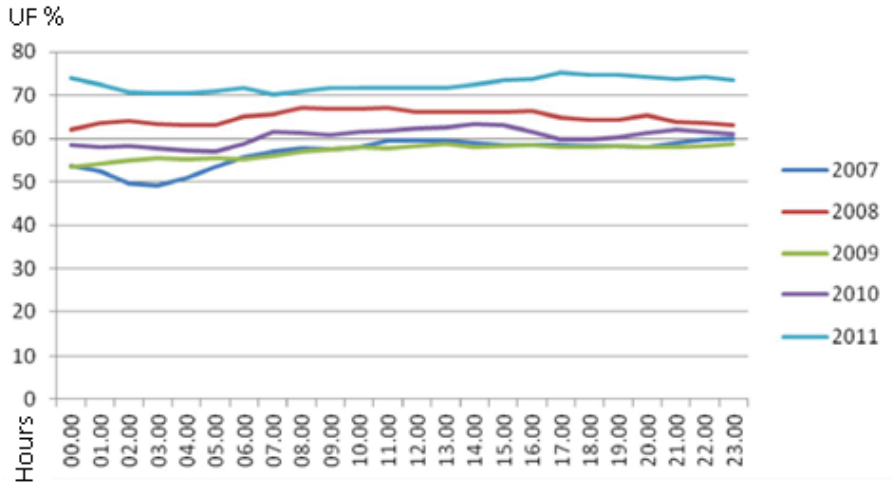

Figure 4-16. Utilization Factors of the Coal Power Plants (Summer Peak)

Natural Gas-Fired Thermal Power Plants

Although natural gas power plants lower their output in low demand hours, at other times, they are working as base load power plants (Figure 4-15, Figure 4-17). This is because of the generation deficit in Turkey and some thermal congestion due to lack of transmission elements. However, with the help of renewable generation, this trend is not expected to continue in the future [1]. Indeed, in 2010 - 2014 Strategic Plan of the Ministry of Energy and Natural Resources, it is stated that the share of Natural Gas-Fired PPs in generation should be decreased by increasing the share of renewable energy power plants. Therefore, in the dispatch algorithm, it is reasonable to treat the natural gas fired power plants as peak generators, in other words, after other fuel typed generators are dispatched, the natural gas power plants will be dispatched if needed and the utilization factors of the in-service generators will be taken as 85 %.

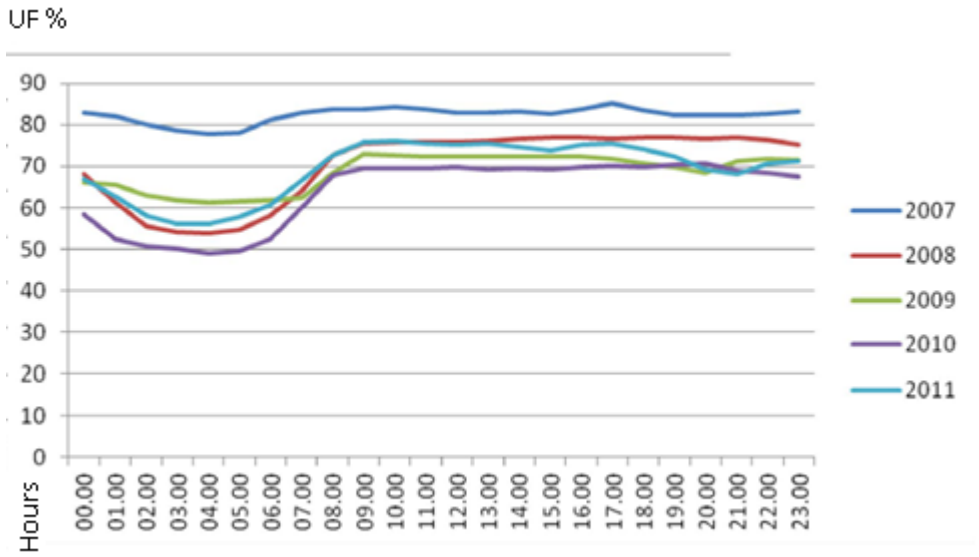

Figure 4-17. Utilization Factors of the Natural Gas Power Plants (Summer Peak)

Geothermal Power Plants

In Turkey, the number of geothermal power plants is limited. The average capacity factor of the geothermal PPs is found to be around 85 % and in the dispatch for summer peak of 2017, the utilization factor is taken as the same.

Wind Power Plants

In scope of RITM project, the selected outputs of the wind power plants of installed power are being monitored in Turkey [15]. Using the measurement data in 2011, the seasonal wind power generation duration curves are prepared in order to give insight about the probability of the WPPs' outputs. The deduced capacity factors of summer season can be found in Table 4-1. Since, the optimization will be about the decision of maximum wind power penetration to the grid, in long term planning, it is reasonable to consider the high scenario values. Therefore, it is feasible to take the utilization factor of wind power plants as 53 % at the instant of summer peak.

Table 4-1. The Capacity Factors of the WPPs in 2011

Scaled Time in Generation Duration Curve:	Low Scenario (75 %)	Base Scenario (50 %)	High Scenario (25 %)
Capacity Factor	34 %	45 %	53 %

Hydroelectric Power Plants

In Turkey, there are large hydro plants with dams; as well as the number run of river type hydro plants are increasing. In order to find the utilization factors of the hydro plants, hydro plants are separated into two: Hydro power plants with dam and run of river (ROR) type hydro power plants. Then, the hydro atlas of Ministry of Energy and Natural Resources [64] is used and hydro PPs are grouped by their locations of basins. Lastly, generation duration curves are constructed and the most probable outputs are guessed. As can be followed from Table 4-2, the utilization factors of the run of river type hydro power plants are lower than the hydro power plants with dam in summer peak; since, the hydro power plants with dams serve as peak generators.

Table 4-2. The Utilization Factors of Hydro Power Plants (Summer Peak)

Basin	HPP (With Dams)	HPP (ROR)
Batı Karadeniz, Kızılırmak, Yeşilırmak Basin (Basin number: 13, 14, 15)	% 70	% 64
Doğu Akdeniz, Seyhan, Ceyhan Basin (Basin number: 17, 18, 19, 20)	% 70	% 14
Fırat - Dicle, Van Basin (Basin number: 21, 25)	% 79	% 35
Doğu Karadeniz, Çoruh, Aras Basin (Basin number: 22, 23, 24)	% 52	% 23

Fuel Oil Fired Thermal Power Plants

Since fuel oil is expensive, it has lost its advantage and share in the generation. As a result, the contribution from this type is negligible and it is not considered in the dispatch algorithm.

International Contracts

Turkish electricity network is in connection with 7 countries; namely, Greece, Bulgaria, Georgia, Nakhichevan, Iran, Iraq and Syria [65].

Turkish government is planning to export electricity to Syria and Iraq in the following years. From Georgia, Turkish government plans to import electricity through a back to back HVDC substation which is already established in Akhaltsikhe. These plans are also implemented while constructing the generation dispatch scenario for summer peak of 2017.

In this study, year 2017 will be simulated; therefore, it is also needed to know the future generation units. In Turkey, generating plants have to apply for a generating license from EMRA. EMRA then, consults the transmission system operator about the evaluation of transmission system connection possibility. Therefore, in order to represent the future generating units, the list which includes the installed capacity of the future generating units, their possible connection points to the grid and the probable year when they will be in service, is obtained from TSO and those generators are included in the system data. By this way, the total installed capacity of Turkish generating system will reach to 90 GW in 2017.

4.4.1.2. Load Forecast

The demand for the electricity in Turkey has been increasing for the past decades except the economic crises (Figure 2-6). The demand forecast is out of scope of this study and the results of master plan analyses performed for TSO (TEIAS) by Power

Systems Department in TUBITAK will be used in this study [66]. In the master plan analyses of TUBITAK, extrapolation model is applied to the past 15 years of energy consumption data. The algorithm used in that study is the top to bottom algorithm, that is to say, firstly from the yearly consumption data, gross consumption is found from logarithmic extrapolation. Then, by using the logarithmic correlation with gross consumption and monthly peaks, the peak demand is calculated for each month. Lastly, peak demand is distributed to each transformer substation with a scaling factor which is decided from their last 5 years of energy consumption data. For those substations which will be in service in future, the demand is estimated by how much load shifting will be accomplished from nearby substations. With an optimistic scenario in growth, the peak demand is expected to reach 49 GW during 2017 summer peak of 2017.

In order to limit the size and complexity of the system, in this study, step-down transformers are not represented. Instead, loads are shifted to the transmission level. In order to include the effect of power loss in step-down transformers, 1 % of the load is added to actual load. As the step-down transformers are not represented, the overloads in the step-down transformers cannot be detected in the study. However, this does not create a problem in the long term planning; since, the transmission operator replaces step-down transformers when their loadings reach a certain limit.

4.4.1.3. Transmission Elements

In Turkey, at transmission level, there are 3 different voltage levels; namely, 380 kV, 154 kV, and 66 kV. However, 66 kV level is planned to be replaced with 154 kV level in the near future. In each voltage range, there are transmission lines and transformers. The thermal ratings of the overhead lines depend on the environment temperature; therefore, for different seasons; the ratings of the overhead lines are different. Since summer peak of 2017 will be analyzed in the algorithm, the summer ratings of the elements are used. In addition to existing system elements, TEIAS investment plan for transmission network is also taken into account.

After preparing the network data, the generation dispatch and the load forecast of summer peak of 2017, next steps are to obtain the locations of WPPs which will lead to maximum wind power generation and to investigate the effects on the grid.

4.4.2. Optimization of Wind Power Production by Linear Programming

In this part of the study, the optimal locations for WPPs which will lead to maximum wind power generation will be determined. This work will consist of studies of two cases: In Case 1, the regional wind power connection capacities declared by TEIAS in November 2013 [8] will be used and a total 3 GW of wind power integration according to those limits will be analyzed. In Case 2, the declared capacities will not be taken into account and the best locations for WPP establishment with the same amount of total installed capacity will be found. In addition, each case will be investigated twice: Regarding and disregarding the thermal limits of the transmission elements. In Case 1-A and Case 2-A, the thermal limits of transmission elements are not taken into account and the effect of the wind power penetration from optimal locations which will lead maximum wind power generation will be analyzed. In Case 1-B and Case 2-B, the thermal limits of transmission elements are taken into account and optimal locations of WPPs which will provide maximum wind power generation while satisfying the thermal constraints are determined. For both cases, linear programming will be utilized with the DC load flow equations. The summary of the cases studied to determine optimal locations of WPPs is presented in Table 4-3.

Table 4-3. The Summary of the Cases Studied to Determine the Optimal Locations of WPPs

Case Number	Regional Wind Power Connection Capacities declared by TEIAS	The Thermal Limits of the Transmission Elements
Case 1-A	✓	×
Case 1-B	✓	✓
Case 2-A	×	×
Case 2-B	×	✓

Linear programming will be used to determine the optimal locations. Linear programming is a technique for the optimization of a linear objective function, subject to a number of linear equality and linear inequality constraints [67]. Its feasible region is a convex polyhedron, which is a set defined as the intersection of finitely many half spaces, each of which is defined by a linear inequality. Its objective function is a real-valued affine function defined on this polyhedron. A linear programming algorithm finds a point in the polyhedron where this function has the smallest (or largest) value if such a point exists.

Mathematically, linear programming (linear optimization) finds the solution of an optimization problem where the objective function and the constraint equations are linear:

$$\text{Maximize } C^T X$$

Subject to:

$$A_{eq}\, X \;=\; b_{eq} \tag{4-1}$$

$$A\, X \leq b \tag{4-2}$$

$$X_{min} \leq X \leq X_{max} \tag{4-3}$$

where,

Equation (4-1) defines the linear equality constraints of *X*,

Equation (4-2) defines the linear inequality constraints of *X*,

Equation (4-3) defines the lower bound and upper bound limits of *X*.

There are many solution methods for linear programming problems [68]. In this study, Matlab '*linprog*' function [69] will be used and the constructed equality and inequality constraints will be inputted to the function to solve the linear optimization problem.

4.4.2.1. Variables in the Optimization Problem

The variable vector, X, in the optimization problem is the vector which consists of the variables in the algorithm. The solution of the linear programming gives the optimal values of the X. Since, DC load flow model and approach will be utilized in this study, generator outputs, bus voltage angles and power flow through the transmission elements are the variables. In addition to that, the aim is to find the optimal locations for wind power penetration; therefore, those are also included in the variable vector. The structure of the X vector is given in Table 4-4.

Table 4-4. Structure of X Vector in the Optimization Problem

$$\boldsymbol{X} = \begin{bmatrix} \boldsymbol{P_G} \\ \boldsymbol{P_W} \\ \boldsymbol{\Theta_V} \\ \boldsymbol{P_T} \end{bmatrix}$$

where,

$\boldsymbol{P_G}$ is a N_G x 1 vector consisting of the active power outputs of the existing generators (in MW),

N_G is the total number of existing generators,

$\boldsymbol{P_W}$ is a N_W x 1 vector consisting of the installed capacity of newly established WPPs (in MW),

N_W is the total number of the eligible locations for WPP establishment evaluated in Section 4.1,

$\boldsymbol{\Theta_V}$ is a N_B x 1 vector consisting of the phase angles of the network bus voltages (in radian),

N_B is the total number of the buses,

$\boldsymbol{P_T}$ is a N_T x 1 vector consisting of the real power flows through the transmission lines (in MW),

N_T is the number of the transmission elements.

4.4.2.2. Objective function in the Optimization Problem

The function to be maximized is chosen to be the total annual wind energy production (MWh) from eligible locations for WPP establishment; since, the aim is to maximize the use of local renewable resources. In other words, the annual wind power production from newly established wind power plants is to be maximized and its dual, negative of itself, is to be minimized:

$$C^T X = \frac{8760}{100} * \sum_{k=1}^{N_W} CF_k * P_{W_k} \tag{4-4}$$

where,

$C^T X$ represents the total annual wind power production from eligible locations (in MWh),

N_W is the total number of eligible locations for WPP establishment,

CF_k represents the annual capacity factor of the wind power plant at k^{th} eligible location (in %),

P_{W_k} represents the installed capacity of the newly established wind power plant at k^{th} eligible location (in MW).

To construct the objective function which is the total annual wind power production from eligible locations, the multiplying indices of P_{W_k} will be $\frac{8760}{100} * CF_k$; whereas, multiplying factors of the other variables in *X* vector will be 0.

The format of the C vector is given in Table 4-5 and the construction of the objective function, $C^T X$, is shown in Table 4-6 where $\boldsymbol{CF}$ represents the vector consists of the capacity factors of the wind power plants.

Table 4-5. Structure of *C* Vector in the Optimization Problem

$\mathbf{0}_{N_G \text{ x } 1}$
$\frac{\mathbf{8760}}{\mathbf{100}} * \boldsymbol{CF}_{N_W \text{x } 1}$
$\mathbf{0}_{N_B \text{ x } 1}$
$\mathbf{0}_{N_T \text{ x } 1}$

Table 4-6. Constructing the Objective Function in the Optimization Problem

$\mathbf{0}$	$\mathbf{8.76} * \boldsymbol{CF}$	$\mathbf{0}$	$\mathbf{0}$	$\boldsymbol{P_G}$	=	$8.76 * \sum_{k=1}^{N_W} CF_k * P_{W\,k}$
				$\boldsymbol{P_W}$		
				$\boldsymbol{\Theta_V}$		
				$\boldsymbol{P_T}$		

4.4.2.3. Constraints in the Optimization Problem

Linear Equalities: $\boldsymbol{A_{eq}\, X = b_{eq}}$

The linear constraints which are used in the optimization will be derived from the DC load flow bus equations for each bus i and branch equations for each branch between bus i and bus j.

- **Bus Equations for each Bus i: $A_{eq1}\,X = b_{eq1}$**

The bus equations will be constructed using the power balance of a node. The power entering a node from generating sources minus the power that is leaving must be equal to the load at the bus (Equation (4-5)).

$$\sum P_{G_i} + \sum P_{W_i} - \sum P_{T_i} = \sum P_{L_i} \tag{4-5}$$

where,

$\sum P_{G_i}$: Total generation from existing generators connected to bus i (in MW),

$\sum P_{W_i}$: Total new wind power penetration from bus i (in MW),

$\sum P_{T_i}$: Sum of line flows leaving from bus i (in MW),

$\sum P_{L_i}$: Total load at bus i (in MW).

The construction of A_{eq1} and b_{eq1} matrices which consist of the bus equations (Equation (4-5)) for each bus in the algorithm can be summarized as in Table 4-7.

Table 4-7. Bus Equations

$A_{eq1_{P_G}}$	$A_{eq1_{P_W}}$	$A_{eq1_{\Theta_V}}$	$A_{eq1_{P_T}}$	P_G	=	b_{eq1}
				P_W		
				Θ_V		
				P_T		

where,

$A_{eq1_{P_G}}$: An N_B x N_G matrix. The multiplying indices corresponding to existing generating units connected to bus i must be made 1 in order to result

in the total active power generation from the existing generators connected to bus i ($\sum P_{G_i}$) . The other indices are zero.

$\boldsymbol{A_{eq1_{P_W}}}$: An N_B x N_W matrix. The multiplying indices corresponding to the eligible wind power plant locations connected to bus *i* must be made 0.53 in order to result in the total wind power penetration from bus i ($\sum P_{W_i}$). The other indices are zero.

$\boldsymbol{A_{eq1_{\Theta_V}}}$: An N_B x N_B matrix. Phase angles do not involve in node equations; therefore, this is a zero matrix.

$\boldsymbol{A_{eq1_{P_T}}}$: An N_B x N_T matrix. The multiplying indices corresponding to the branches leaving from bus i must be made -1; whereas, the indices corresponding to the branches entering to bus *i* must be made 1 in order to obtain the sum of line flows leaving from bus i ($-\sum P_{T_i}$). The other indices are zero.

$\mathbf{b_{eq1}}$: An N_B x 1 vector. The i^{th} row of the vector corresponds to total load connected to bus i ($\sum P_{L_i}$).

- **Branch Flow Equations for each Branch between Bus i and Bus j: $\boldsymbol{Aeq_2\, X = beq_2}$**

The branch flow equations will be constructed using DC power flow equations (Equation (4-6)):

$$P_{T_{ij}} - \frac{\theta i - \theta j}{Xij} = 0 \tag{4-6}$$

where,

$P_{T_{ij}}$: Line flow from bus i to bus j (in MW),

θ_i: Phase angle of bus i voltage (in radian),

θ_j : Phase angle of bus j voltage (in radian),

X_{ij} : Branch series reactance between bus i and bus j (in micro ohm).

Then, the construction of A_{eq2} and b_{eq2} matrices, which consist of the branch flow equations (Equation (4-6)) for each transmission element in the optimization problem, can be summarized as in Table 4-8.

Table 4-8. Branch Flow Equations

$\boldsymbol{A_{eq2_{P_G}}}$	$\boldsymbol{A_{eq2_{P_W}}}$	$\boldsymbol{A_{eq2_{\Theta_V}}}$	$\boldsymbol{A_{eq2_{P_T}}}$	$\boldsymbol{P_G}$	=	$\mathbf{b_{eq2}}$
				$\boldsymbol{P_W}$		
				$\boldsymbol{\Theta_V}$		
				$\boldsymbol{P_T}$		

where,

$\boldsymbol{A_{eq2_{P_G}}}$: An N_T x N_G matrix. Generator outputs are not involved in branch flow equations; therefore, it is a zero matrix.

$\boldsymbol{A_{eq2_{P_W}}}$: An N_T x N_W matrix. New wind penetrations are not involved in branch flow equations; therefore, it is a zero matrix.

$\boldsymbol{A_{eq2_{\Theta_V}}}$: An N_T x N_B matrix. For the branch ij, the multiplying factor of θ_i is $\frac{-1}{Xij}$; whereas, the multiplying factor of θ_j is $\frac{1}{Xij}$ in order to construct $\frac{-(\theta i-\theta j)}{Xij}$. The other indices are zero.

$\boldsymbol{A_{eq2_{P_T}}}$: An N_T x N_T matrix. The multiplying index of power flow through the branch ij is 1, to construct $P_{T_{ij}}$ .The other indices are zero, making $\boldsymbol{A_{eq2_{P_T}}}$ an identity matrix.

$\mathbf{b_{eq2}}$: An N_T x 1 null vector which represents the right side of Equation (4-6).

After constructing the bus equations and branch flow equations, the construction of resultant linear equality constraint matrices A_{eq} and b_{eq} which define the DC load flow equations can be summarized as Table 4-9.

Table 4-9. The Linear Equality Constraints

$A_{eq1_{P_G}}$	$A_{eq1_{P_W}}$	$A_{eq1_{\Theta_V}}$	$A_{eq1_{P_T}}$	P_G	=	b_{eq1}
$A_{eq2_{P_G}}$	$A_{eq2_{P_W}}$	$A_{eq2_{\Theta_V}}$	$A_{eq2_{P_T}}$	P_W		b_{eq2}
				Θ_V		
				P_T		

Linear Inequalities: $A\,X \leq b$

The representations of the linear inequalities will be different for the cases that are going to be simulated in this study.

In Case 1, regional wind power connection capacities declared by TEIAS (Figure 4-14) will define the inequality constraints in the linear optimization. The installed power of the newly established wind power plants in these 47 regions should be smaller than or equal to the declared limits by TSO.

$$\sum_{for\ k \in Region\ r} P_{W_k} \leq P_{WC_r} \tag{4-7}$$

where,

P_{W_k} is the installed power of newly established WPP at the k^{th} eligible location in Region r (in MW),

P_{WC_r} is the declared regional wind power connection capacity of Region r (in MW).

Then, the inequality equations which represent Case 1 can be summarized as in Table 4-10.

Table 4-10. Inequality Equations for Case 1

$\boldsymbol{A_{1P_G}}$	$\boldsymbol{A_{1P_W}}$	$\boldsymbol{A_{1\Theta_V}}$	$\boldsymbol{A_{1P_T}}$	$\boldsymbol{P_G}$	$\leq$	$\mathbf{b_1}$
				$\boldsymbol{P_W}$		
				$\boldsymbol{\Theta_V}$		
				$\boldsymbol{P_T}$		

where,

$\boldsymbol{A_{1P_G}}$: An N_R x N_G matrix. Existing generator outputs are not involved in inequality constraints; therefore, it is a zero matrix. Here, N_R is 47 which is the total number of regions in Figure 4-14.

$\boldsymbol{A_{1P_W}}$: An N_R x N_W matrix. For eligible wind power locations which are in Region r, the corresponding multiplying indices will be 1.

$\boldsymbol{A_{1\Theta_V}}$: An N_R x N_B matrix. Bus voltage angles are not involved in inequality constraints; therefore, it is a zero matrix.

$\boldsymbol{A_{1P_T}}$: An N_R x N_T matrix. Line flows are not involved in inequality constraints; therefore, it is a zero matrix.

$\mathbf{b_1}$: An N_R x 1 vector. It represents the right side of Equation (4-7) and includes the announced regional wind power connection capacities (Figure 4-14).

In Case 2, in order to find the best locations for WPP establishment in Turkey, integration of wind power plants will be investigated disregarding the limiting capacities from TEIAS. Therefore, in this case, the only limiting inequality constraint will be the sum of installed capacity of wind power plants being smaller than 3 GW.

$$\sum_{for\ all\ locations} P_{W_k} \leq 3000 \tag{4-8}$$

where,

P_{W_k} is the installed capacity of new wind power plant at k^{th} location (MW).

Then, Table 4-11 represents the linear inequality constraints for Case 2 in the optimization algorithm.

Table 4-11. Inequality Equations for Case 2

A_{2P_G}	A_{2P_W}	$A_{2\Theta_V}$	A_{2P_T}	P_G	≤	b_2
				P_W		
				Θ_V		
				P_T		

where,

A_{2P_G} : A 1 x N_G null matrix.

A_{2P_W}: A 1 x N_W all-ones matrix.

$A_{2\Theta_V}$: A 1 x N_B null matrix.

A_{2P_T}: A 1 x N_T null matrix.

b_2: is a scalar with a value of 3000 which represents the right side of Equation (4-8).

Lower and Upper Bounds: $X_{min} \leq X \leq X_{max}$

The lower and upper bounds of the variables will be obtained from the thermal limits of the transmission elements and the maximum possible installed capacity of that location.

- ***Lower Bound Vector:*** X_{min}

The lower bound vector which defines the minimum limits of the variables in the algorithm is presented in Table 4-12.

Table 4-12. The Structure of Lower Bound Vector

$\mathbf{X}_{\mathbf{min}_{\boldsymbol{G}}}$
$\mathbf{X}_{\mathbf{min}_{\boldsymbol{W}}}$
$\mathbf{X}_{\mathbf{min}_{\boldsymbol{\Theta}}}$
$\mathbf{X}_{\mathbf{min}_{\boldsymbol{T}}}$

where,

$\mathbf{X}_{\mathbf{min}_{\boldsymbol{G}}}$: An N_G x 1 vector: The indices correspond to active power outputs of the existing generators from generation dispatch except the slack bus which has the minimum limit as -∞.

$\mathbf{X}_{\mathbf{min}_{\boldsymbol{W}}}$: An N_W x 1 null vector: The minimum installed capacity of new WPP is 0, in other words, no establishment.

$\mathbf{X}_{\mathbf{min}_{\boldsymbol{\Theta}}}$: An N_B x 1 vector: The minimum bus voltage angle can be -∞ except for the slack bus voltage whose phase angle is forced to be 0.

$\mathbf{X}_{\mathbf{min}_{\boldsymbol{T}}}$: An N_T x 1 vector: The minimum power flow through each branch is restricted by the negative of its thermal capacity.

- ***Upper Bound Vector***: $\boldsymbol{X_{max}}$

The upper bound vector which defines the maximum limits of the variables in the algorithm is presented in Table 4-13.

Table 4-13. The Structure of Upper Bound Vector

$\boldsymbol{X}_{\boldsymbol{max}_{\boldsymbol{G}}}$
$\boldsymbol{X}_{\boldsymbol{max}_{\boldsymbol{W}}}$
$\boldsymbol{X}_{\boldsymbol{max}_{\boldsymbol{\Theta}}}$
$\boldsymbol{X}_{\boldsymbol{max}_{\boldsymbol{T}}}$

where,

$\boldsymbol{X_{max_G}}$: An N_G x 1 vector: The indices correspond to the active power outputs of the existing generators from generation dispatch except the slack bus which has the maximum limit as ∞.

$\boldsymbol{X_{max_W}}$: An N_W x 1 vector: The maximum installed capacity of the new WPP will be limited by 30 MW for eligible locations.

$\boldsymbol{X_{max_\Theta}}$: An N_B x 1 vector: The maximum bus voltage angle can be ∞ except for the slack bus voltage whose phase angle is forced to be 0.

$\boldsymbol{X_{max_T}}$: An N_T x 1 vector: The maximum power flow through each branch is restricted by its thermal capacity.

The flowchart of the developed algorithm to find the optimal locations of WPPs in Turkey is summarized in Figure 4-18. As inputs, the expected summer peak of 2017 data which include the generation dispatch, the load forecast and the electricity network data are prepared. In addition to that, the results of the studies presented in Chapter 3 which include the feasible data points for WPP establishment, their annual capacity factors, their connection TSs and their region according to the declared map of TEIAS (Figure 4-14) will be inputted to the algorithm.

Using the above mentioned inputs, the equations which will be used in the linear optimization are constructed: The objective function (Equation (4-4)) to maximize the annual wind power generation is constructed using the calculated annual capacity factors of each eligible data point. Then, using the network data and DC load flow equations (Equation (4-5) and Equation (4-6)), the linear equality constraints are constructed. Next step is to construct the inequality constraints: As two different cases will be simulated, two different linear inequality equation sets will be constructed as given in Equation (4-7) for Case 1, and Equation (4-8) for Case 2.

When all equations and their corresponding matrices are constructed, the last step is to input the upper and lower bound limits of the variables to the built-in function of Matlab; namely, '*linprog*' to solve the linear optimization problem.

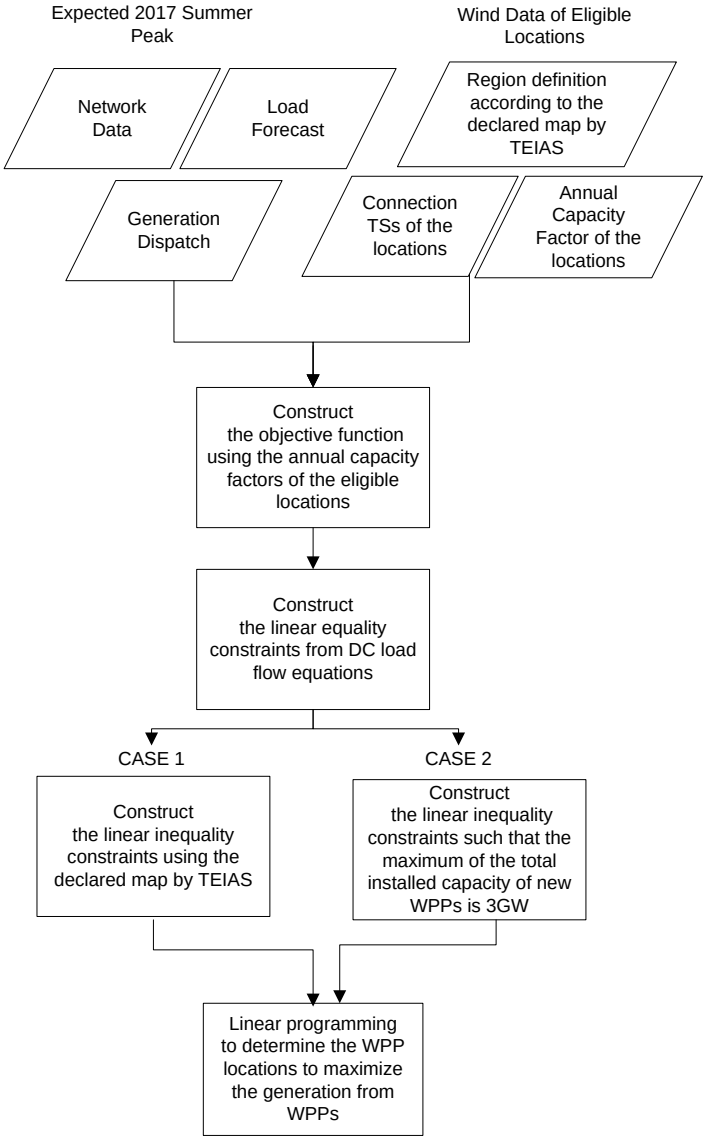

Figure 4-18. The Flowchart of the Optimization to Find the Optimal Locations of WPPs

4.4.3. Results of the Optimization

As stated, two cases will be investigated in the optimization algorithm: In Case 1, the optimal locations of WPPs will be selected regarding the regional wind power connection capacities announced by TEIAS [8]. In Case 2, the declared regional connection capacities by TEIAS will not be taken into account in order to find the

best locations for WPP establishment in Turkey. In addition to that, Case 1 and Case 2 will be investigated twice: In Case 1-A and Case 2-A, the thermal limits of the transmission elements will be ignored and the best locations which lead maximum wind power generation and their effects will be investigated. In Case 1-B and Case 2-B, the thermal limits of the transmission elements will be taken into account and the locations which lead maximum wind power generation while satisfying the thermal limits are found. Each case will be investigated in terms of the selected locations of new wind power plants, the annual average wind power production and the effect on thermal loadings of the network elements.

4.4.3.1. Case 1: Optimal WPP Locations Bounded by the Regional Wind Power Connection Capacities Declared by TEIAS

In Case 1, the regional capacities declared by TEIAS will be taken into account and the optimal places for WPPs will be found accordingly. In Case 1-A, the optimization problem will be solved ignoring the thermal limits of the network elements in order to see the best locations which will lead the maximum annual wind power generation in Turkey.

The result of Case 1-A is presented in Figure 4-19, in which the optimal locations for WPP installment while satisfying the declared capacities from TEIAS are shown. Many of the selected locations are in Çanakkale, Balıkesir, Mersin, and Trakya regions. From Table A-1 in Appendix A, it can also be followed that the declared regional wind power connection capacities by TEIAS in those 4 regions are around 800 MW which are more than one fourth of the declared total capacity, 3 GW.

Since, in Case 1-A, the optimization is solved without the thermal constraints of transmission elements, several transmission elements are overloaded which can be seen in Table 4-14. However, overloads in the transmission elements are very slight. Only, Diliskelesi – Gebzekimya branch is critically overloaded. However, as there are many generating units in the nearby area, by a minor re-dispatch in outputs of the generators, the overload can be avoided.

Table 4-14. Overloaded Transmission Elements in Case 1-A

From Bus Name	To Bus Name	Summer Rating (MVA)	Case 1-A Loading (%)
Tekirdag	Malkara	110	100.85
Bursasan-B	Bosen	153	100.43
Bursa3	Otosansit	206	101.21
Kayabasi	Turhal	110	100.22
Inebolu	Kure	123	102.00
Resadiye	Tuna-H	206	100.25
Ismetpasa	Sogutsen	110	100.75
Diliskelesi	Gebzekimya	153	118.68

The annual wind power production from newly installed WPPs is calculated as 8.771 TWh from the result of the optimization. The total installed capacity of the wind power plants are 3 GW; then, the average capacity factor of the newly established wind power plants can be calculated according to Equation (3-32):

$$\frac{8.771 * 10^{12}}{3 * 10^{9} * 8760} * 100\ \% = 33.375\ \%$$

In Case 1-B, both the thermal limits of the transmission elements and the regional constraints declared by TEIAS (Figure 4-14) are taken into account while solving the linear optimization. Since, in Case 1-A, several transmission elements are overloaded in the optimal solution, in Case 1-B, the locations of the WPPs are slightly modified due to thermal limits. In Figure 4-20, the selected locations in Case 1-B are shown. Again, the selected locations are in correlation with the capacity factors.

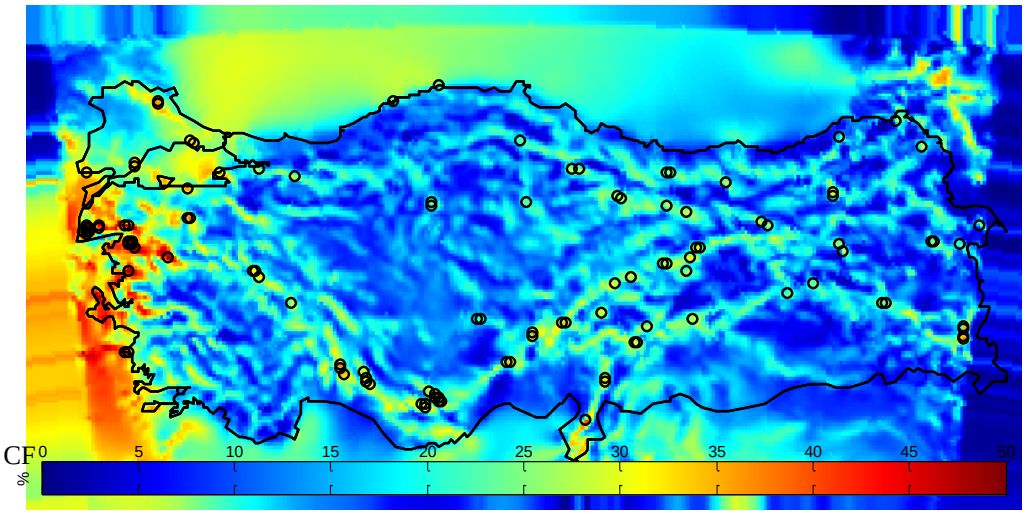

Figure 4-19. Optimal Locations of WPPs in Case 1-A

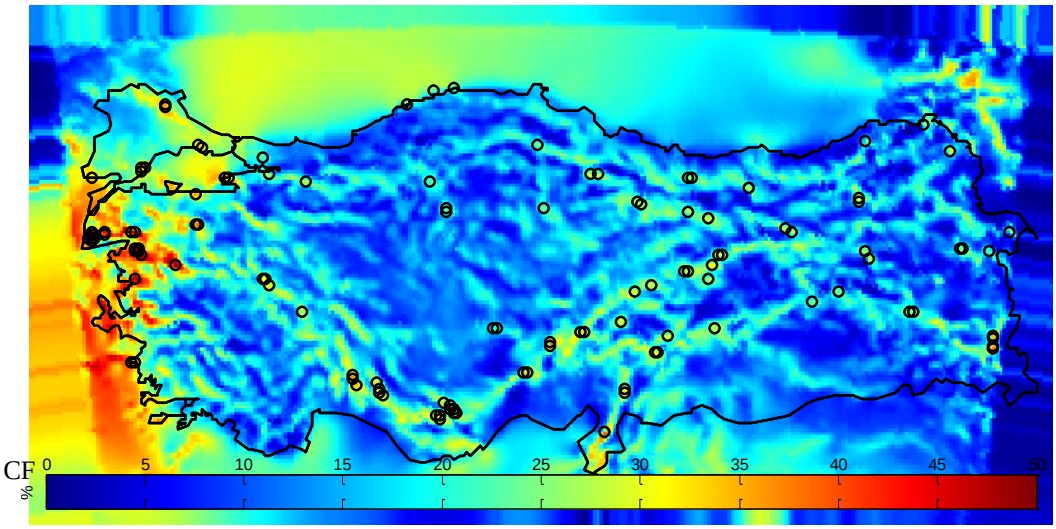

Figure 4-20. Optimal Locations of WPPs in Case 1-B

Since; in Case 1-B, the thermal constraints are taken into consideration, no transmission elements are overloaded. However, this results in slightly lower wind power generation: 8.76412 TWh is the result of the optimization. Then, the average

capacity factor of the newly established wind power plants can be calculated according to Equation (3-32):

$$\frac{8.76412 * 10^{12}}{3 * 10^{9} * 8760} * 100\ \% = 33.349\ \%$$

As the overloads are not severe, the result of the optimization has not dramatically changed: There is only a slight decrease in annual wind power production and average capacity factor.

In Table 4-15, the comparison of the selected locations in simulated two cases is presented. As can be followed, in 6 locations, the wind power is curtailed and needed to be moved to a different location with lower capacity factor in the same region due to thermal constraints.

Table 4-15. Comparison of the Optimal Locations between Case 1-A and Case 1-B

Lat. (°)	Lon. (°)	Connected TS	Wind Outputs		Difference (MW)	CF (%)	Region #
			Case 1-A (MW)	Case 1-B (MW)			
41.7902	32.4139	Bartin	30.00	26.58	-3.42	23.11	13
40.5587	32.8882	Ismetpasa	0.00	3.42	3.42	22.42	13
39.8418	28.2658	Kemalpasa	20.00	9.93	-10.07	34.20	21
40.5803	28.9046	Gemlik	0.00	10.07	10.07	31.93	21
42.0229	33.3482	Inebolu	30.00	25.86	-4.14	23.46	23
41.9632	32.9872	Cide	0.00	4.14	4.14	23.40	23
40.6215	29.7556	Ford	30.00	15.61	-14.39	26.41	37
40.8843	29.5921	Diliskelesi	0.00	14.39	14.39	22.44	37
40.0581	37.9811	Susehri	30.00	27.39	-2.61	28.82	43
38.8863	37.2394	Kangal	20.00	22.61	2.61	27.61	43
40.1860	36.9972	Almus	30.00	26.30	-3.70	29.27	45
40.1849	37.0679	Akinci-H	10.00	13.70	3.70	29.14	45

4.4.3.2. Case 2: Optimal WPP Locations in Turkey

In Case 2, the linear optimization will be solved disregarding the regional wind power connection capacities declared by TEIAS in order to find the best locations for WPP establishment in Turkey.

In Case 2-A, the linear optimization is solved disregarding the thermal constraints. In Figure 4-21, the optimal locations for WPP establishment are shown. Each black circle represents an installed capacity of 30 MW. As expected from the capacity factor map, all of the selected locations are in Çanakkale, Balıkesir, and Izmir regions.

Since; the optimization is solved without the thermal limits of the transmission elements, several transmission elements are overloaded which can be seen in Table 4-16. Especially; in Izmir region, there are severe overloads due to the new wind power integration.

Table 4-16. Overloaded Transmission Elements in Case 2-A

From Bus Name	To Bus Name	Summer Rating (MVA)	Case 2-A Loading (%)
Aliaga OSB	Cakmaktepe	206	146.96
Diliskelesi	Gebzekimya	153	137.87
Uzundere	Karabaglar-B	206	120.78
Uzundere	Karabaglar-B	206	120.78
Bursasan-B	Bosen	153	118.08
Bursa 3	Otosansit	206	110.85
Urla	Kocadag-R	110	105.35
Tekirdag	Malkara	110	104.06
Ambarli-DG (400 kV)	Ambarli-DG (154 kV)	150	103.59
Ambarli-DG (400 kV)	Ambarli-DG (154 kV)	150	103.59

The annual wind power production is calculated as 11.6223 TWh from the result of the optimization. The total installed capacity of new wind power plants is 3 GW; then, the average capacity factors of all newly established wind power plants can be calculated according to Equation (3-32):

$$\frac{11.6223 * 10^{12}}{3 * 10^{9} * 8760} * 100\ \% = 44.22\ \%$$

In Case 2-B, the optimization will be solved by taking the thermal constraints into account. Since; in Case 2-A, several transmission elements are overloaded in the optimal solution; in Case 2-B, the locations of the WPPs are modified due to thermal limits of the transmission elements. In Figure 4-22, the selected locations resulted from the linear optimization are shown. Especially, in Hatay, Izmir, Bursa, Adapazari and Balikesir regions, the optimal locations of WPPs are different than Case 2-A due to thermal limits of the transmission elements.

Since, in Case 2-B, thermal constraints are taken into consideration, no transmission elements are overloaded. However, this results in lower wind power generation: 11.19668 TWh is the result of the optimization. Then, the average capacity factors of the newly established wind power plants can be calculated according to Equation (3-32):

$$\frac{11.19668 * 10^{12}}{3 * 10^{9} * 8760} * 100\% = 42.60\ \%$$

In Table 4-17, the comparison of the optimal locations between Case 2-A and Case 2-B is shown. As can be seen, in many locations, the wind power is curtailed due to thermal limits of the transmission elements and wind power is penetrated from a different area which has lower capacity factor. Different than Case 1, there are many locations whose outputs must be shifted due to thermal constraints. Especially, in Bursa region, due to generation deficit and thermal congestions, new WPP locations are selected near the area. In addition, in Izmir and Balikesir regions, the optimal

locations of WPPS in Case 2-A are shifted due to thermal limits of the transmission elements.

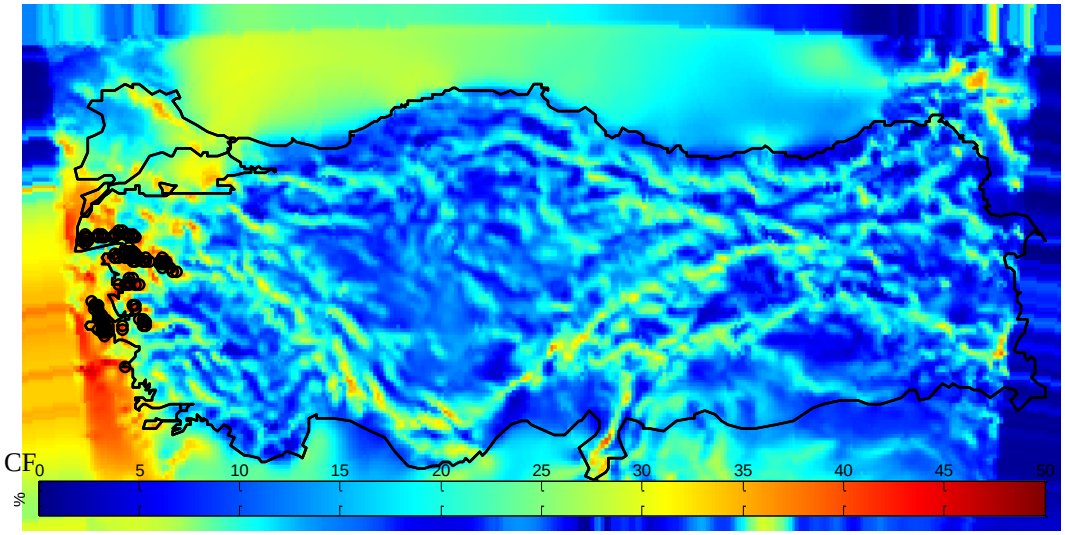

Figure 4-21. Optimal Locations of WPPs in Case 2-A

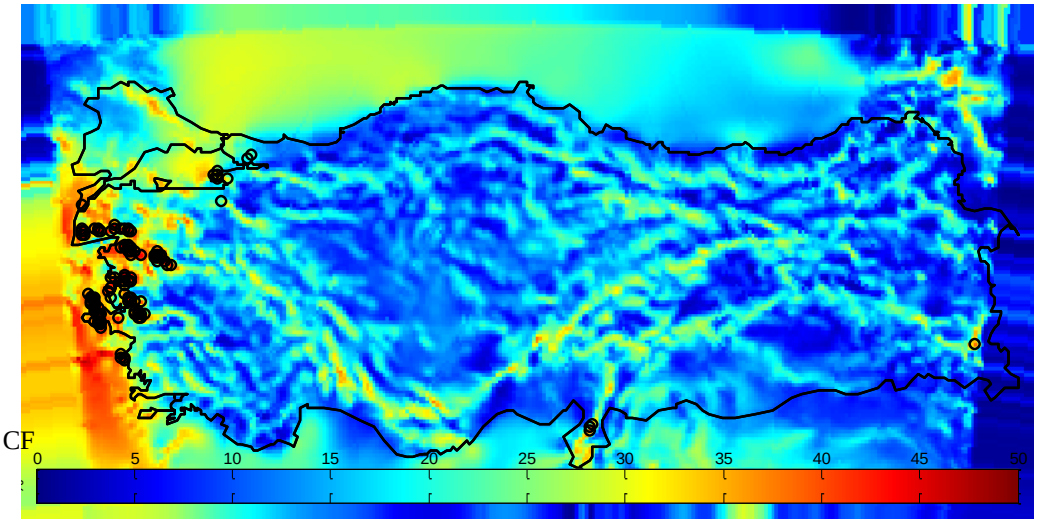

Figure 4-22. Optimal Locations of WPPs in Case 2-B

Table 4-17. Comparison of the Optimal Locations between Case 2-A and Case 2-B

Lat. (°)	Lon. (°)	Connected TS	Wind Outputs		Difference (MW)	CF (%)	Region #
			Case 2-A (MW)	Case 2-B (MW)			
39.0092	27.0926	Duzova-R	30.00	0.00	-30.00	46.00	32
39.2968	27.3396	Bergama	30.00	0.00	-30.00	45.81	32
39.3365	27.1251	Bergama	30.00	0.00	-30.00	44.95	32
39.014	27.1618	Yuntdagi-R	30.00	0.00	-30.00	44.58	32
39.2875	27.2007	Bergama	30.00	0.00	-30.00	44.35	32
39.6591	27.0881	Edremit	30.00	0.00	-30.00	43.67	12
39.6834	26.6628	Akcay	30.00	11.49	-18.51	43.48	12
39.4393	27.0432	Edremit	30.00	0.00	-30.00	43.12	12
39.7521	26.8659	Akcay	30.00	0.00	-30.00	42.74	12
39.4247	26.8344	Ayvalik	30.00	0.00	-30.00	42.47	12
39.3318	27.0556	Edremit	30.00	0.00	-30.00	42.46	12
39.5451	26.2577	Sares	30.00	0.00	-30.00	42.19	22
39.6472	26.1743	Sares	30.00	0.00	-30.00	42.17	22
38.32	26.549	Kocadag-R	30.00	12.56	-17.44	42.07	32
39.4978	27.1066	Edremit	30.00	0.00	-30.00	41.97	12
38.2227	26.6987	Urla	30.00	0.00	-30.00	41.89	32
38.3788	26.611	Kocadag-R	30.00	0.00	-30.00	41.82	32
38.9507	27.0296	Duzova-R	30.00	0.00	-30.00	41.62	32
39.7618	27.0057	Edremit	30.00	0.00	-30.00	41.59	12
39.6934	26.8024	Akcay	30.00	0.00	-30.00	41.48	12
39.3759	26.9103	Ayvalik	30.00	0.00	-30.00	41.42	12
38.1689	26.705	Urla	30.00	0.00	-30.00	41.33	32
38.2423	26.9723	Tahtali	30.00	0.00	-30.00	41.27	32
39.3552	27.4032	Soma-A	30.00	0.00	-30.00	41.26	40
38.2764	26.6923	Urla	30.00	0.00	-30.00	41.23	32
39.3709	26.8408	Ayvalik	30.00	0.00	-30.00	41.18	12
39.3807	26.9799	Edremit	30.00	0.00	-30.00	41.12	12
38.9158	27.3121	Izmir-Havza	30.00	0.00	-30.00	41.04	32

Table 4-17. (continued)

Lat. (°)	Lon. (°)	Connected TS	Wind Outputs		Difference (MW)	CF (%)	Region #
			Case 2-A (MW)	Case 2-B (MW)			
39.306	27.4786	Soma-A	30.00	0.00	-30.00	41.01	40
39.6733	26.5232	Sares	30.00	0.00	-30.00	40.97	22
38.7749	26.8413	Almak	0.00	30.00	30.00	40.72	32
37.656	27.1074	Kusadasi	0.00	30.00	30.00	40.65	11
38.3198	27.3086	Isiklar-B	0.00	30.00	30.00	40.27	32
38.5254	27.1474	Ulucak	0.00	30.00	30.00	40.23	32
38.8527	27.18	Seyitali-R	0.00	30.00	30.00	40.11	32
38.7162	26.7787	Almak	0.00	30.00	30.00	40.11	32
38.8574	27.249	Seyitali-R	0.00	30.00	30.00	40.06	32
38.9361	26.8223	Aliaga 1	0.00	30.00	30.00	40.03	32
36.5262	36.2974	Belen-R	0.00	30.00	30.00	39.89	29
38.476	26.4608	Cesme	0.00	30.00	30.00	39.88	32
38.3335	27.5142	Kemalpasa	0.00	30.00	30.00	39.85	32
37.705	27.0335	Kusadasi	0.00	30.00	30.00	39.85	11
38.8969	27.0358	Cakmaktepe	0.00	30.00	30.00	39.78	32
38.5441	27.4224	Manisa	0.00	30.00	30.00	39.69	40
36.4724	36.2965	Antakya 2	0.00	30.00	30.00	39.23	29
37.6023	27.1134	Kusadasi	0.00	30.00	30.00	39.14	11
36.5794	36.3654	Iskenderun1	0.00	30.00	30.00	38.71	29
40.0875	26.2591	Kumlimani	0.00	30.00	30.00	38.19	22
37.8645	43.9195	Bagisli	0.00	18.40	18.40	38.18	42
38.5348	27.2849	Universite	0.00	30.00	30.00	38.17	32
38.633	27.1353	Ulucak	0.00	30.00	30.00	37.95	32
38.848	27.111	Cakmaktepe	0.00	30.00	30.00	35.76	32
40.584	28.9755	Gemlik	0.00	30.00	30.00	34.52	21
40.5803	28.9046	Gemlik	0.00	30.00	30.00	31.93	21
40.5301	28.9803	Gemlik	0.00	30.00	30.00	31.44	21
38.7942	27.1171	Cakmaktepe	0.00	30.00	30.00	31.21	32

Table 4-17. (continued)

Lat. (°)	Lon. (°)	Connected TS	Wind Outputs		Difference (MW)	CF (%)	Region #
			Case 2-A (MW)	Case 2-B (MW)			
40.5373	29.1219	Gemlik	0.00	30.00	30.00	29.85	21
40.6378	28.9707	Gemlik	0.00	3.70	3.70	29.46	21
38.6137	26.8601	Alcuk	0.00	30.00	30.00	28.20	32
40.1533	29.0137	Bursa 3	0.00	12.17	12.17	24.72	21
40.8843	29.5921	Diliskelesi	0.00	30.00	30.00	22.44	37
40.881	29.5209	Diliskelesi	0.00	1.68	1.68	19.78	37

This completes the analyses about the integration of wind power plants with total installed capacity of 3 GW into Turkish grid. As expected, the maximum wind power generation value belongs to Case 2-A, in which no constraints are inputted. It is followed by Case 2-B, in which only the thermal limits of the transmission elements are taken into account. Annual wind energy production is lower in Case 1, in which the regional wind power connection capacities by TEIAS are taken into consideration as regional constraints in the optimization problem, compared to Case 2 in which no regional constraints are applied. By declaring the regional connection capacities, TEIAS aims to disperse the generation and have WPP penetration from every side of Turkey. As it was seen, only a few transmission elements are slightly overloaded in Case 1-A. Therefore, the declared capacities by TEIAS enable wind power penetration from all locations in Turkey without endangering the system security. However, as investigated in Case 2-B, locations which will lead more wind power production can be found without any overloads in the transmission elements. It must be noted that, in this case, a careful selection of WPP locations is required and connection capacities should be declared based on connection transformer substations rather than regional capacities.

CHAPTER 5

CONCLUSION AND FUTURE WORK

5.1. Conclusions

The work accomplished in this thesis consists of two main parts: Firstly, the wind energy potential in Turkey is investigated in terms of Weibull distribution parameters, average wind speed values, wind power density variations and expected capacity factor distributions.

Concerning the analyses for the determination of the wind power potential in Turkey, conclusions below are drawn:

- The Ministry of Energy and Natural Resources has prepared a wind atlas including average wind speeds of Turkey and expected capacity factors of the wind power plants. However, this work lacks of Weibull distribution parameters, wind power density values and seasonal analyses.

- TUBITAK Marmara Research Center has prepared a database including forecasts of the wind speed, the wind direction, the ambient temperature and the air pressure values for every 6 km x 6 km area of Turkey for every hour of last 8 years. In Matlab software, necessary algorithms are developed to investigate the variation of wind parameters.

- In order to find Weibull parameters of the wind speed, the direction of the wind is also necessary. There is a strong correlation between the wind speed and wind direction; therefore; while analyzing Weibull parameters, the direction segments should be separately investigated.

- The average wind speed is an important indicator to differentiate between strong and weak winds; however; it is not sufficient. The wind power density and the expected capacity factor of the wind power plant should also be calculated.

- Average wind speeds are highest in Çanakkale, Balıkesir, Izmir and Hatay regions. For seasonal analyses, summer and winter seasons are better than the spring season.

- To calculate the wind power density, which is said to be the most revealing character of the power, at a specified region, air density values are needed. Using the ambient temperature, pressure and long term humidity values, the average air density values at all locations in Turkey are calculated based on 6 km x 6 km areas.

- Air density values and Weibull parameters are used to calculate the wind power densities. The highest values of the wind power densities are found in Çanakkale, Balıkesir, Izmir, Hatay and Trakya regions.

- By selecting an appropriate wind turbine, capacity factors of the probable investments are calculated. Capacity factors; hence, the wind power productions, are highest in summer and winter seasons.

- All results are visualized via maps in order to easily find locations. A simple; but, mostly preferred Plate Carrée map transformation is used to accomplish that aim.

- Lastly, using the wind rose algorithm, calculated results using database values are compared with the actual measurement data from RITM project for Yahyalı WPP. It is seen that calculated values are able to detect the variation of wind parameters and are consistent with the actual data.

In the second part of the thesis, the integration of the wind power to Turkish grid and the optimal locations for WPPs are investigated. Conclusions concerning that work are drawn below:

- Every location with high wind speed may not be suitable for wind power plant establishment; therefore, areas which are not suitable for wind power plant establishment are found using Google Earth and relevant information.

- As elimination criteria to find those infeasible locations, the calculated wind power density values in Chapter 3, urban areas, altitude data and locations which are already licensed are used.

- Using Turkish substation data, TSs which are close to or in the city center, the substations of large PPs and the GISs are eliminated from the possible connection list and the eligible TSs for WPP connection are found. In addition to the existing TSs, the announced 7 wind basin substations are also added to the list.

- TEIAS has already confirmed nearly 10 GW of wind power plants' connection to grid. In November 2013, TEIAS announced a total of 3 GW of new regional wind power connection capacities in 47 regions. New applications will be evaluated according to this plan.

- In order to analyze the wind power integration to the grid, summer peak load data of 2017 are prepared using the investment plan of TEIAS, load

forecast results of TUBITAK Master Plan and generation curves corresponding to summer peaks of past 5 years.

- Two cases are simulated in order to investigate the optimal locations for WPP establishment which will lead to maximum wind power production. In both cases, linear programming optimization method is used with DC load flow linear equations and each case is investigated twice by regarding and disregarding the thermal constraints from the thermal limits of the transmission elements. However, the inequality constraints in each case are different: In Case 1, the announced regional wind power connection capacities by TEIAS are used as inequality constrains and the optimal locations are selected according to these regional constrains. It is seen that, although the average wind energy production is less due to selection of the locations which have lower capacity factors, overloads in transmission elements are not severe and even if thermal constraints from the thermal limits of the transmission elements are inputted, curtailments due to congestions are very slight.

- In Case 2, the declared regional wind power connection capacities by TEIAS are not taken into account in order to see the best locations for WPP establishment without any regional constraints. It is seen that, although the annual average wind power generation is higher than Case 1; the transmission elements are severely overloaded leading to an insecure network. When the thermal limits of the transmission elements are inputted as transmission constraints, there are many locations whose outputs have to be curtailed and penetrated from different transformer substations.

- From the results of Case 1, it can be stated that the declared regional capacities by TEIAS do not require additional investments; therefore; are important in order to secure the system. In addition, by announcing capacities from every region, WPP investments in every part of Turkey are promoted. However, as investigated in Case 2, locations which will lead

more wind power production can be found without endangering the system security. It must be noted that, in this case, a careful selection of WPP locations is required and connection capacities should be declared based on connection transformer substations rather than regional capacities.

5.2. Suggestions for Future Work

The renewable energy is a very important topic which is investigated by many academicians and researchers all over the world. Therefore, there are many other issues which are not under the scope of this study, but could be investigated in more detail in future studies. Following topics could be researched in future works:

- The areas that were under investigation in this study are 6 km x 6 km, which is indeed a large area. However, at the current time, this is the only available data in Turkey. Therefore, in order to increase the resolution of the study and have more accurate results, necessary data collection techniques can be improved.

- In scope of RITM project, actual measurements from selected wind power plants are being recorded. When this actual measurement period and the number of included WPPs in RITM project increase; the work in Chapter 3, the investigation of wind power potential in Turkey, can be repeated by using the actual measurement data.

- Another important topic in Turkey in terms of the renewable energy is the solar power plants. With a similar database about the solar power, the investigation of the solar power in Turkey and optimal locations which will lead to maximum solar generation can be determined.

- Lastly, in Chapter 4, in order to determine optimal locations for wind power plants, the DC load flow equations were used with linear

programming. For future studies, it is possible to use AC load flow with nonlinear optimization methods. More accurate results can be obtained by the use of AC load flow.

REFERENCES

[1] T.C. Enerji ve Tabii Kaynaklar Bakanlığı, "ETKB 2010-2014 Dönemi Stratejik Planı," [Online]. Available: http://www.enerji.gov.tr/yayinlar_raporlar/ETKB_2010_2014_Stratejik_Plani.pdf. [Accessed 10 03 2014].

[2] EPDK, "Turkish Energy Market: An Investors Guide," 2012. [Online]. Available: http://www.epdk.org.tr/documents/strateji/rapor_yayin/yatirimciel_kitabi/Sgb_Rapor_Yayin_Yatirimciel_Kitabi_Eng_2012_Mb3JG91tFh1B.pdf. [Accessed 02 03 2014].

[3] B. Ummels, "Power System Operation with Large-Scale Wind Power in Liberalised Environments," Labor Grafimedia bv, Utrecht, 2009.

[4] European Centre for Medium-Range Weather Forecasts, "ECMWF," [Online]. Available: http://www.ecmwf.int/. [Accessed 21 03 2014].

[5] Technical University of Denmark, "WAsP," [Online]. Available: http://www.wasp.dk/. [Accessed 14 03 2014].

[6] VESTAS Wind Turbines, [Online]. Available: http://www.vestas.com/. [Accessed 02 02 2014].

[7] MathWorks, [Online]. Available: http://www.mathworks.com/. [Accessed 14 03 2014].

[8] TEİAŞ, "Bölgesel Bazda Sisteme Bağlanabilecek Rüzgâr Enerjisine Dayalı Üretim Tesisi Kapasiteleri," 29 11 2013. [Online]. Available: http://www.teias.gov.tr/duyurular/RUZGAR.HTM. [Accessed 20 12 2013].

[9] T. Ackermann, Wind Power in Power Systems, Stockholm: John Wiley & Sons Ltd, 2005.

[10] RWE Npower Renewables, "Wind Turbine Power Calculations," [Online]. Available: http://www.raeng.org.uk/education/diploma/maths/pdf/exemplars_advanced/23_wind_turbine.pdf. [Accessed 18 03 2014].

[11] Michigan State University, "NWHS Physics Equations Page," [Online]. Available: https://www.msu.edu/~tuckeys1/highschool/physics/p_equations.htm.

[Accessed 15 03 2014].

[12] Vestas, "V112-3.0 MW Wind Turbine Brochure," [Online]. Available: http://www.vestas.com/Files/Filer/EN/Brochures/Vestas_V_112_web_100309.pdf. [Accessed 18 03 2014].

[13] S. S. Soman, H. Zareipour, O. Malik and P. Mandal, "A Review of Wind Power and Wind Speed Forecasting Methods With Different Time Horizons," in *North American Power Symposium (NAPS)*, Arlington, TX, 2010.

[14] Y.-K. Wu and J.-S. Hong, "A Literature Review of Wind Forecasting Technology in the World," in *Power Tech, IEEE*, Lausanne, 2007.

[15] "Rüzgar Gücü İzleme ve Tahmin Merkezi," TÜBİTAK MAM, Meteoroloji Genel Müdürlüğü, Yenilenebilir Enerji Genel Müdürlüğü, [Online]. Available: http://www.ritm.gov.tr/root/index.php. [Accessed 16 03 2014].

[16] University of Massachusetts Amherst: Wind Energy Center, "Wind Power: Capacity Factor, Intermittency, and What Happens When the Wind Does not Blow," [Online]. Available: http://www.umass.edu/windenergy/publications/published/communityWindFactSheets/RERL_Fact_Sheet_2a_Capacity_Factor.pdf. [Accessed 14 03 2014].

[17] G. Strbac, A. Shakoor, M. Black, D. Pudjianto and T. Bopp, "Impact of Wind Generation on the Operation and Development of the UK Electricity Systems," Elsevier, 2007.

[18] H. Agabus, Large-Scale Integration of Wind Energy into the Power System Considering the Uncertainty Information, Tallinn: Tallinn University of Technology, 2009.

[19] EPDK, "Elektrik Piyasası Şebeke Yönetmeliği," [Online]. Available: http://www.epdk.gov.tr/index.php/elektrik-piyasasi/mevzuat?id=89. [Accessed 18 03 2014].

[20] H. Holttinen, P. Meibom, A. Orths, V. F. Hulle and C. Ensslin, "Design and Operation of Power Systems with Large Amounts of Wind Power," in *Global Wind Power Conference*, Adelaide, Australia, 2006.

[21] A. Badelin, Large Scale Integration of Wind Power in the Russian Power Supply: Analysis, Issues, Strategy, Kassel: University of Kassel, 2007.

[22] A. Smith, "Quantifying Exports and Minimising Curtailment: From 20% to 50% Wind Penetration in Denmark," BIEE, 2010.

[23] Yenilenebilir Enerji Genel Müdürlüğü, "Rüzgar Enerjisi Teknik Potansiyelleri Atlası: REPA," [Online]. Available: http://www.eie.gov.tr/YEKrepa/REPA-duyuru_01.html. [Accessed 19 03 2014].

[24] Türkiye Rüzgar Enerjisi Birliği, "Türkiye Rüzgar Enerjisi İstatistik Raporu," TÜREB, 2013.

[25] EPDK, "Elektrik Piyasası Üretim Lisansları," [Online]. Available: http://lisans.epdk.org.tr/epvys-web/faces/pages/lisans/elektrikUretim/elektrikUretimOzetSorgula.xhtml. [Accessed 02 03 2014].

[26] TEİAŞ, [Online]. Available: http://www.teias.gov.tr/. [Accessed 02 01 2014].

[27] EPDK, "Elektrik İletim Sistemi Arz Güvenilirliği ve Kalitesi Yönetmeliği," [Online]. Available: http://www.epdk.gov.tr/index.php/elektrik-piyasasi/mevzuat?id=167. [Accessed 12 03 2014].

[28] P. Dvorak, "Wind Power Engineering: Building Wind Farms is Easy, Transmission Lines are Tough," [Online]. Available: http://www.windpowerengineering.com/construction/building-wind-farms-easy-transmission-lines-tough/. [Accessed 11 02 2014].

[29] MathWorks, "Documentation Center: wblfit," [Online]. Available: http://www.mathworks.com/help/stats/wblfit.html. [Accessed 16 03 2014].

[30] S. J. v. Donk, . L. E. Wagner, E. L. Skidmore and J. Tatarko, "Comparison of the Weibull Model with Measured Wind Speed Distributions for Stochastic Wind Generation," *American Society of Agricultural Engineers*, vol. 48(2), p. 503−510, 2005.

[31] J. Seguro and T. Lambert, "Modern Estimation of the Parameters of the Weibull Wind Speed Distribution for Wind Energy Analysis," *Journal of Wind Engineering and Industrial Aerodynamics*, no. 85, pp. 75-84, 2000.

[32] MathWorks, "Documentation Center: wblpdf," [Online]. Available: http://www.mathworks.com/help/stats/wblpdf.html. [Accessed 18 03 2014].

[33] MathWorks, "Documentation Center: wblcdf," [Online]. Available: http://www.mathworks.com/help/stats/wblcdf.html. [Accessed 18 03 2014].

[34] V. Yılmaz, H. Aras and H. Çelik, "Statistical Analysis of Wind Speed Data," *Journal of Eng. & Arch.Fac. Eskişehir Osmangazi University,* vol. XVIII, no. 2, 2005.

[35] E. K. Akpinar and S. Akpinar, "A Statistical Analysis of Wind Speed Data Used in Installation of Wind Energy Conversion Systems," *Energy Conversion and Management*, no. 46, pp. 515-532, 2005.

[36] A. N. Celik, "A Statistical Analysis of Wind Power Density Based on the Weibull and Rayleigh Models at the Southern Region of Turkey," *Renewable Energy*, no. 29, pp. 593-604, 2003.

[37] Iowa Energy Center, "How to Analyze Wind Data," [Online]. Available: http://www.iowaenergycenter.org/wind-energy-manual/wind-and-wind-

power/how-to-analyze-wind-data/. [Accessed 18 03 2014].

[38] A. Hahmann, J. Badger, N. G. Mortensen and J. C. Hansen, "From Trades to Turbines: The Art and Science of Wind Energy Resource Assessment," [Online]. Available: http://www.wasaproject.info/docs/5_windatlasintro2010.pdf. [Accessed 18 03 2014].

[39] WAsP, "Wind Speed Distributions and AEP," [Online]. Available: http://130.226.56.171/Support/FAQ/WebHelp/Wasp9.htm#WindSpeedDistributions.htm. [Accessed 18 03 2014].

[40] C. Awasthi, A. Gour and P. Mukesh, "Observed Wind Climate and Weibull Distribution at RGPV Energy Park, Bhopal (India) Using WAsP," *International Journal of Emerging Technology and Advanced Engineering,* vol. 3, no. 8, 2013.

[41] P. H. Dana, "Map Projection Overview," 1995. [Online]. Available: http://www.colorado.edu/geography/gcraft/notes/mapproj/mapproj_f.html. [Accessed 18 03 2014].

[42] E. M. Delmelle, *Map Projection Properties: Considerations for Small Scale GIS Applications,* New York: The Faculty of Graduate School of State University of New York, 2001.

[43] National Aeronautics and Space Administration, "World Wind," [Online]. Available: http://worldwind31.arc.nasa.gov/svn/trunk/WorldWind/src/gov/nasa/worldwind/globes/FlatGlobe.java. [Accessed 18 03 2014].

[44] The Research Institute for Advanced Computer Science (RIACS), "World Wind Map Tile System," [Online]. Available: http://www.riacs.edu/research/projects/worldwind/extending/wwtilesystem.pdf. [Accessed 18 03 2014].

[45] A. P. Kirvan, "Latitude and Longitude," [Online]. Available: http://www.ncgia.ucsb.edu/giscc/units/u014/u014.html. [Accessed 18 03 2014].

[46] T. Hughes, "Estimating and Calculating Air Density," Environmental Verification and Analysis Center, The University of Oklahoma, [Online]. Available: http://www.ocgi.okstate.edu/owpi/EducOutreach/Library/Lesson2_airdensity.pdf. [Accessed 15 03 2014].

[47] T.C. Orman ve Su İşleri Bakanlığı: Meteoroloji Genel Müdürlüğü, "Türkiye İklim Sınıflandırması," [Online]. Available: http://www.meteor.gov.tr/FILES/genel/sss/iklimveridegerlendir.pdf. [Accessed 15 03 2014].

[48] S. Sensoy, M. Demircan, Y. Ulupınar and İ. Balta, "Türkiye İklimi," [Online]. Available: http://www.mgm.gov.tr/FILES/iklim/turkiye_iklimi.pdf. [Accessed 12 02 2014].

[49] R. S. Davis, "Equation for the Determination of the Density of Moist Air," *Metrologia*, no. 29, pp. 67-70, 1992.

[50] C. M. Grinstead and J. L. Snell, "Expected Value and Variance," in *Introduction to Probability*, New Hampshire, Dartmouth College, pp. 225-271.

[51] Department of Mathematics and Statistics: University at Albany, "About the Gamma Function," [Online]. Available: http://math.albany.edu/~hammond/course/calcnotes/gamma.pdf. [Accessed 16 03 2014].

[52] T.C. Resmi Gazete, "Rüzgâr Enerjisine Dayalı Lisans Başvurularının Teknik Değerlendirilmesi Hakkında Yönetmelik," 2008. [Online]. Available: http://www.resmigazete.gov.tr/eskiler/2008/11/20081109-3.htm. [Accessed 18 03 2014].

[53] International Electrotechnical Commission, IEC International Standards regarding Wind Turbines: IEC 61400-2, 2006, p. 21.

[54] The Department of Mathematics at Virginia Tech, "Probability and Cumulative Distribution Functions," [Online]. Available: http://www.math.vt.edu/people/qlfang/class_home/Lesson2021.pdf. [Accessed 18 03 2014].

[55] MathWorks, "Matlab Central File Exchange: Wind Rose," [Online]. Available: http://www.mathworks.com/matlabcentral/fileexchange/17748-windrose. [Accessed 18 03 2014].

[56] T.C. Çevre ve Şehircilik Bakanlığı, "ÇED Süreci," [Online]. Available: http://www.csb.gov.tr/gm/ced/index.php?Sayfa=sayfaicerik&IcId=673#CED. [Accessed 11 03 2014].

[57] V. Smil, "The Universal Link: Energetics, Energy, and Power," in *Energy in Nature and Society*, Cambridge, Massachusetts, the MIT Press, 2008, pp. 1-23.

[58] Google Earth, [Online]. Available: http://www.google.com/earth/. [Accessed 14 12 2013].

[59] EPDK, "Milli Parklar, Tabiat Anıtları, Tabiat Koruma Alanları ve Tabiat Parkları Pafta Listesi," [Online]. Available: http://www.epdk.gov.tr/index.php/elektrik-piyasasi/lisans. [Accessed 16 03 2014].

[60] Northern Ireland Planning Portal, "Renewable Energy: Spacing of Turbines," [Online]. Available:

http://www.planningni.gov.uk/index/policy/policy_publications/planning_statements/pps18/pps18_annex1/pps18_annex1_wind/pps18_annex1_technology/pps18_annex1_spacing.htm. [Accessed 11 03 2014].

[61] D. G. L. Johnson, "Wind Power Plants: Turbine Placement," in *Wind Energy Systems*, Manhattan, KS, University Reprints, 2006, pp. 9.1-9.4.

[62] K. Yıldır, "Türkiye'de Rüzgar Santrallerinin İletim Sistemi Bağlantıları," in *Rüzgâr Enerjisi Çalıştayı, TÜREB*, İstanbul, 2013.

[63] TEİAŞ, "Ani, Maksimum, Minimum ve Kış Tüketim Günlerinin Yük Eğrileri," [Online]. Available: http://www.teias.gov.tr/yukdagitim/yillik_menu.htm. [Accessed 18 03 2014].

[64] T.C. Enerji ve Tabii Kaynaklar Bakanlığı: Yenilenebilir Enerji Genel Müdürlüğü, "YEGM Tarafından Mühendislik Hizmetleri Yürütülen Hidroelektrik Santral Projeleri," [Online]. Available: http://www.eie.gov.tr/hes/index.aspx. [Accessed 18 02 2014].

[65] TEİAŞ, "Mevcut Enterkonneksiyon Hatlarının Net Transfer Kapasiteleri," TEİAŞ, Ankara, 2013.

[66] TÜBİTAK MAM & TEİAŞ, "2013 - 2022 Yılları Türkiye İletim Sistemi Bölgesel Talep Tahmin ve Şebeke Analiz Çalışması," TEİAŞ, Ankara, 2013.

[67] H. Bradley, "Applied Mathematical Programming," in *Solving Linear Programs*, Addison-Wesley, 1977, pp. 38-69.

[68] Y. Zhang, "Solving Large Scale Linear Programs by Interior-Point Methods under the MATLAB Environment," Department of Mathematics and Statics: University of Maryland Baltimore County, Baltimore, Maryland, 1996.

[69] MathWorks, "Documentation Center: linprog," [Online]. Available: http://www.mathworks.com/help/optim/ug/linprog.html. [Accessed 16 02 2014].

APPENDIX A

THE REGIONAL WIND POWER CONNECTION CAPACITIES DECLARED BY TEIAS

Table A-1. The Regional Wind Power Connection Capacities Declared by TEIAS [8]

Region Number	Cities	Maximum Capacity (MW)
1	Adana	120
2	Adıyaman	40
3	Afyonkarahisar	30
4	Ağrı, Iğdır	110
5	Aksaray, Kırşehir, Nevşehir	40
6	Amasya, Samsun	60
7	Ankara, Kırıkkale, Çankırı	60
8	Antalya	100
9	Ardahan, Kars	40
10	Artvin, Rize, Trabzon	30
11	Aydın, Muğla	50
12	Balıkesir	160
13	Bartın, Zonguldak, Karabük	30
14	Batman, Mardin, Diyarbakır, Şanlıurfa	60
15	Bayburt, Gümüşhane, Giresun	40
16	Bilecik, Eskişehir, Kütahya	50
17	Bingöl, Tunceli	50
18	Bitlis, Muş	40
19	Bolu, Düzce, Sakarya	30

Table A-1 (continued)

Region Number	Cities	Maximum Capacity (MW)
20	Burdur, Denizli, Uşak	30
21	Bursa	110
22	Çanakkale	260
23	Çorum, Kastamonu, Sinop	60
24	Edirne	30
25	Elazığ	30
26	Erzincan	70
27	Erzurum	110
28	Gaziantep, Kilis	40
29	Hatay	30
30	Isparta	60
31	İstanbul	50
32	İzmir	50
33	Kahramanmaraş, Osmaniye	40
34	Karaman, Mersin	250
35	Kayseri, Niğde	60
36	Kırklareli	60
37	Kocaeli, Yalova	30
38	Konya	30
39	Malatya	80
40	Manisa	30
41	Ordu	50
42	Siirt, Şırnak, Hakkari	30
43	Sivas	80
44	Tekirdağ	50
45	Tokat	40
46	Van	70
47	Yozgat	30
	Total:	3000